Award Number: W81XWH-11-1-0270

TITLE: Enhancement of Radiation Therapy in Prostate Cancer by DNA-PKcs Inhibitor

PRINCIPAL INVESTIGATOR: Debabrata Saha, Ph.D.

CONTRACTING ORGANIZATION: University of Texas Southwestern Medical Center
Dallas, TX 75390-7208

REPORT DATE: September 2015

TYPE OF REPORT: Final Addendum

PREPARED FOR: U.S. Army Medical Research and Materiel Command
Fort Detrick, Maryland 21702-5012

REPORT DOCUMENTATION PAGE

Form Approved
OMB No. 0704-0188

1. REPORT DATE	**2. REPORT TYPE**	**3. DATES COVERED**
September 2015	Final Addendum	1 July 2014 – 30 June 2015

4. TITLE AND SUBTITLE

Enhancement of Radiation Therapy in Prostate Cancer by DNA-PKcs Inhibitor

5a. CONTRACT NUMBER

5b. GRANT NUMBER
W81XWH-11-1-0270

5c. PROGRAM ELEMENT NUMBER

6. AUTHOR(S)

Debabrata Saha, Ph.D.

E-Mail: Debabrata.Saha@utsouthwestern.edu

5d. PROJECT NUMBER

5e. TASK NUMBER

5f. WORK UNIT NUMBER

7. PERFORMING ORGANIZATION NAME(S) AND ADDRESS(ES)

University of Texas Southwestern Medical Center
Dallas, TX 75390-7208

8. PERFORMING ORGANIZATION REPORT NUMBER

9. SPONSORING / MONITORING AGENCY NAME(S) AND ADDRESS(ES)
U.S. Army Medical Research and Materiel Command
Fort Detrick, Maryland 21702-5012

10. SPONSOR/MONITOR'S ACRONYM(S)

11. SPONSOR/MONITOR'S REPORT NUMBER(S)

12. DISTRIBUTION / AVAILABILITY STATEMENT
Approved for Public Release; Distribution Unlimited

13. SUPPLEMENTARY NOTES

14. ABSTRACT

Prostate cancer (PCa) is the second leading cause of cancer death (~30,000/year) in men in the USA. Surgery and radiotherapy are the most effective therapies to treat PCa patients. However, both these forms of treatment, show significant tumor recurrence with locally aggressive disease, metastasis and the morbidity in patients. Several biological disorders are thought to underlie the cause of prostate cancer. One such factor is a tumor suppressor gene DAB2IP which encodes a member of the Ras-GAP protein family. Genome wide Single Nucleotide Polymorphism (SNP) association studies in a large number of patients indicated that DAB2IP is linked with the risk of aggressive prostate cancer. DAB2IP deficient PCa cells are resistant to radiation treatment. Therefore, to improve radiation killing of these aggressive PCa cells, this proposal will explore the radiosensitizing property of NU7441, a specific kinase inhibitor of DNA-PKcs.

15. SUBJECT TERMS
Radiation therapy, Prostate cancer, Radio-sensitization, DNA-Double strand break, cell cycle

16. SECURITY CLASSIFICATION OF:			**17. LIMITATION OF ABSTRACT**	**18. NUMBER OF PAGES**	**19a. NAME OF RESPONSIBLE PERSON**
a. REPORT	**b. ABSTRACT**	**c. THIS PAGE**			USAMRMC
U	U	U	UU	108	**19b. TELEPHONE NUMBER** *(include area code)*

Table of Contents

Introduction

Prostate cancer (PCa) is the second leading cause of cancer death (~30,000/year) in men in the USA. Surgery and radiotherapy are the most effective therapies to treat PCa patients. However, both these forms of treatment, show significant tumor recurrence with locally aggressive disease, metastasis and the morbidity in patients. Several biological disorders are thought to underlie the cause of prostate cancer. One such factor is a tumor suppressor gene DAB2IP which encodes a member of the Ras-GAP protein family. Genome wide Single Nucleotide Polymorphism (SNP) association studies in a large number of patients indicated that DAB2IP is linked with the risk of aggressive prostate cancer. DAB2IP deficient PCa cells are resistant to radiation treatment. Therefore, to improve radiation killing of these aggressive PCa cells, this proposal will explore the radiosensitizing property of NU7441, a specific kinase inhibitor of DNA-PKcs. Three specific aims were proposed:

Aim 1: To test whether a DNA-PKcs inhibitor can radio-sensitize DAB2IP deficient aggressive PCa cells under normoxic and hypoxic conditions.

Aim 2: To study the role of DNA-PKcs in HIF-1α stabilization under hypoxic conditions in DAB2IP deficient prostate cancer cells.

Aim 3: To investigate the combined effect of a DNA-PK inhibitor and radiation therapy in a rodent orthotopic (OT) PCa model using image guided radiation therapy (IGRT).

Body:

Following tasks were proposed during the No Cost Extension Period:

Mostly the experiments proposed in the Aim 3 in the original proposal will be performed. Briefly; To determine the efficacy of the combined treatment, we will establish these groups (1) control, (2) radiation (12Gyx3), (3) radiation (12Gyx2), (4) radiation (12Gyx1), (5) NU7441 (25mg/kg), (6) NU7441+radiation (12Gyx3), (7) NU7441+radiation (12Gyx2), (8) NU7441+radiation (12Gyx2). We will measure the tumor volume using the Ultra Sound guided (USG) imaging and bioluminescence imaging (BLI). For Immunohistological analysis, we will establish similar animal groups and collect the tumor samples at different time points after treatment for (i) pimonidazole staining, (ii) HIF-1α expression level, (iii) Ki 67 staining (proliferation), (iv) γH2AX staining (For DNA damage/repair response) (v) DNA-PKcs staining (to differentiate normal and tumor tissue) and (v) Apoptosis Study. We will also analyze the radiation induced damage to the adjacent organs bladder and rectum by histology.

Key Research Accomplishment:

Aim 3.1 Tumor growth study with radiation and NU7441

We implanted PC3KD-luc cells orthotopically inside the prostate of adult male nude rats, but our results showed a loss of bioluminescence signal as the tumor grows, which led us to use ultrasound as the primary tumor measurement tool instead of BLI to determine the effect of combined treatment of radiation and NU7441. We found that the PC3KD-luc tumor is highly aggressive and it reaches a size bigger than 5,000 mm^3 in 3 weeks. At the beginning we attempted hypo-fractionated radiation dose which was 3 fractions of 12 Gy every 48h. Our pilot study showed that this regimen (12 Gy X 3) has an ablative effect on prostate tumor (Figure 1) and also associated with rectum toxicity. We therefore, reduce the radiation dose to 10 Gy per fraction for 2 fractions. NU7441 (25mg/kg/day for 5 days) was administered intraperitoneal 1 hour prior to radiation treatment. Our results showed NU7441 alone slightly delayed the tumor growth compare to control animals. However, irradiation (10Gy X 2) has a significant impact on tumor growth, and combination treatment (NU7441 + radiation) further delayed the tumor growth compared to irradiation only group (Figure 2B). Tumor volumes in all groups were measured by ultrasound and the representative ultrasound images were shown in Figure 2A. Our data showed that the combination of radiation and NU7441 is highly effective in the treatment of locally aggressive prostate cancer.

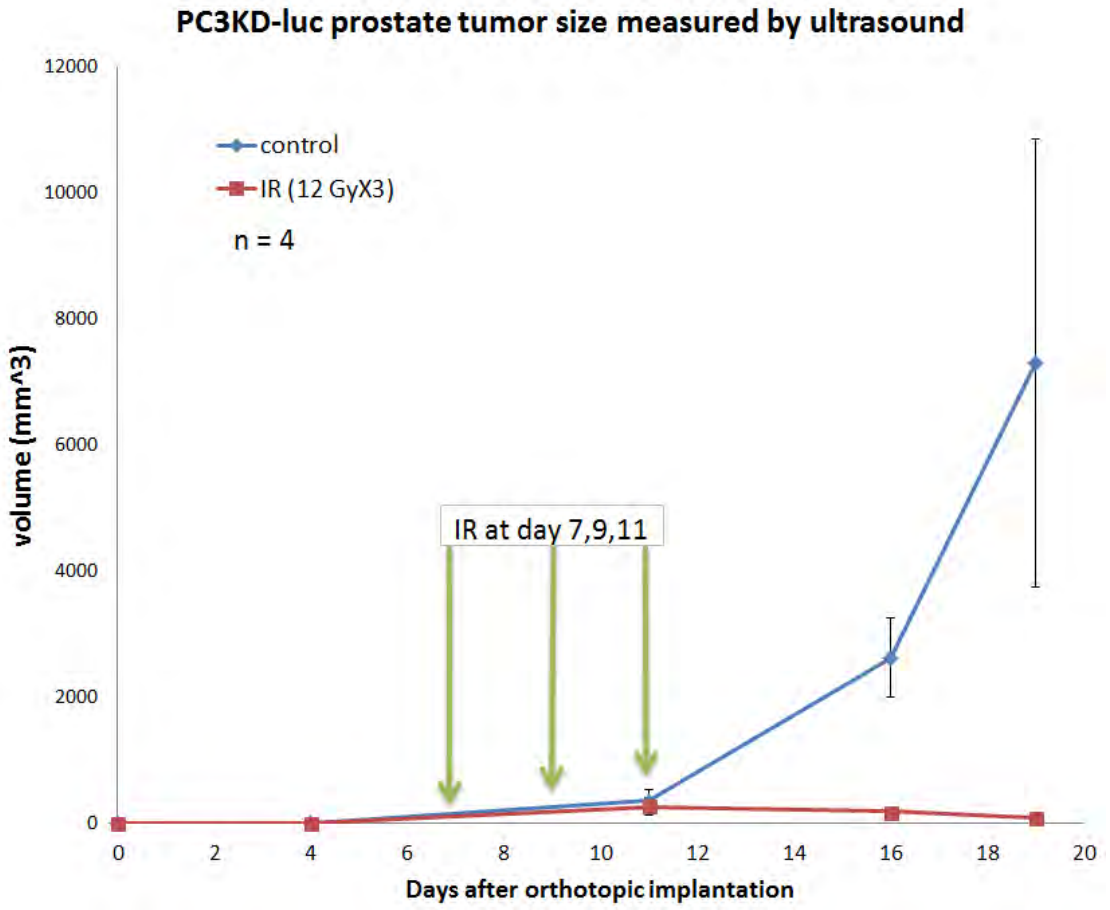

Figure 1. PC3KD prostate tumor radiation response. PC3KD cells were surgically implanted into the right prostate lobe of athymic nude rats and the tumor growth was monitored by Ultrasound and BL imaging. Animals were radiated when the tumor volume was 100 to 200mm^3 using XRad-320 irradiator.

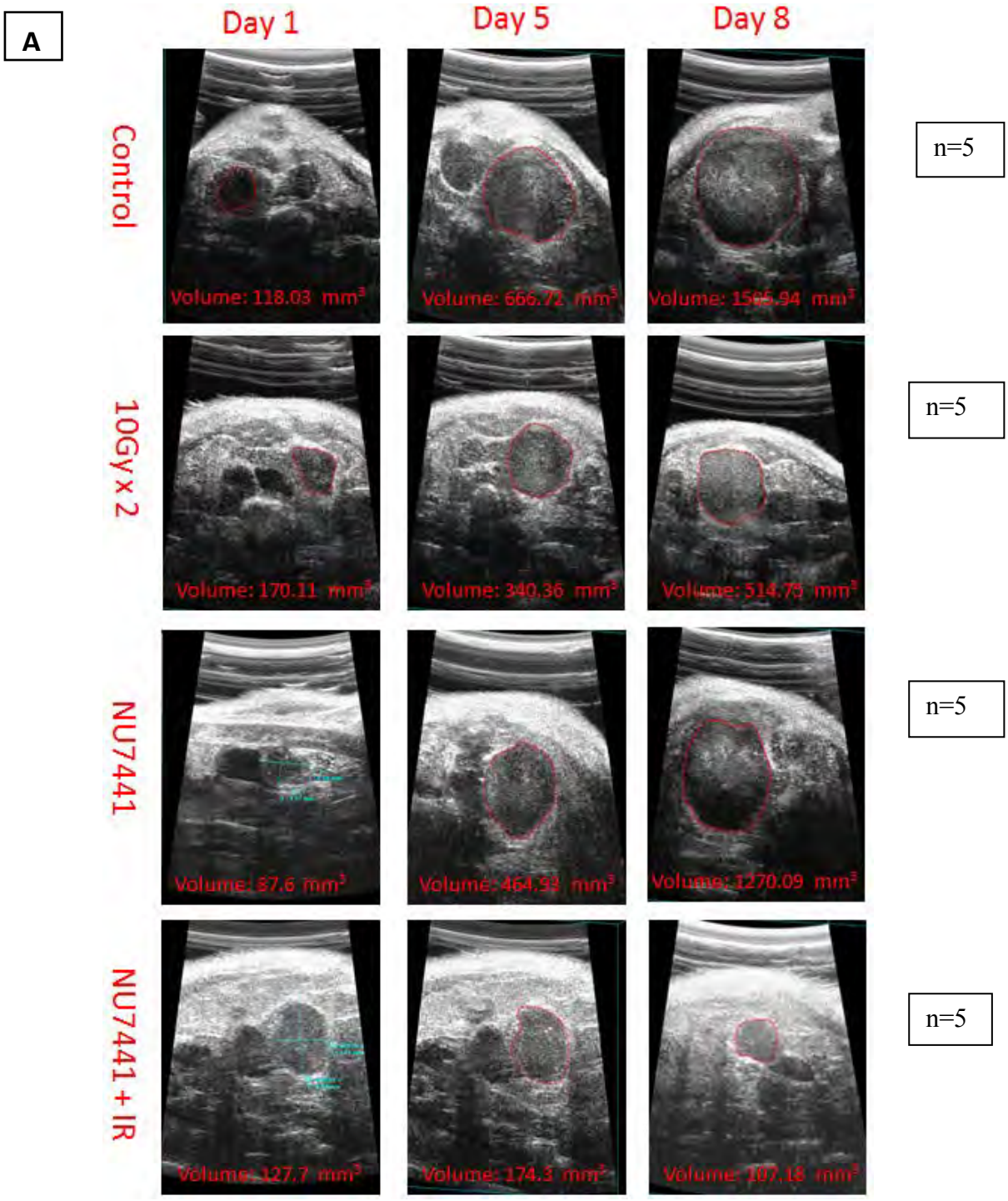

Figure 2A. Ultrasound Imaging was performed on the VisualSonics Vevo 770 Imaging System using the real-time Micro Visualization scan head RMV716 (11–24 MHz) specific for rats. Rats were anesthetized and the transducer head was placed transverse to the pelvis of the rats in supine position. Images were obtained by resolving various depths of tissue into the center of optimum resolution plane to ensure clear images throughout the tumor volume.

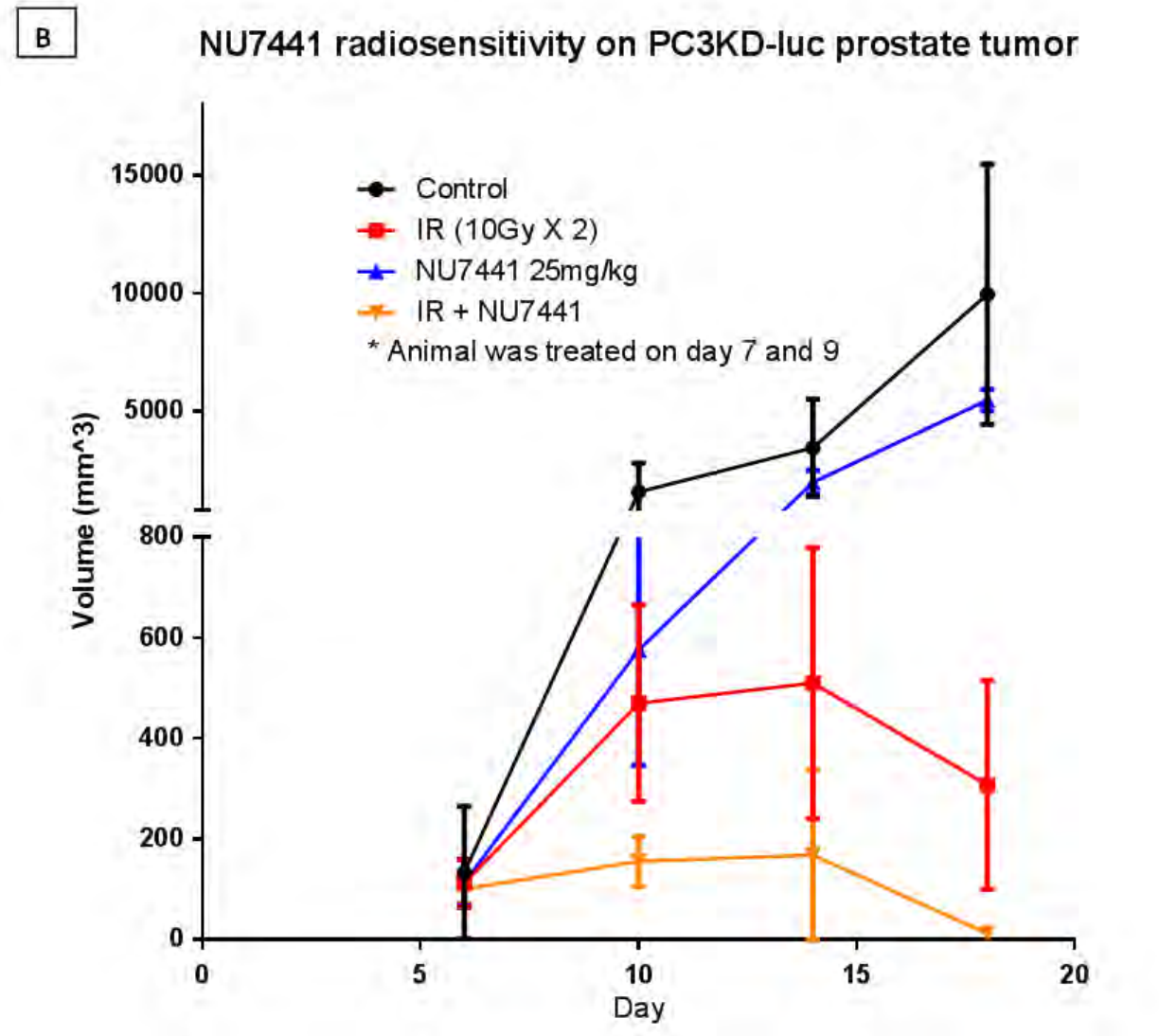

Figure 2B. Tumor growth delay in response to the combined treatment of radiation and NU7441. PC3KD cells were surgically implanted into the right prostate lobe of athymic nude rats. Initial tumor growth was detected by BL imaging after that and the tumor growth in all treatment groups was monitored by Ultrasound imaging as shown in Figure 2A. Animals were radiated when the tumor volume was 100 to 200mm^3 using XRad-320 irradiator. Two fractions of 10 Gy were given 48 hrs apart while the NU7441 (25mg/kg/day) was administered intraperitoneal for 5 consecutive days.

Aim 3.2: Immunohistological analysis of the treatment efficacy:
Our study demonstrated that almost complete tumor ablation was achieved in response to the combined treatment of radiation and NU7441. We further analyze the combined effect of radiation and NU7441on the prostate tumor, normal prostate tissues and the surrounding organ 3 weeks after the final treatment. We previously reported that OT prostate model clearly showed the tumor outline in the right prostate while left prostate remains normal (Tumati et al). Therefore, we performed immuno histochemical analysis specifically looking at the DNA damage response after the combined treatment of radiation and NU7441. We use both gH2AX and 53BP1 as the marker for DNA double strand damage. We observed significant residual level of gH2AX and 53BP1 nuclear staining in animals received both radiation and the combined treatment (Figure 3A). It was also observed that in radiation alone and in combined treatment groups, distinct prostate glandular structure was visible while those were absent in the control and NU7441 treated groups. The glandular structures were noticed mostly in the peripheral regions of the prostate as shown in Figure 3B.

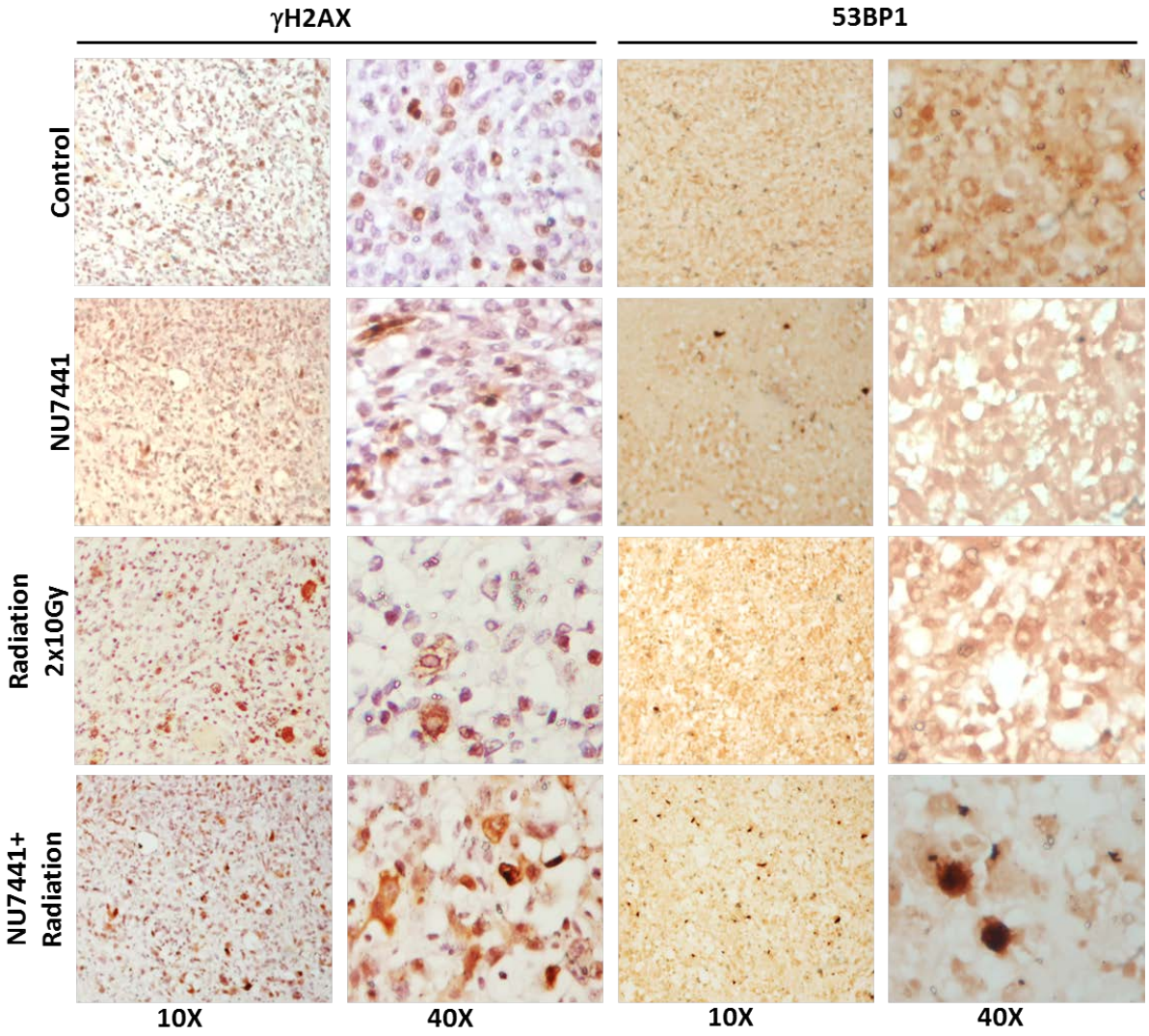

Figure 3A: Immunohistochemical (IHC) detection of gamma γH2AX and 53BP1 positive cells in paraffin embedded prostate cancer sections: γH2AX and 53BP1 as the markers of DNA double-strands breaks detects unrepaired cells in treated and untreated prostate cancers post-irradiation. Antibodies for γH2AX and 53BP1 were obtained from Millipore and BD Bioscience respectively. For IHC analysis, antibodies were used at 1:100 dilutions and counter stained with hematoxylin. Images were captured in 10x and 40x magnification.

Figure 3B: IHC analysis of the tumor samples treated with radiation and radiation+NU7441. As mentioned

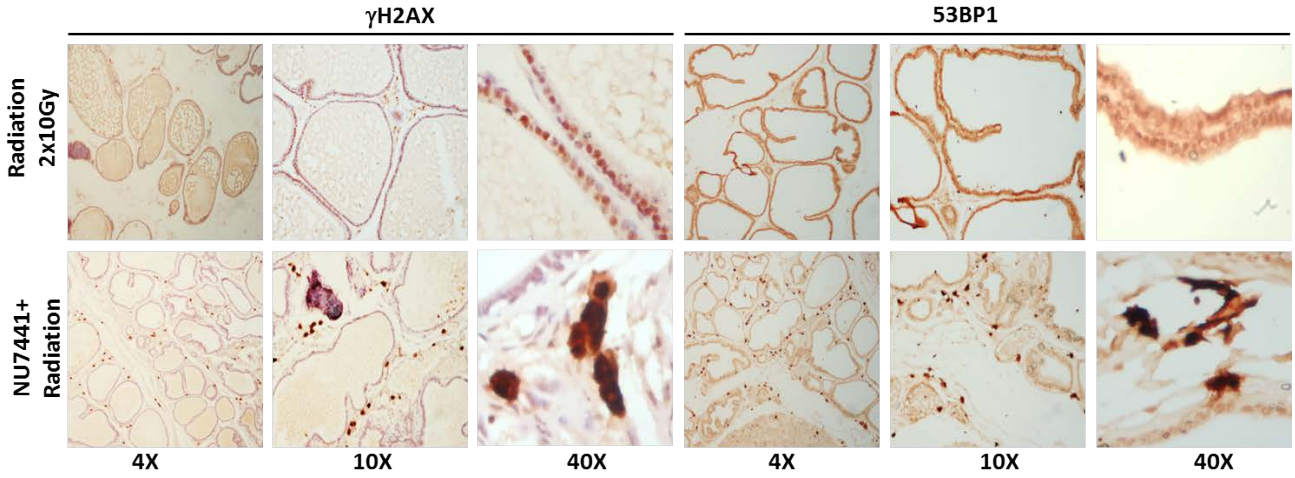

earlier that significant tumor control was achieved in these two groups and evident by detecting the glandular structure.

Ki-67 Staining in prostate cancer samples

Ki-67 is a nuclear non-histone protein highly expressed in proliferating cells but low in non-dividing cells. Ki-67 staining is routinely used as a specific nuclear marker for cell proliferation for many cancers including bladder, brain, breast, kidney, lung, ovary and prostate. In this study, samples from the 4 treatment groups were collected 3 weeks after the final treatment and the paraffin sections were prepared. Sections were stained with rabbit anti-human Ki67 and then incubate with biotinylated goat anti-rabbit IgG followed by incubation with FITC-streptavidin. Slides were examined using a fluorescence microscope with appropriate filters.

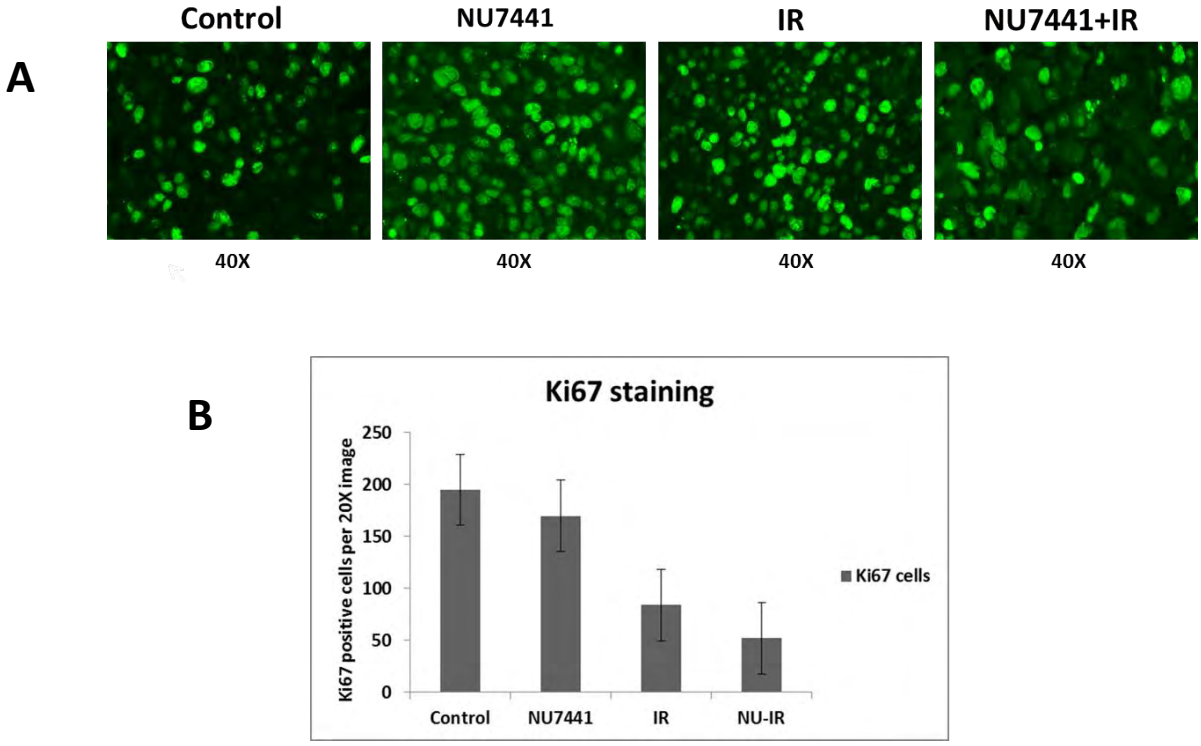

Figure 4: Detection of Ki-67 in implanted prostate tumors treated with DNA-PK inhibitor NU7441 followed by radiation exposure: (A) Ki-67 staining of the prostate cancer samples treated with, (i) control, (ii) NU7441, (iii) IR and (iv) IR+radiation. Animals were sacrificed 3 weeks after the treatment and samples were collected and stained with Ki-67. (B) Ki-67 positive cells (bright fluorescent) were counted and plotted.

Our results showed that the number of Ki-67 positive cells were significantly low in both radiation (IR) and combined treatment groups (NU7441+IR) whereas in the drug alone group number of Ki-67 positive cells were similar to control animal group indicating that radiation alone and the combined treatment groups were highly effective in preventing the prostate tumor progression.

TUNEL Staining for detecting apoptosis in prostate cancer samples

TUNEL assay is widely used technique for assessing the apoptosis in tissue section. As our Ki-67 staining demonstrated a significant inhibition of tumor cell proliferation in the combined treatment group, therefore, we performed TUNEL assay to detect the apoptotic cell death in all tumor samples. The sections from all treatment groups were subjected to TUNEL staining. Our results clearly showed that the number of TUNEL positive cells (green) were significantly high in the combined treatment groups (NU7441+IR). A higher level of TUNEL positive cell were also observed in the IR group whereas, very few TUNEL positive cells were noticed in the drug alone and the control group

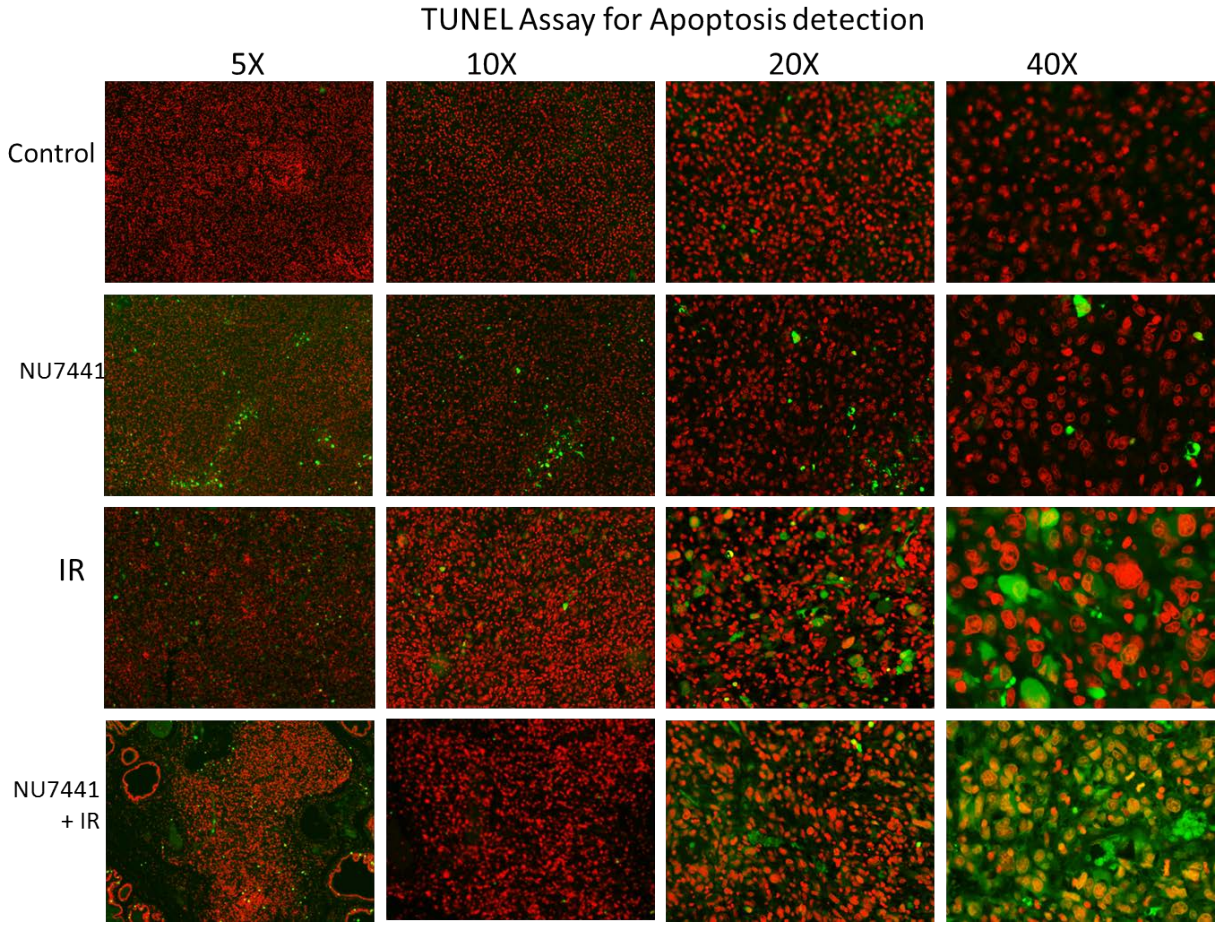

Figure 5. Detection of Apoptosis in implanted prostate tumors treated with DNA-PK inhibitor NU7441 followed by radiation exposure: Implanted tumors on rat exposed to radiation (10Gy X2) with and without drug NU7441 (25mg/kg 1 hour before radiation). Control and irradiated tumors were observed for growth and after 3 weeks, animals were sacrificed and tumors were collected for histological analysis. Paraffin embedded tumor sections were used to detect apoptosis by Terminal deoxynucleotidyl transferase dUTP nick end labeling (TUNEL) assay. Immunofluorescent images were captured by Zeiss Axio Imager fluorescent microscope. Green fluorescence (FITC) indicates TUNEL positive cells and red fluorescence indicates counterstain Propidium iodide. Higher number of green cells indicate hyper apoptosis. Images from the center of the tumors.

Aim 3.3: Analysis of the potential damage to bladder and rectum from irradiation and radiation + Nu7441

To observe the potential damage to bladder and rectum from irradiation and radiation + NU7441, we separated animals into control, NU7441, IR (10 Gy X 2), and combination (IR + NU7441). Bladder and rectum will be collected and compared in response to treatment. In our initial study (reported in the 2014 progress report), we found the irradiation treatment of 12Gy X 3 causing severe GI tract toxicity (Figure 4). In order to minimize the GI toxicity, we introduced a new treatment plan (10Gy X 2) was applied in the following studies.

Figure 6. Rectum toxicity of irradiation. A blocked GI tract was discovered 4 weeks after dissecting a rat received irradiation (12Gy X 3).

Ten days after treatment, animals were sacrificed. Prostate, bladder, and rectum were collected and fixed in 10% formalin and paraffin blocks were prepared. Then the tissue sections of different organs were stained with H & E. In control animal, majority of prostate was invaded by tumor, the same as in NU7441group; while the tumor was well contained inside of prostate in both IR only and combination treatment groups (**Figure 7 A-B)**. Rectum looked normal in all groups. Because of the tumor size the bladder was squeezed in the control and the NU7441 group but no metastasis was noticed in rectum and the bladder. Our data suggest that irradiation (10Gy X 2) only and combination (10Gy X 2 + NU7441) treatment had no noticeable toxicity to prostate surrounding organs such as rectum and bladder.

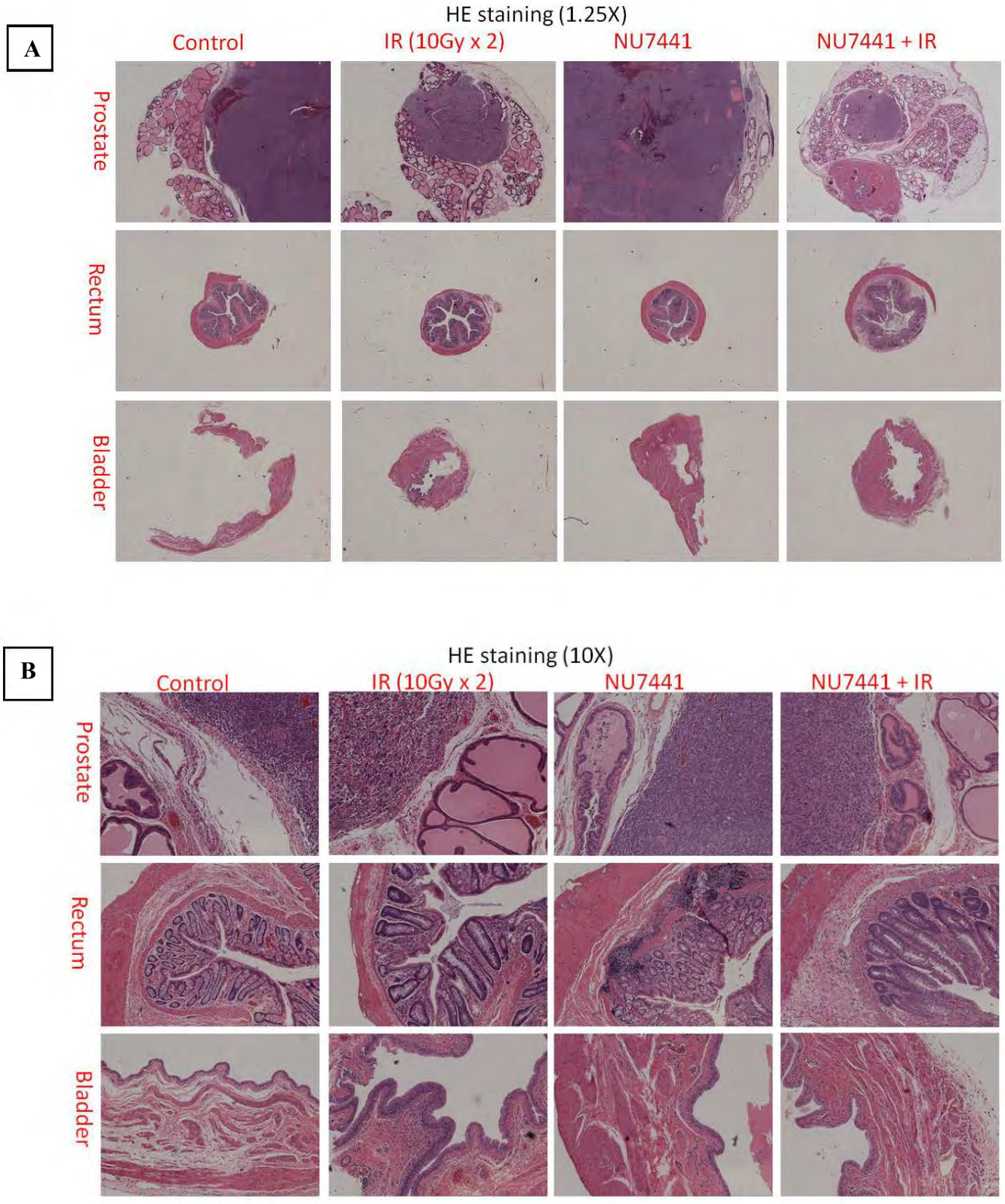

HIF-1a expression level in the PC3KD tumors:

We found that prostate tumors develop large areas of hypoxia heterogeneously spread throughout the tumor. These areas of hypoxia may explain the high amount of resistance to radiation therapy (Figure 6, A-C). Hypoxia staining in the rat prostate tumor was performed using the Hypoxyprobe™-1 plus kit (Hypoxyprobe Inc., Burlington, MA). Hypoxyprobe-1 (pimonidazole HCl) was administered i.p. (120 mg/kg) in tumor bearing rats.

Two hours later, the animal was sacrificed; tumor tissue was collected and fixed in 4% formalin solution for 48 h. Paraffin sections were prepared for IHC analysis. The following samples were stained from the control group animals. Similar type staining pattern was observed in NU7441 treated animal group. We also performed hypoxia staining in animals received radiation and combined therapy but due to smaller tumor volume and necrosis were unable to detect hypoxic region.

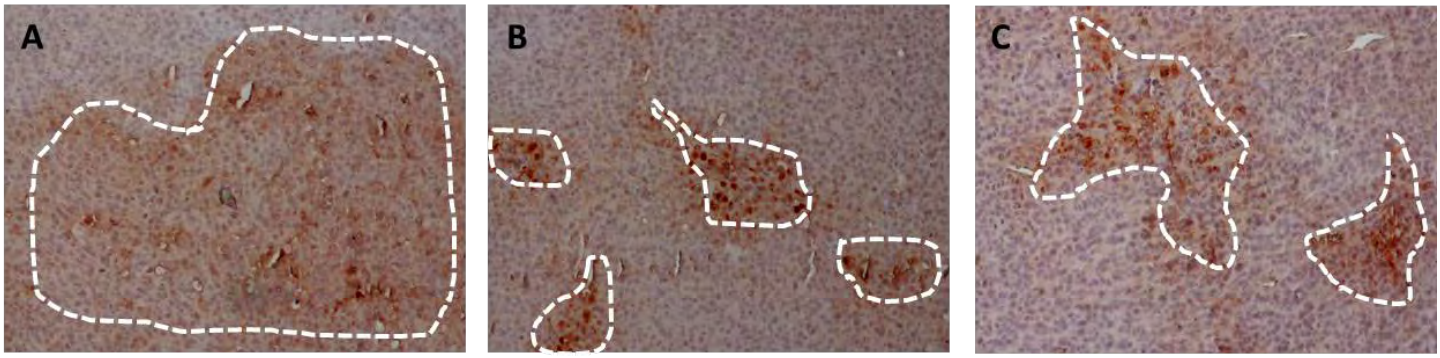

Figure 8: Hypoxyprobe-1 (pimonidazole HCl) was administered i.p. (120 mg/kg) in tumor bearing rats. Two hours later, the animal was sacrificed; tumor tissue was collected and fixed in 4% formalin solution for 48 h. Paraffin sections were prepared for IHC analysis. Hyproxyprobe-1 MAb1 (1:50) was used as the primary antibody and the Biotin-conjugated F(ab')2 (1:500) was used as the secondary antibody. Then samples were treated with Streptavidin peroxidase followed by DAB and then counter stained with Hematoxylin. Hypoxic areas were marked with white boundary (A-C).

Continuation of Task 7:
Last year we reported DAB2IP localized at kinetochore and played a significant role in spindle assembly check point regulation during mitosis. We made a significant progress in this area. Our new observation showed that using Time-lapse imaging that allows calculating the time from NEB (nuclear envelop break down) until anaphase onset, which can reflect the status of mitotic progression. We use HeLa cells stably expressing a histone H2B-GFP fusion protein were transfected with control or DAB2IP siRNA, and then monitored under a confocal microscope. Consistent with our previous observation, the percentage of mitotic cells with misaligned and lagging chromosomes were markedly increase after DAB2IP knockdown (Figure 7 A), indicating that depletion of DAB2IP will lead to abnormal organization of spindle structure. As a result, the DAB2IP-KD cells exhibit prolonged unperturbed mitosis progression when compared with control cells.

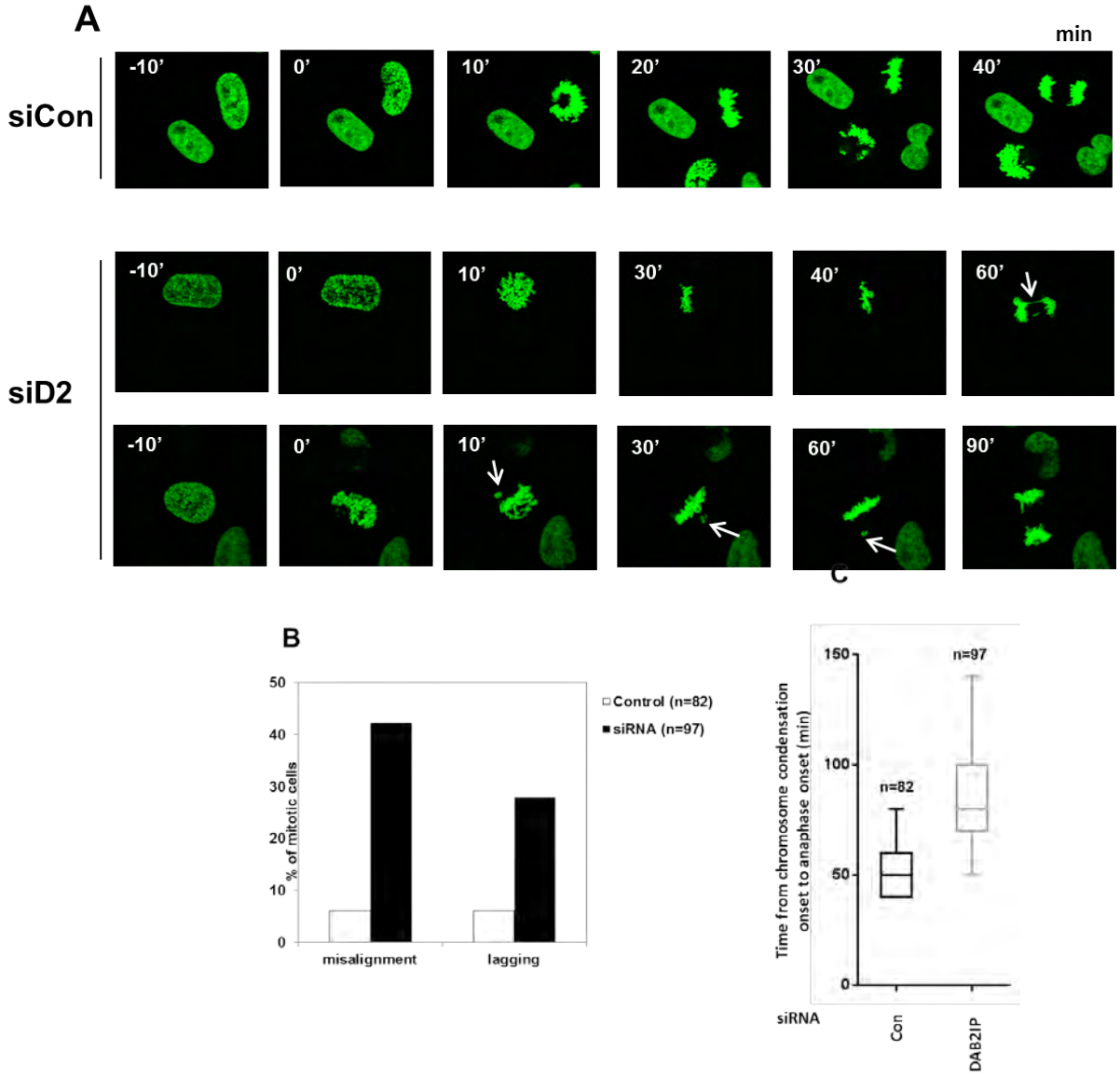

Figure 9: Depletion of DAB2IP leads to chromosome misalignment and chromosome missegregation. **A,** HeLa-H2B-GFP cells transfected with control or DAB2IP siRNA were monitored by time-lapse confocal microscopy. Live images were taken every 10 minutes with X60 objective. Representative images of the chromosome condensation-to-anaphase transition are shown 48 hours after siRNA transfection. **B,** mitotic cells with misaligned and lagging chromosomes was quantified. **C,** the durations of the chromosome condensation-to-anaphase transitions were determined.

Reportable outcomes:

1. A manuscript entitled "Pretreatment Biopsy Analysis of DAB2IP Identifies Subpopulation of High-Risk Prostate Cancer Patients with Worse Survival Following Radiation Therapy" Jacobs et al has been accepted in the Journal of Cancer Medicine. The accepted manuscript attached.

2. A manuscript entitled "Tumor Suppressor Protein DAB2IP Participates in Spindle Assembly Checkpoint and Maintains Chromosomal Stability" by Lan Yu et al is currently under review and the submitted version is attached.

3. Debabrata Saha (PI) presented a poster on "Tumor Suppressor Protein DAB2IP Participates in Spindle Assembly Checkpoint and Maintains Chromosomal Stability" at the radiation Biology Meeting in Wolfsberg, Switzerland on June 20 -22, 2015

Conclusion:

This is the final report of this project. We have discovered a novel role of the DABIP protein in the progression of Prostate Cancer. Our retrospective clinical studies clearly demonstrated that men with high risk prostate cancer have decreased tumor expression of DAB2IP and showed a poor outcome of definitive radiation therapy. Our current findings also reveal a novel activity of DAB2IP in modulating the spindle assembly checkpoint (SAC) which is essential for maintaining chromosomal stability that is often lost in cancer cells. For the last 4 years of we have made significant progress in the area of prostate cancer research and achieved a high level of scientific excellence. We have published 5 articles and 1 is currently under review and another one will be submitted by the end of October, 2015. We sincerely thank the Department of defense to provide us the wonderful opportunity to conduct this research which opens up a completely new area in the field of Prostate cancer research.

References: References are included in the attached manuscript.

Appendices:

Following 3 documents are attached:

1. A manuscript entitled “Pretreatment Biopsy Analysis of DAB2IP Identifies Subpopulation of High-Risk Prostate Cancer Patients with Worse Survival Following Radiation Therapy” Jacobs et al has been accepted in the Journal of Cancer Medicine. The accepted manuscript attached.

2. A manuscript entitled “Tumor Suppressor Protein DAB2IP Participates in Spindle Assembly Checkpoint and Maintains Chromosomal Stability” by Lan Yu et al is currently under review and the submitted version is attached.

3. Debabrata Saha (PI) presented a poster on “Tumor Suppressor Protein DAB2IP Participates in Spindle Assembly Checkpoint and Maintains Chromosomal Stability” at the radiation Biology Meeting in Wolfsberg, Switzerland on June 20 -22, 2015

Cancer Medicine Open Access

Pretreatment Biopsy Analysis of DAB2IP Identifies Subpopulation of High-Risk Prostate Cancer Patients with Worse Survival Following Radiation Therapy

Journal:	*Cancer Medicine*
Manuscript ID:	CAM4-2015-07-0202.R2
Wiley - Manuscript type:	Original Research
Search Terms:	biomarkers, survival, prostate cancer, translational research

Abstract:

Objective: Decreased expression of tumor suppressor DAB2IP is linked to aggressive cancer and radiation resistance in several malignancies, but clinical survival data is largely unknown. We hypothesized that pretreatment DAB2IP reduction would predict worse prostate cancer-specific survival (PCSS).

Methods: Immunohistochemistry of pretreatment biopsies was scored by an expert genitourinary pathologist. Other endpoints analyzed include freedom from biochemical failure (FFBF), castration resistance-free survival (CRFS), and distant metastasis-free survival (DMFS).

Results: Seventy-nine patients with NCCN-defined high-risk prostate cancer treated with radiotherapy from 2005-2012 at our institution were evaluated. Twenty-eight percent (22/79) of pretreatment biopsies revealed DAB2IP-reduction. The median follow up times were 4.8 years and 5.3 years for patients in the DAB2IP-reduced group and DAB2IP-retained group, respectively. Patients with reduced DAB2IP demonstrated worse outcome compared to patients retaining DAB2IP, including FFBF (4-year: 34% vs. 92%; $p<0.0001$), CRFS (4-year: 58% vs. 96%; $p=0.0039$), DMFS (4-year: 58% vs. 100%; $p=0.0006$), and PCSS (5-year: 83% vs. 100%; $p=0.0102$). Univariate analysis showed T stage, N stage, and Gleason score were statistically significant variables. Pretreatment tumor DAB2IP status remained significant in multivariable analyses.

Conclusion: This study suggests that about one-fourth of men with high-risk prostate cancer have decreased tumor expression of DAB2IP. This subpopulation with reduced DAB2IP has a suboptimal response and worse malignancy-specific survival following radiation therapy and androgen deprivation. DAB2IP loss may be a genetic explanation for the observed differences in aggressive tumor characteristics and radiation resistance. Further study into improving treatment response and survival in this subpopulation is warranted.

Reviewers' comments:

Reviewer: 1

The revised manuscript is improved now. the authors responded each comments from reviewers.

Reviewer: 2

This study reported that reduced DAB2IP was associated with poor prognosis of prostate cancer based on 79 patients after radiation therapy and androgen deprivation. The findings are attractive and the authors have answered the reviewers' comments. I have several other comments as follows:

1. The information in Table 2, 3 and 4 were not enough. I suggest the authors reorganize these tables and include the numbers, median times, HRs and 95CI%s as well as P values in these Tables. The statistical method should be noted in these Tables.
2. In Table 4, stepwise regression analysis is not suggested. In stead, DAB2IP expression levels should be treated as the main risk factor and the other known factors including stage, gleason score, and treatment are included in the multivariate regression model as covariables.
3. The kaplan meier curve for overall survival is also informative and should be provided.

Reviewer 1 did not have any additional negative comments to address. We have responded to Reviewer 2's comments in the following point-by-point fashion:

1. Reviewer 2 suggests that we note the statistical method used in Tables 2, 3, and 4. We do this on page 7 in our method's section where we state that Kaplan-Meier estimates and log-rank tests were computed to estimate the FFBF, CRFS, DMFS, PCSS, and OS. Therefore, the data in Table 2 and Table 3 were calculated using log-rank. As stated below in point #2, the information in Table 4 was obtained by Cox regression. We have added the statistical method used to the legends of Tables 2, 3, and 4 on page 17 to make it more clear.

Review 2 also suggested that we include additional information such as the hazard ratios and 95% confidence intervals in addition to the P values. However, "because the logrank test is purely a test of significance it cannot provide an estimate of the size of the difference between the groups or a confidence interval" (Bland, JM and Altman, DG. "The logrank test." *BMJ*. 2004 May 1; 328(7447): 1073). Therefore, we are unable to add this information to the tables of interest. One way we are able to accommodate this reviewer's suggestion with the statistical results on hand is by adding hazard ratios to Table 4 since this table was calculated using Cox regression. We have added this information and uploaded the new tables.

2. The reviewer is correct that stepwise regression analysis was not performed in Table 4. In the method's section of the manuscript on page 7 we clearly state that we performed univariate Cox regression (not stepwise) to identify significant clinical risk factors that could be significantly associated with each endpoint, and that afterwards multivariate analysis using a backward model selection was conducted for each factor that met the inclusion criterion $p<0.15$ by univariate analysis. The wording of these statistical methods was approved by our expert statistician who calculated the statistics and confirmed their accuracy.

3. The Kaplan-Meier curve for overall survival has been added and is labeled Figure 1E on page 17.

Abstract

Objective: Decreased expression of tumor suppressor DAB2IP is linked to aggressive cancer and radiation resistance in several malignancies, but clinical survival data is largely unknown. We hypothesized that pretreatment DAB2IP reduction would predict worse prostate cancer-specific survival (PCSS).

Methods: Immunohistochemistry of pretreatment biopsies was scored by an expert genitourinary pathologist. Other endpoints analyzed include freedom from biochemical failure (FFBF), castration resistance-free survival (CRFS), and distant metastasis-free survival (DMFS).

Results: Seventy-nine patients with NCCN-defined high-risk prostate cancer treated with radiotherapy from 2005-2012 at our institution were evaluated. Twenty-eight percent (22/79) of pretreatment biopsies revealed DAB2IP-reduction. The median follow up times were 4.8 years and 5.3 years for patients in the DAB2IP-reduced group and DAB2IP-retained group, respectively. Patients with reduced DAB2IP demonstrated worse outcome compared to patients retaining DAB2IP, including FFBF (4-year: 34% vs. 92%; $p<0.0001$), CRFS (4-year: 58% vs. 96%; $p=0.0039$), DMFS (4-year: 58% vs. 100%; $p=0.0006$), and PCSS (5-year: 83% vs. 100%; $p=0.0102$). Univariate analysis showed T stage, N stage, and Gleason score were statistically significant variables. Pretreatment tumor DAB2IP status remained significant in multivariable analyses.

Conclusion: This study suggests that about one-fourth of men with high-risk prostate cancer have decreased tumor expression of DAB2IP. This subpopulation with reduced DAB2IP has a suboptimal response and worse malignancy-specific survival following radiation therapy and androgen deprivation. DAB2IP loss may be a genetic explanation for the observed differences in

aggressive tumor characteristics and radiation resistance. Further study into improving treatment response and survival in this subpopulation is warranted.

Introduction

Prostate cancer is the most common male malignancy and the second leading cause of cancer-related death in the United States with 220,800 cases and 27,540 deaths expected in 2015[1], of which 20-30% have high-risk features[2]. For high-risk prostate cancer defined by the National Comprehensive Cancer Network (NCCN) as Stage ≥ cT3a, Gleason score ≥ 8, or prostate-specific antigen (PSA) ≥ 20, standard treatment guidelines include definitive radiation therapy with neo-adjuvant, concurrent, and long-term androgen deprivation therapy in the United States[3]. In spite of standard therapy, long-term outcomes are suboptimal with 5-year biochemical progression-free survival of 60-70% and 5-year overall survival of 75-85%[4-7]. Synthesizing all this data, one in four to five men with prostate cancer is diagnosed with high-risk disease and despite treatment for their locally advanced malignancy, roughly 30-40% of these men suffer a relapse which accounts for most prostate cancer deaths.

Being able to predict the patients that portend worse outcome at the time of diagnosis may provide means to offer patients an alternative, more effective therapy. Biomarkers that can readily identify patients most likely to fail conventional therapy is warranted, and investigations of the molecular pathway involved in this poor outcome may further lead to future therapeutic interventions. One such potential biomarker is DOC-2/DAB2 interactive protein (DAB2IP).

DAB2IP, a member of the RAS-GAP protein family, is a novel and putative tumor suppressor. DAB2IP protein is a potent growth inhibitor by inducing G(0)/G(1) cell cycle arrest and is proapoptotic in response to stress[8]. Decreased expression of DAB2IP has been associated

with aggressive prostate cancer and radiation resistance in cell culture models[9-11], rats[12], and human tumors[13, 14]. The mechanism underlying radiation resistance of DAB2IP-deficient tumors can be explained by elevated ATM expression and activation, increased S phase cell distribution, accelerated DNA double-strand break repair kinetics, evasion of apoptosis, and increased autophagy following ionizing radiation[9-11, 15]. Loss of DAB2IP expression initiates epithelial-to-mesenchymal transition which leads to multiple lymph node and distant organ metastases[16]. Other than radiation resistance, loss of DAB2IP may promote castration resistance[14]. This is because one of DAB2IP's functions is to inhibit androgen receptor-mediated cell growth and gene activation in prostate cells via both androgen-dependent and androgen-independent mechanisms[17].

Decreased expression of DAB2IP is often detected in aggressive prostate cancer cells, and this loss of DAB2IP is primarily due to altered epigenetic regulation of its promoter particularly by histone acetylation[18-20]. *DAB2IP* promoter methylation is frequently present in human breast cancer as well which plays a key role in DAB2IP inactivation and lymph node metastasis[21]. Other than breast and prostate cancer, decreased DAB2IP expression by promoter methylation has been identified in several other malignancies including hepatocellular carcinoma[22], lung cancer[23], and gastrointestinal tumors[24]. Another recently identified mechanism leading to the loss of DAB2IP protein is proteasome degradation mediated by oncogenic S-phase kinase-associated protein-2 (Skp2)[25].

DAB2IP is also down-regulated in bladder cancer with aggressive phenotypes[26]. DAB2IP-knockdown of bladder cancer cells by siRNA exhibit increased clonogenic survival in response to ionizing radiation compared with control cells expressing an endogenous level of DAB2IP[15]. The radiation resistance of DAB2IP deficient bladder cancer translates into worse

cancer-specific survival[27]. Furthermore, low levels of DAB2IP were detected in a hepatocellular carcinoma subclass from patients with poor survival[28]. Taken together, these studies suggest that loss of DAB2IP may portend worse survival in multiple different malignancies.

Enhancer of Zeste homolog 2 (EZH2), a histone lysine methyltransferase, suppresses DAB2IP gene expression by recruiting both polycomb repressor complex and histone deacetylase 1 to the *DAB2IP* promoter region[29]. Overexpression of EZH2 has been shown to drive prostate cancer progression, and studies have shown that clinically localized tumors that express high levels of EZH2 have worse outcome[30, 31].

Our pilot study, which analyzed 46 men's diagnostic prostate biopsies for DAB2IP expression and had short follow up, showed that decreased DAB2IP tumor expression correlated with worse clinical outcome in the high-risk population[14]. This same pilot study also analyzed 48 biopsy specimens for EZH2 expression. While increasing expression of EZH2 trended toward worse outcome it was not statistically significant in our high-risk cohort. This current study attempted to answer our hypothesis that with longer follow up and increased sample size, pretreatment tumor status of DAB2IP would ultimately predict worse prostate cancer-specific survival (PCSS).

Material and Methods

Patient selection

All patients with prostate cancer treated with external beam radiation at the University of Texas Southwestern Medical Center between December 2005 and July 2012 were identified. Of the 658 patients identified, 138 patients met the NCCN guidelines for high-risk classification (Stage ≥ T3a, or Gleason score ≥ 8, or PSA ≥ 20) and did not receive any surgical management.

Patients with metastases prior to initial radiation therapy (i.e. M1 stage disease) were excluded from the study. All patients were treated definitively with external beam radiotherapy using a variety of techniques, including dynamic arc therapy and intensity modulated radiation therapy (IMRT). All patients were treated with a prostate prescription dose exceeding 72 Gy. Patient data was coded into a secured database according to our institution review board approved study protocol.

Of the patients identified, only those patients who had preserved pretreatment prostate biopsy tissue available and whose biopsies had a sufficient tumor sample available for analysis were included in the study. Each patient in this study underwent transrectal ultrasound guided prostate biopsy and the total number of cores obtained ranged from 4-33 with 12 being the most common number of cores obtained (n=54). Based on the pathology report, the core with the highest Gleason score was chosen for immunohistochemistry staining. If multiple cores tied for the highest Gleason score, then the core with the highest percentage of neoplastic cells that still had benign normal prostate tissue (i.e. not 100% neoplastic cells) was chosen.

Specimen characteristics, staining, and quantification

Diagnostic needle biopsies were mounted in paraffin, and 3-4 μm sections were prepared for standard hematoxylin and eosin staining. Standard immunohistochemistry analysis was performed for DAP2IP and EZH2. Immunostaining was performed using the Benchmark XT automated stainer (Ventana, Tuscan, AZ, USA). Briefly, formalin-fixed, paraffin-embedded tissue microarray sections were cut at 3-4 μm and air-dried overnight. The sections were de-paraffinized, rehydrated, subjected to heat-induced epitope retrieval, and then incubated with anti-EZH2 (clone:SP129, Ventana, prediluted) or anti-DAB2IP[32] (homegrown, 1:150) primary

antibodies. UltraView universal detection system (Ventana) was used for signal detection. The slides were developed using 3-3'-diaminobenzidine chromogen and counterstained with hematoxylin. Specific positive and negative (slides incubated without primary antibody) controls were utilized for each run of immunostains and checked for validation of the assay. Controls for anti-EZH2 antibody included tissue from prostate and breast adenocarcinoma and normal lymph node that are known to have high EZH2 expression. Anti-EZH2 protocol was standardized according to the directions in the package insert. This antibody is intended for *in vitro* diagnostic use. Protocol for anti-DAP2IP was performed as published previously[32].

Tumor and benign prostate tissue stained with each marker were evaluated by an experienced genitourinary pathologist who was blinded to patient clinical information. Each case was evaluated for the extent (percentage of positive cells) and intensity of staining. The average intensity of positive tumor cells was given a grade (G) score: G0, none; G1, weak; G2, intermediate; and G3, strong. DAB2IP positivity was evaluated as cytoplasmic expression. EZH2 was evaluated as nuclear pattern of expression. Compared to DAB2IP expression in the benign 'control' prostate tissue surrounding the neoplastic cells, tumor DAB2IP status was categorized as retained (same or stronger expression) or reduced (weaker expression). EZH2 expression was scored as the intensity of staining, G0-G3.

Study design

The five clinical endpoints in this study were freedom from biochemical failure (FFBF), castration resistance-free survival (CRFS), distant metastasis-free survival (DMFS), overall survival (OS), and prostate cancer-specific survival (PCSS). FFBF was determined using the Phoenix definition, which denotes a PSA increase of $\geq$ 2.0 ng/mL above the nadir PSA level.[33]

CRFS was defined as ≥ 2 episodes of rising PSA while on standard hormone therapy in the setting of testosterone levels < 50 ng/ml, or if patients were started on second line therapy as first line hormone therapy was deemed to have failed at the clinical oncologist's discretion. DMFS was determined from clinical chart review documenting date of known metastasis by imaging. PCSS was defined as death due to prostate cancer, radiation toxicity, or unknown cause with distant metastasis or castration resistance. Time to each endpoint was calculated from the first day of radiation therapy.

Statistical analysis

Kaplan-Meier estimates and log-rank tests were computed to estimate the FFBF, CRFS, DMFS, PCSS, and OS. Univariate Cox regression analyses were conducted to identify significant clinical risk factors that could be significantly associated with each endpoint, including T stage, N stage, Gleason score, pretreatment PSA, total radiation dose, hormone therapy, and duration of hormone therapy. Fisher's exact test was used to evaluate statistical differences among these factors based on the status of the tumor biomarker. Finally, multivariate analysis using a backward model selection was conducted for each factor that met the inclusion criterion $p<0.15$ by univariate analysis.

Results

DAB2IP results

Seventy-nine patients with high-risk prostate cancer treated with definitive radiation therapy from 2005-2012 met the inclusion criteria and were evaluated. Twenty-eight percent (22/79) of patients revealed DAB2IP-reduction while 72% (57/79) retained DAB2IP. The

median follow up times were 4.8 years and 5.3 years for patients in the DAB2IP-reduced group and DAB2IP-retained group, respectively. Statistical differences of clinicopathological factors include more advanced T stage (p=0.0149), higher pretreatment PSA (p=0.0379), and more aggressive Gleason score (p=0.0048) all within the DAB2IP-reduced group. There were no significant differences in patient age at diagnosis, N stage, total radiation dose, hormone therapy, or duration of hormone therapy received (see Table 1).

Pretreatment tumor reduction of DAB2IP as evidenced by prostate biopsy samples correlated strongly with worse outcome in every endpoint measured except death from any cause (see Table 2). Reduced DAB2IP portended a significantly worse FFBF (p<0.0001), CRFS (p=0.0039), DMFS (p=0.0006), and PCSS (p=0.0102). Kaplan-Meier estimates of these four significant endpoints can be seen in Figure 1. By four years post-radiotherapy, the biochemical failure rate was a staggering 66% in the DAB2IP-reduced group compared to only 8% in the DAB2IP-retained group at that point. By five years post-radiotherapy, the prostate cancer-specific mortality rate was 17% in the DAB2IP-reduced group whereas no one in the DAB2IP-retained group had died due to their malignancy.

Sixteen of the 79 high-risk patients in the DAB2IP cohort had met the criteria for castration resistance. Thirteen of these patients had testosterone data available to confirm that the PSA continued to rise despite a testosterone level <50 ng/ml. The median testosterone level for these 13 patients was 3 ng/ml and the levels ranged from undetectable to 32 ng/ml. The remaining 3 patients were determined to have clinically become castration resistant because of a rising PSA despite adding a second agent to their androgen deprivation therapy.

EZH2 results

Ninety-seven patients with high-risk prostate cancer treated with definitive radiation therapy from 2005-2012 met the inclusion criteria and were evaluated. Ninety-eight percent (95/97) of patients expressed EZH2 as follows: 2% (2/97) were G0, 10% (10/95) were G1, 68% (66/97) were G2, and 20% (19/97) were G3. The median time to follow up was 4.6 years in the EZH2 cohort. Stratified EZH2 expression was not statistically significant for any outcome (see Table 3).

Nine patients in the EZH2 study elected to not receive hormone therapy. Of these, one patient did not express EZH2, one patient had G1 expression, and the remaining seven patients all had G2 expression. Importantly, none of these nine patients died from any cause let alone from their malignancy. Furthermore, even though every patient with the highest expression of EZH2 (G3) received androgen deprivation, these patients demonstrated the worst outcomes at four years for FFBF, CRFS, and DMFS.

Univariate and multivariate analysis

Univariate analysis using Cox regression of typical prognostic variables revealed that only T stage, N stage, and Gleason score correlated with outcome. Higher T stages were significantly associated with worse FFBF ($p=0.0477$), CRFS ($p=0.0379$), DMFS ($p=0.0082$), and PCSS ($p=0.0105$). N1 stage was significantly associated with worse FFBF ($p=0.0003$), CRFS ($p=0.0132$), and DMFS ($p<0.0001$) but not PCSS ($p=0.2782$). Higher Gleason scores were significantly associated with worse FFBF ($p=0.0007$), CRFS ($p=0.0043$), DMFS ($p=0.0083$), and PCSS ($p=0.0031$). None of the prognostic variables were significantly associated with OS.

Table 4 shows all variables that were significant for each outcome after multivariable analysis. Pretreatment tumor DAB2IP status remained significant in the multivariable analysis

for FFBF (p=0.0026), CRFS (p=0.0043), and DMFS (p=0.0009). The two other significant variables on multivariable analysis include Gleason score (FFBF p=0.0428; CRFS p=0.0409; DMFS p=0.0174) and T stage (DMFS p=0.0252). Multivariate analysis could not be conducted for PCSS because zero patients had died due to prostate cancer in the subgroups of retained-DAB2IP, T1c-T2b stages, N0 stage, or Gleason scores 6-8. Interestingly, not only was DAB2IP significant for each measureable outcome after multivariable analysis, but it was always the most highly significant variable.

Discussion

DAB2IP is a putative tumor suppressor and member of the RAS-GAP family. Decreased expression of the protein DAB2IP is associated with aggressive disease[13, 14] and radiation resistance[9, 15, 34, 35]. Down-regulation of DAB2IP has mostly been attributed to epigenetic regulation involving methylation of the promoter region mediated by EZH2[18-20], though Skp2-mediated proteasome degradation[25] and genetic variants (i.e. mutations)[13, 36, 37] may also play a role. Decreased DAB2IP has been identified in several cancers other than prostate, including breast[21, 38], hepatocellular[22, 28], lung[23], gastrointestinal[24], and bladder[15, 26].

Based on strong preclinical data indicating the role of DAB2IP in radiation response in prostate cancer cells, we performed a pilot study to determine its clinical importance[14]. Our prior pilot study analyzed 46 men's diagnostic prostate biopsies with high-risk disease for DAB2IP expression and showed a strong correlation between pretreatment tumor DAB2IP reduction and worse clinical outcome with only 2.7 years of median follow up. With longer follow up and increased sample size, we hypothesized that pretreatment tumor status of DAB2IP would also predict worse malignancy-specific survival (PCSS). In addition to studying DAB2IP, we also

sought to determine the potential prognostic role of its upstream regulator, EZH2, after increasing the sample size and follow up time.

In this study we show that pretreatment tumor DAB2IP status and not EZH2 correlates with worse rates of biochemical failure, castration resistance, and distant metastasis after the standard of care treatment for these high-risk prostate cancer patients including definitive radiation therapy and androgen deprivation. Additionally, our results confirmed our hypothesis that DAB2IP reduction ultimately leads to significantly increased mortality due to prostate cancer. Five of the six patients (83%) in this study that died due to their malignancy had an initial Eastern Cooperative Oncology Group (ECOG) score of 0 and therefore performance status did not confound our results. Based on the numerical data included in the opening introductory paragraph of this manuscript and our observation that about one-fourth of high-risk prostate cancer patients have decreased expression of DAB2IP, we estimate that between 12,000 and 18,000 men treated annually in the United States have suboptimal response to the current standard of care treatment.

Another important finding from this study is that the tumors with reduced DAB2IP expression were statistically more likely to have a more advanced T stage, higher pretreatment PSA, and more aggressive Gleason score. Whether down-regulation of DAB2IP is the molecular cause of these more aggressive clinicopathologic findings or whether the decreased DAB2IP expression selectively occurs in aggressive tumors remains unclear.

Nearly all high-risk prostate cancer samples in this study expressed EZH2. Rather than predict cancers with poor therapeutic response, EZH2 levels may help screen for higher risk cancers. Nevertheless, it's interesting to note that tumors with the highest expression of EZH2 (G3) demonstrated the worst outcomes at four years for FFBF, CRFS, and DMFS, which is

congruent with the idea that increased EZH2 leads to methylation of the *DAB2IP* promotor and reduction in DAB2IP expression. Since regulation of DAB2IP expression is not the sole function of EZH2, it makes sense that it would not be as potent of a prognostic biomarker compared to DAB2IP which modulates different signal cascades associated with cell proliferation, survival, apoptosis, and metastasis.

Based on the results presented herein, DAB2IP may be able to differentiate the worst cases amongst the already high-risk group of prostate cancer patients that are at greatest risk for treatment failure prior to initiation of standard therapy. Potential clinical application is that in the future we may be able to effectively use tumor DAB2IP expression from a patient's biopsy specimen as a means of determining curability of their cancer with standard radiation-based therapeutic regimens.

Future research may be directed toward creating molecularly-based therapeutic strategies to upregulate DAB2IP and restore the tumor suppressor's presence within the neoplastic cells or by targeting downstream effectors. DNA methyltransferase inhibitors as well as histone deacetylase inhibitors can both induce expression of the *DAB2IP* gene[19, 20]. Cytolethal distending toxin (CTD) from Campylobacter jejuni significantly elicited cell death in DAB2IP-deficient prostate cancer cells when combined with radiotherapy[39]. Restoring DAB2IP may also improve castration resistance in addition to radiation resistance as DAB2IP expression inversely correlates with androgen receptor activation status particularly in recurrent or metastatic prostate cancer patients[17].

The DAB2IP pathway is an important potential target for improving the treatment of multiple malignancies (not just prostate cancer) and enhancing multiple modalities (not just radiation therapy). For example, KU55933 which suppresses ATM phosphorylation upon

irradiation could be applied in the radiotherapy of bladder cancer patients with a DAB2IP gene defect[15]. Furthermore, other than improving radiation responsiveness, targeting the DAB2IP pathway may also improve response to chemotherapy[35]. Inhibiting EZH2 through siRNA has been shown to increase DAB2IP expression[29] and reverse chemoresistance[40]. Improving chemotherapy response could improve survival in this population as patients with reduced DAB2IP in bladder cancer treated with surgery and adjuvant chemotherapy had worse cancer-specific survival[26].

One limitation of this study includes the way in which tumor DAB2IP status is characterized as reduced or retained. We were not able to identify a specific intensity level threshold below which DAB2IP should be considered reduced, especially since some samples stained better than others with the antibody. Instead, we compared the tumor staining with the surrounding normal prostate tissue as the control to know whether the tumor retained normal DAB2IP expression or reduced the protein's expression. The limitation of this definition comes when the entire stained sample is tumor and there are no benign glands with which to compare, or when there are very few glands with which to compare and they are all atrophic with high DAB2IP expression. Perhaps this problem could be avoided via a prospective study using fresh tissue and not relying on a retrospective study with tissues at varying ages.

Another limitation of this study is not having a separate cohort of patients that received a non-radiation intervention such as prostatectomy with which to compare. At this point we do not definitively know whether DAB2IP reduction is a poor prognostic indicator regardless of the intervention, or if it really is a marker of radiation resistance. Additionally, since the tissue specimens were obtained from biopsy, there is a clear limitation of potential heterogeneity of pathological findings and the immunostaining not always reflecting the characteristics of all

cancer foci in each patient. Also, even though we were able to increase the sample size by over 70% from our prior study and obtain over 2 more years of additional follow up data, the sample size and follow up time remain limitations. DAB2IP requires further studies to validate its role in this cohort of patients and to further determine whether it may also be a predictive marker of response to radiation therapy.

In conclusion, based on our results about one-fourth of men with high-risk prostate cancer and well over 10,000 men in the United States annually may have reduced tumor expression of DAB2IP which makes their tumors more radioresistant and aggressive. This subpopulation with reduced DAB2IP has a suboptimal response and significantly higher prostate cancer-specific mortality despite standard of care treatment with radiation therapy and androgen deprivation. Targeting the DAB2IP pathway may be a promising area for future drug development to improve the effectiveness of radiation and chemotherapy in multiple malignancies. Further study into improving the radiation response and survival in this subpopulation is warranted.

References

1. Siegel RL, et al. Cancer statistics, 2015. *CA: A Cancer Journal for Clinicians* 2015; **65**(1): 5-29.
2. Punnen S, et al. The epidemiology of high-risk prostate cancer. *Current Opinion in Urology* 2013; **23**(4): 331-6.
3. Mohler JL. The 2010 NCCN Clinical Practice Guidelines in Oncology on Prostate Cancer. *Journal of the National Comprehensive Cancer Network* 2010; **8**(2): 145.
4. Horwitz EM, et al. Ten-year follow-up of radiation therapy oncology group protocol 92-02: a phase III trial of the duration of elective androgen deprivation in locally advanced prostate cancer. *J Clin Oncol* 2008; **26**(15): 2497-504.
5. Bolla M, et al. Duration of androgen suppression in the treatment of prostate cancer. *N Engl J Med* 2009; **360**(24): 2516-27.
6. Bolla M, et al. External irradiation with or without long-term androgen suppression for prostate cancer with high metastatic risk: 10-year results of an EORTC randomised study. *Lancet Oncol* 2010; **11**(11): 1066-73.

7. Hanks GE, et al. Phase III trial of long-term adjuvant androgen deprivation after neoadjuvant hormonal cytoreduction and radiotherapy in locally advanced carcinoma of the prostate: the Radiation Therapy Oncology Group Protocol 92-02. *J Clin Oncol* 2003; **21**(21): 3972-8.
8. Xie D, et al. DAB2IP coordinates both PI3K-Akt and ASK1 pathways for cell survival and apoptosis. *Proceedings of the National Academy of Sciences* 2009; **106**(47): 19878-83.
9. Kong Z, et al. Downregulation of human DAB2IP gene expression in prostate cancer cells results in resistance to ionizing radiation. *Cancer research* 2010; **70**(7): 2829-39.
10. Xie D, et al. DAB2IP coordinates both PI3K-Akt and ASK1 pathways for cell survival and apoptosis. *Proceedings of the National Academy of Sciences of the United States of America* 2009; **106**(47): 19878-83.
11. Yu L, et al. DAB2IP regulates autophagy in prostate cancer in response to combined treatment of radiation and a DNA-PKcs inhibitor. *Neoplasia* 2012; **14**(12): 1203-12.
12. Tumati V, et al. Development of a locally advanced orthotopic prostate tumor model in rats for assessment of combined modality therapy. *International Journal of Oncology* 2013; **42**(5): 1613-9.
13. Duggan D, et al. Two genome-wide association studies of aggressive prostate cancer implicate putative prostate tumor suppressor gene DAB2IP. *Journal of the National Cancer Institute* 2007; **99**(24): 1836-44.
14. Jacobs C, et al. DOC-2/DAB2 Interacting Protein Status in High-Risk Prostate Cancer Correlates With Outcome for Patients Treated With Radiation Therapy. *International Journal of Radiation Oncology*Biology*Physics* 2014; **89**(4): 729-35.
15. Zhang T, et al. The ATM inhibitor KU55933 sensitizes radioresistant bladder cancer cells with DAB2IP gene defect. *International Journal of Radiation Biology* 2015; **91**(4): 368-78.
16. Xie D, et al. Role of DAB2IP in modulating epithelial-to-mesenchymal transition and prostate cancer metastasis. *Proceedings of the National Academy of Sciences* 2010; **107**(6): 2485-90.
17. Wu K, et al. The role of DAB2IP in androgen receptor activation during prostate cancer progression. *Oncogene* 2014; **33**(15): 1954-63.
18. Chen H, et al. Epigenetic regulation of a novel tumor suppressor gene (hDAB2IP) in prostate cancer cell lines. *The Journal of biological chemistry* 2003; **278**(5): 3121-30.
19. Chen H, et al. Differential Regulation of the Human Gene DAB2IP in Normal and Malignant Prostatic Epithelia: Cloning and Characterization. *Genomics* 2002; **79**(4): 573-81.
20. Chen H, et al. Epigenetic Regulation of a Novel Tumor Suppressor Gene (hDAB2IP) in Prostate Cancer Cell Lines. *Journal of Biological Chemistry* 2003; **278**(5): 3121-30.
21. Dote H, et al. Aberrant Promoter Methylation in Human DAB2 Interactive Protein (hDAB2IP) Gene in Breast Cancer. *Clinical Cancer Research* 2004; **10**(6): 2082-9.
22. Qiu G-H, et al. Differential expression of hDAB2IPA and hDAB2IPB in normal tissues and promoter methylation of hDAB2IPA in hepatocellular carcinoma. *Journal of Hepatology* 2007; **46**(4): 655-63.
23. Yano M, et al. Aberrant promoter methylation of human DAB2 interactive protein (hDAB2IP) gene in lung cancers. *International Journal of Cancer* 2005; **113**(1): 59-66.
24. Dote H, et al. Aberrant promoter methylation in human DAB2 interactive protein (hDAB2IP) gene in gastrointestinal tumour. *Br J Cancer* 2005; **92**(6): 1117-25.
25. Tsai Y-S, et al. The role of homeostatic regulation between tumor suppressor DAB2IP and oncogenic Skp2 in prostate cancer growth; 2014.
26. Shen Y-J, et al. Downregulation of DAB2IP results in cell proliferation and invasion and contributes to unfavorable outcomes in bladder cancer. *Cancer Science* 2014; **105**(6): 704-12.
27. Zhu JN, et al. DAB2IP expression in bladder transitional cell carcinoma and its correlation with clinical outcome. *Journal of Sichuan University Medical science edition* 2014; **45**(4): 591-4.

28. Calvisi DF, et al. Inactivation of Ras GTPase-activating proteins promotes unrestrained activity of wild-type Ras in human liver cancer. *Journal of Hepatology* 2011; **54**(2): 311-9.
29. Chen H, et al. Down-regulation of human DAB2IP gene expression mediated by polycomb Ezh2 complex and histone deacetylase in prostate cancer. *The Journal of biological chemistry* 2005; **280**(23): 22437-44.
30. Rhodes DR, et al. Multiplex biomarker approach for determining risk of prostate-specific antigen-defined recurrence of prostate cancer. *Journal of the National Cancer Institute* 2003; **95**(9): 661-8.
31. Varambally S, et al. The polycomb group protein EZH2 is involved in progression of prostate cancer. *Nature* 2002; **419**(6907): 624-9.
32. Wang Z, et al. The Mechanism of Growth-inhibitory Effect of DOC-2/DAB2 in Prostate Cancer: CHARACTERIZATION OF A NOVEL GTPase-ACTIVATING PROTEIN ASSOCIATED WITH N-TERMINAL DOMAIN OF DOC-2/DAB2. *Journal of Biological Chemistry* 2002; **277**(15): 12622-31.
33. Roach M, et al. Defining biochemical failure following radiotherapy with or without hormonal therapy in men with clinically localized prostate cancer: Recommendations of the RTOG-ASTRO Phoenix Consensus Conference. *International journal of radiation oncology, biology, physics* 2006; **65**(4): 965-74.
34. Kong Z, et al. Epothilone B confers radiation dose enhancement in DAB2IP gene knock-down radioresistant prostate cancer cells. *International journal of radiation oncology, biology, physics* 2010; **78**(4): 1210-8.
35. Wu K, et al. The Mechanism of DAB2IP in Chemoresistance of Prostate Cancer Cells. *Clinical Cancer Research* 2013; **19**(17): 4740-9.
36. Yang L, et al. A Common Genetic Variant (97906C>A) of DAB2IP/AIP1 Is Associated with an Increased Risk and Early Onset of Lung Cancer in Chinese Males. *PLoS ONE* 2011; **6**(10): e26944.
37. Xu S, et al. Association of the variant rs2243421 of human DOC-2/DAB2 interactive protein gene (hDAB2IP) with gastric cancer in the Chinese Han population. *Gene* 2013; **515**(1): 200-4.
38. Conway K, et al. DNA methylation profiling in the Carolina Breast Cancer Study defines cancer subclasses differing in clinicopathologic characteristics and survival. *Breast Cancer Research : BCR* 2014; **16**(5): 450.
39. Lai C-H, et al. Sensitization of radio-resistant prostate cancer cells with a unique cytolethal distending toxin. *Oncotarget* 2014; **5**(14): 5523-34.
40. W Z, et al. siRNA silencing EZH2 reverses cisplatin-resistance of human non-small cell lung and gastric cancer cells. *Asian Pacific Journal of Cancer Prevention* 2015; **16**(6): 2425-30.

Table and Figure Legends:

Table 1. Comparing clinicopathological factors based on tumor DAB2IP expression. PSA, prostate-specific antigen.

Table 2. Pretreatment tumor reduction of DAB2IP portends significantly worse outcome as calculated by log-rank. CRFS, castration resistance-free survival; DMFS, distant metastasis-free survival; FFBF, freedom from biochemical failure; PCSS, prostate cancer-specific survival.

Table 3. Stratified EZH2 expression was not statistically significant for any outcome as calculated by log-rank. CRFS, castration resistance-free survival; DMFS, distant metastasis-free survival; FFBF, freedom from biochemical failure; PCSS, prostate cancer-specific survival.

Table 4. Statistically significant variables on multivariate analysis by endpoint as calculated by Cox regression.

Figure 1. Kaplan Meier and log-rank analysis comparing (A) freedom from biochemical failure, (B) castration resistance-free survival, (C) distant metastasis-free survival, (D) prostate cancer-specific survival, and (E) overall survival based on pretreatment tumor DAB2IP status.

Abstract

Objective: Decreased expression of tumor suppressor DAB2IP is linked to aggressive cancer and radiation resistance in several malignancies, but clinical survival data is largely unknown. We hypothesized that pretreatment DAB2IP reduction would predict worse prostate cancer-specific survival (PCSS).

Methods: Immunohistochemistry of pretreatment biopsies was scored by an expert genitourinary pathologist. Other endpoints analyzed include freedom from biochemical failure (FFBF), castration resistance-free survival (CRFS), and distant metastasis-free survival (DMFS).

Results: Seventy-nine patients with NCCN-defined high-risk prostate cancer treated with radiotherapy from 2005-2012 at our institution were evaluated. Twenty-eight percent (22/79) of pretreatment biopsies revealed DAB2IP-reduction. The median follow up times were 4.8 years and 5.3 years for patients in the DAB2IP-reduced group and DAB2IP-retained group, respectively. Patients with reduced DAB2IP demonstrated worse outcome compared to patients retaining DAB2IP, including FFBF (4-year: 34% vs. 92%; $p<0.0001$), CRFS (4-year: 58% vs. 96%; $p=0.0039$), DMFS (4-year: 58% vs. 100%; $p=0.0006$), and PCSS (5-year: 83% vs. 100%; $p=0.0102$). Univariate analysis showed T stage, N stage, and Gleason score were statistically significant variables. Pretreatment tumor DAB2IP status remained significant in multivariable analyses.

Conclusion: This study suggests that about one-fourth of men with high-risk prostate cancer have decreased tumor expression of DAB2IP. This subpopulation with reduced DAB2IP has a suboptimal response and worse malignancy-specific survival following radiation therapy and androgen deprivation. DAB2IP loss may be a genetic explanation for the observed differences in

aggressive tumor characteristics and radiation resistance. Further study into improving treatment response and survival in this subpopulation is warranted.

Introduction

Prostate cancer is the most common male malignancy and the second leading cause of cancer-related death in the United States with 220,800 cases and 27,540 deaths expected in 2015[1], of which 20-30% have high-risk features[2]. For high-risk prostate cancer defined by the National Comprehensive Cancer Network (NCCN) as Stage ≥ cT3a, Gleason score ≥ 8, or prostate-specific antigen (PSA) ≥ 20, standard treatment guidelines include definitive radiation therapy with neo-adjuvant, concurrent, and long-term androgen deprivation therapy in the United States[3]. In spite of standard therapy, long-term outcomes are suboptimal with 5-year biochemical progression-free survival of 60-70% and 5-year overall survival of 75-85%[4-7]. Synthesizing all this data, one in four to five men with prostate cancer is diagnosed with high-risk disease and despite treatment for their locally advanced malignancy, roughly 30-40% of these men suffer a relapse which accounts for most prostate cancer deaths.

Being able to predict the patients that portend worse outcome at the time of diagnosis may provide means to offer patients an alternative, more effective therapy. Biomarkers that can readily identify patients most likely to fail conventional therapy is warranted, and investigations of the molecular pathway involved in this poor outcome may further lead to future therapeutic interventions. One such potential biomarker is DOC-2/DAB2 interactive protein (DAB2IP).

DAB2IP, a member of the RAS-GAP protein family, is a novel and putative tumor suppressor. DAB2IP protein is a potent growth inhibitor by inducing G(0)/G(1) cell cycle arrest and is proapoptotic in response to stress[8]. Decreased expression of DAB2IP has been associated

with aggressive prostate cancer and radiation resistance in cell culture models[9-11], rats[12], and human tumors[13, 14]. The mechanism underlying radiation resistance of DAB2IP-deficient tumors can be explained by elevated ATM expression and activation, increased S phase cell distribution, accelerated DNA double-strand break repair kinetics, evasion of apoptosis, and increased autophagy following ionizing radiation[9-11, 15]. Loss of DAB2IP expression initiates epithelial-to-mesenchymal transition which leads to multiple lymph node and distant organ metastases[16]. Other than radiation resistance, loss of DAB2IP may promote castration resistance[14]. This is because one of DAB2IP's functions is to inhibit androgen receptor-mediated cell growth and gene activation in prostate cells via both androgen-dependent and androgen-independent mechanisms[17].

Decreased expression of DAB2IP is often detected in aggressive prostate cancer cells, and this loss of DAB2IP is primarily due to altered epigenetic regulation of its promoter particularly by histone acetylation[18-20]. *DAB2IP* promoter methylation is frequently present in human breast cancer as well which plays a key role in DAB2IP inactivation and lymph node metastasis[21]. Other than breast and prostate cancer, decreased DAB2IP expression by promoter methylation has been identified in several other malignancies including hepatocellular carcinoma[22], lung cancer[23], and gastrointestinal tumors[24]. Another recently identified mechanism leading to the loss of DAB2IP protein is proteasome degradation mediated by oncogenic S-phase kinase-associated protein-2 (Skp2)[25].

DAB2IP is also down-regulated in bladder cancer with aggressive phenotypes[26]. DAB2IP-knockdown of bladder cancer cells by siRNA exhibit increased clonogenic survival in response to ionizing radiation compared with control cells expressing an endogenous level of DAB2IP[15]. The radiation resistance of DAB2IP deficient bladder cancer translates into worse

cancer-specific survival[27]. Furthermore, low levels of DAB2IP were detected in a hepatocellular carcinoma subclass from patients with poor survival[28]. Taken together, these studies suggest that loss of DAB2IP may portend worse survival in multiple different malignancies.

Enhancer of Zeste homolog 2 (EZH2), a histone lysine methyltransferase, suppresses DAB2IP gene expression by recruiting both polycomb repressor complex and histone deacetylase 1 to the *DAB2IP* promoter region[29]. Overexpression of EZH2 has been shown to drive prostate cancer progression, and studies have shown that clinically localized tumors that express high levels of EZH2 have worse outcome[30, 31].

Our pilot study, which analyzed 46 men's diagnostic prostate biopsies for DAB2IP expression and had short follow up, showed that decreased DAB2IP tumor expression correlated with worse clinical outcome in the high-risk population[14]. This same pilot study also analyzed 48 biopsy specimens for EZH2 expression. While increasing expression of EZH2 trended toward worse outcome it was not statistically significant in our high-risk cohort. This current study attempted to answer our hypothesis that with longer follow up and increased sample size, pretreatment tumor status of DAB2IP would ultimately predict worse prostate cancer-specific survival (PCSS).

Material and Methods

Patient selection

All patients with prostate cancer treated with external beam radiation at the University of Texas Southwestern Medical Center between December 2005 and July 2012 were identified. Of the 658 patients identified, 138 patients met the NCCN guidelines for high-risk classification (Stage ≥ T3a, or Gleason score ≥ 8, or PSA ≥ 20) and did not receive any surgical management.

Patients with metastases prior to initial radiation therapy (i.e. M1 stage disease) were excluded from the study. All patients were treated definitively with external beam radiotherapy using a variety of techniques, including dynamic arc therapy and intensity modulated radiation therapy (IMRT). All patients were treated with a prostate prescription dose exceeding 72 Gy. Patient data was coded into a secured database according to our institution review board approved study protocol.

Of the patients identified, only those patients who had preserved pretreatment prostate biopsy tissue available and whose biopsies had a sufficient tumor sample available for analysis were included in the study. Each patient in this study underwent transrectal ultrasound guided prostate biopsy and the total number of cores obtained ranged from 4-33 with 12 being the most common number of cores obtained (n=54). Based on the pathology report, the core with the highest Gleason score was chosen for immunohistochemistry staining. If multiple cores tied for the highest Gleason score, then the core with the highest percentage of neoplastic cells that still had benign normal prostate tissue (i.e. not 100% neoplastic cells) was chosen.

Specimen characteristics, staining, and quantification

Diagnostic needle biopsies were mounted in paraffin, and 3-4 μm sections were prepared for standard hematoxylin and eosin staining. Standard immunohistochemistry analysis was performed for DAP2IP and EZH2. Immunostaining was performed using the Benchmark XT automated stainer (Ventana, Tuscan, AZ, USA). Briefly, formalin-fixed, paraffin-embedded tissue microarray sections were cut at 3-4 μm and air-dried overnight. The sections were de-paraffinized, rehydrated, subjected to heat-induced epitope retrieval, and then incubated with anti-EZH2 (clone:SP129, Ventana, prediluted) or anti-DAB2IP[32] (homegrown, 1:150) primary

antibodies. UltraView universal detection system (Ventana) was used for signal detection. The slides were developed using 3-3'-diaminobenzidine chromogen and counterstained with hematoxylin. Specific positive and negative (slides incubated without primary antibody) controls were utilized for each run of immunostains and checked for validation of the assay. Controls for anti-EZH2 antibody included tissue from prostate and breast adenocarcinoma and normal lymph node that are known to have high EZH2 expression. Anti-EZH2 protocol was standardized according to the directions in the package insert. This antibody is intended for *in vitro* diagnostic use. Protocol for anti-DAP2IP was performed as published previously[32].

Tumor and benign prostate tissue stained with each marker were evaluated by an experienced genitourinary pathologist who was blinded to patient clinical information. Each case was evaluated for the extent (percentage of positive cells) and intensity of staining. The average intensity of positive tumor cells was given a grade (G) score: G0, none; G1, weak; G2, intermediate; and G3, strong. DAB2IP positivity was evaluated as cytoplasmic expression. EZH2 was evaluated as nuclear pattern of expression. Compared to DAB2IP expression in the benign 'control' prostate tissue surrounding the neoplastic cells, tumor DAB2IP status was categorized as retained (same or stronger expression) or reduced (weaker expression). EZH2 expression was scored as the intensity of staining, G0-G3.

Study design

The five clinical endpoints in this study were freedom from biochemical failure (FFBF), castration resistance-free survival (CRFS), distant metastasis-free survival (DMFS), overall survival (OS), and prostate cancer-specific survival (PCSS). FFBF was determined using the Phoenix definition, which denotes a PSA increase of $\geq$ 2.0 ng/mL above the nadir PSA level.[33]

CRFS was defined as ≥ 2 episodes of rising PSA while on standard hormone therapy in the setting of testosterone levels < 50 ng/ml, or if patients were started on second line therapy as first line hormone therapy was deemed to have failed at the clinical oncologist's discretion. DMFS was determined from clinical chart review documenting date of known metastasis by imaging. PCSS was defined as death due to prostate cancer, radiation toxicity, or unknown cause with distant metastasis or castration resistance. Time to each endpoint was calculated from the first day of radiation therapy.

Statistical analysis

Kaplan-Meier estimates and log-rank tests were computed to estimate the FFBF, CRFS, DMFS, PCSS, and OS. Univariate Cox regression analyses were conducted to identify significant clinical risk factors that could be significantly associated with each endpoint, including T stage, N stage, Gleason score, pretreatment PSA, total radiation dose, hormone therapy, and duration of hormone therapy. Fisher's exact test was used to evaluate statistical differences among these factors based on the status of the tumor biomarker. Finally, multivariate analysis using a backward model selection was conducted for each factor that met the inclusion criterion $p<0.15$ by univariate analysis.

Results

DAB2IP results

Seventy-nine patients with high-risk prostate cancer treated with definitive radiation therapy from 2005-2012 met the inclusion criteria and were evaluated. Twenty-eight percent (22/79) of patients revealed DAB2IP-reduction while 72% (57/79) retained DAB2IP. The

median follow up times were 4.8 years and 5.3 years for patients in the DAB2IP-reduced group and DAB2IP-retained group, respectively. Statistical differences of clinicopathological factors include more advanced T stage (p=0.0149), higher pretreatment PSA (p=0.0379), and more aggressive Gleason score (p=0.0048) all within the DAB2IP-reduced group. There were no significant differences in patient age at diagnosis, N stage, total radiation dose, hormone therapy, or duration of hormone therapy received (see Table 1).

Pretreatment tumor reduction of DAB2IP as evidenced by prostate biopsy samples correlated strongly with worse outcome in every endpoint measured except death from any cause (see Table 2). Reduced DAB2IP portended a significantly worse FFBF (p<0.0001), CRFS (p=0.0039), DMFS (p=0.0006), and PCSS (p=0.0102). Kaplan-Meier estimates of these four significant endpoints can be seen in Figure 1. By four years post-radiotherapy, the biochemical failure rate was a staggering 66% in the DAB2IP-reduced group compared to only 8% in the DAB2IP-retained group at that point. By five years post-radiotherapy, the prostate cancer-specific mortality rate was 17% in the DAB2IP-reduced group whereas no one in the DAB2IP-retained group had died due to their malignancy.

Sixteen of the 79 high-risk patients in the DAB2IP cohort had met the criteria for castration resistance. Thirteen of these patients had testosterone data available to confirm that the PSA continued to rise despite a testosterone level <50 ng/ml. The median testosterone level for these 13 patients was 3 ng/ml and the levels ranged from undetectable to 32 ng/ml. The remaining 3 patients were determined to have clinically become castration resistant because of a rising PSA despite adding a second agent to their androgen deprivation therapy.

EZH2 results

Ninety-seven patients with high-risk prostate cancer treated with definitive radiation therapy from 2005-2012 met the inclusion criteria and were evaluated. Ninety-eight percent (95/97) of patients expressed EZH2 as follows: 2% (2/97) were G0, 10% (10/95) were G1, 68% (66/97) were G2, and 20% (19/97) were G3. The median time to follow up was 4.6 years in the EZH2 cohort. Stratified EZH2 expression was not statistically significant for any outcome (see Table 3).

Nine patients in the EZH2 study elected to not receive hormone therapy. Of these, one patient did not express EZH2, one patient had G1 expression, and the remaining seven patients all had G2 expression. Importantly, none of these nine patients died from any cause let alone from their malignancy. Furthermore, even though every patient with the highest expression of EZH2 (G3) received androgen deprivation, these patients demonstrated the worst outcomes at four years for FFBF, CRFS, and DMFS.

Univariate and multivariate analysis

Univariate analysis using Cox regression of typical prognostic variables revealed that only T stage, N stage, and Gleason score correlated with outcome. Higher T stages were significantly associated with worse FFBF ($p=0.0477$), CRFS ($p=0.0379$), DMFS ($p=0.0082$), and PCSS ($p=0.0105$). N1 stage was significantly associated with worse FFBF ($p=0.0003$), CRFS ($p=0.0132$), and DMFS ($p<0.0001$) but not PCSS ($p=0.2782$). Higher Gleason scores were significantly associated with worse FFBF ($p=0.0007$), CRFS ($p=0.0043$), DMFS ($p=0.0083$), and PCSS ($p=0.0031$). None of the prognostic variables were significantly associated with OS.

Table 4 shows all variables that were significant for each outcome after multivariable analysis. Pretreatment tumor DAB2IP status remained significant in the multivariable analysis

for FFBF (p=0.0026), CRFS (p=0.0043), and DMFS (p=0.0009). The two other significant variables on multivariable analysis include Gleason score (FFBF p=0.0428; CRFS p=0.0409; DMFS p=0.0174) and T stage (DMFS p=0.0252). Multivariate analysis could not be conducted for PCSS because zero patients had died due to prostate cancer in the subgroups of retained-DAB2IP, T1c-T2b stages, N0 stage, or Gleason scores 6-8. Interestingly, not only was DAB2IP significant for each measureable outcome after multivariable analysis, but it was always the most highly significant variable.

Discussion

DAB2IP is a putative tumor suppressor and member of the RAS-GAP family. Decreased expression of the protein DAB2IP is associated with aggressive disease[13, 14] and radiation resistance[9, 15, 34, 35]. Down-regulation of DAB2IP has mostly been attributed to epigenetic regulation involving methylation of the promoter region mediated by EZH2[18-20], though Skp2-mediated proteasome degradation[25] and genetic variants (i.e. mutations)[13, 36, 37] may also play a role. Decreased DAB2IP has been identified in several cancers other than prostate, including breast[21, 38], hepatocellular[22, 28], lung[23], gastrointestinal[24], and bladder[15, 26].

Based on strong preclinical data indicating the role of DAB2IP in radiation response in prostate cancer cells, we performed a pilot study to determine its clinical importance[14]. Our prior pilot study analyzed 46 men's diagnostic prostate biopsies with high-risk disease for DAB2IP expression and showed a strong correlation between pretreatment tumor DAB2IP reduction and worse clinical outcome with only 2.7 years of median follow up. With longer follow up and increased sample size, we hypothesized that pretreatment tumor status of DAB2IP would also predict worse malignancy-specific survival (PCSS). In addition to studying DAB2IP, we also

sought to determine the potential prognostic role of its upstream regulator, EZH2, after increasing the sample size and follow up time.

In this study we show that pretreatment tumor DAB2IP status and not EZH2 correlates with worse rates of biochemical failure, castration resistance, and distant metastasis after the standard of care treatment for these high-risk prostate cancer patients including definitive radiation therapy and androgen deprivation. Additionally, our results confirmed our hypothesis that DAB2IP reduction ultimately leads to significantly increased mortality due to prostate cancer. Five of the six patients (83%) in this study that died due to their malignancy had an initial Eastern Cooperative Oncology Group (ECOG) score of 0 and therefore performance status did not confound our results. Based on the numerical data included in the opening introductory paragraph of this manuscript and our observation that about one-fourth of high-risk prostate cancer patients have decreased expression of DAB2IP, we estimate that between 12,000 and 18,000 men treated annually in the United States have suboptimal response to the current standard of care treatment.

Another important finding from this study is that the tumors with reduced DAB2IP expression were statistically more likely to have a more advanced T stage, higher pretreatment PSA, and more aggressive Gleason score. Whether down-regulation of DAB2IP is the molecular cause of these more aggressive clinicopathologic findings or whether the decreased DAB2IP expression selectively occurs in aggressive tumors remains unclear.

Nearly all high-risk prostate cancer samples in this study expressed EZH2. Rather than predict cancers with poor therapeutic response, EZH2 levels may help screen for higher risk cancers. Nevertheless, it's interesting to note that tumors with the highest expression of EZH2 (G3) demonstrated the worst outcomes at four years for FFBF, CRFS, and DMFS, which is

congruent with the idea that increased EZH2 leads to methylation of the *DAB2IP* promotor and reduction in DAB2IP expression. Since regulation of DAB2IP expression is not the sole function of EZH2, it makes sense that it would not be as potent of a prognostic biomarker compared to DAB2IP which modulates different signal cascades associated with cell proliferation, survival, apoptosis, and metastasis.

Based on the results presented herein, DAB2IP may be able to differentiate the worst cases amongst the already high-risk group of prostate cancer patients that are at greatest risk for treatment failure prior to initiation of standard therapy. Potential clinical application is that in the future we may be able to effectively use tumor DAB2IP expression from a patient's biopsy specimen as a means of determining curability of their cancer with standard radiation-based therapeutic regimens.

Future research may be directed toward creating molecularly-based therapeutic strategies to upregulate DAB2IP and restore the tumor suppressor's presence within the neoplastic cells or by targeting downstream effectors. DNA methyltransferase inhibitors as well as histone deacetylase inhibitors can both induce expression of the *DAB2IP* gene[19, 20]. Cytolethal distending toxin (CTD) from Campylobacter jejuni significantly elicited cell death in DAB2IP-deficient prostate cancer cells when combined with radiotherapy[39]. Restoring DAB2IP may also improve castration resistance in addition to radiation resistance as DAB2IP expression inversely correlates with androgen receptor activation status particularly in recurrent or metastatic prostate cancer patients[17].

The DAB2IP pathway is an important potential target for improving the treatment of multiple malignancies (not just prostate cancer) and enhancing multiple modalities (not just radiation therapy). For example, KU55933 which suppresses ATM phosphorylation upon

irradiation could be applied in the radiotherapy of bladder cancer patients with a DAB2IP gene defect[15]. Furthermore, other than improving radiation responsiveness, targeting the DAB2IP pathway may also improve response to chemotherapy[35]. Inhibiting EZH2 through siRNA has been shown to increase DAB2IP expression[29] and reverse chemoresistance[40]. Improving chemotherapy response could improve survival in this population as patients with reduced DAB2IP in bladder cancer treated with surgery and adjuvant chemotherapy had worse cancer-specific survival[26].

One limitation of this study includes the way in which tumor DAB2IP status is characterized as reduced or retained. We were not able to identify a specific intensity level threshold below which DAB2IP should be considered reduced, especially since some samples stained better than others with the antibody. Instead, we compared the tumor staining with the surrounding normal prostate tissue as the control to know whether the tumor retained normal DAB2IP expression or reduced the protein's expression. The limitation of this definition comes when the entire stained sample is tumor and there are no benign glands with which to compare, or when there are very few glands with which to compare and they are all atrophic with high DAB2IP expression. Perhaps this problem could be avoided via a prospective study using fresh tissue and not relying on a retrospective study with tissues at varying ages.

Another limitation of this study is not having a separate cohort of patients that received a non-radiation intervention such as prostatectomy with which to compare. At this point we do not definitively know whether DAB2IP reduction is a poor prognostic indicator regardless of the intervention, or if it really is a marker of radiation resistance. Additionally, since the tissue specimens were obtained from biopsy, there is a clear limitation of potential heterogeneity of pathological findings and the immunostaining not always reflecting the characteristics of all

cancer foci in each patient. Also, even though we were able to increase the sample size by over 70% from our prior study and obtain over 2 more years of additional follow up data, the sample size and follow up time remain limitations. DAB2IP requires further studies to validate its role in this cohort of patients and to further determine whether it may also be a predictive marker of response to radiation therapy.

In conclusion, based on our results about one-fourth of men with high-risk prostate cancer and well over 10,000 men in the United States annually may have reduced tumor expression of DAB2IP which makes their tumors more radioresistant and aggressive. This subpopulation with reduced DAB2IP has a suboptimal response and significantly higher prostate cancer-specific mortality despite standard of care treatment with radiation therapy and androgen deprivation. Targeting the DAB2IP pathway may be a promising area for future drug development to improve the effectiveness of radiation and chemotherapy in multiple malignancies. Further study into improving the radiation response and survival in this subpopulation is warranted.

References

1. Siegel RL, et al. Cancer statistics, 2015. *CA: A Cancer Journal for Clinicians* 2015; **65**(1): 5-29.
2. Punnen S, et al. The epidemiology of high-risk prostate cancer. *Current Opinion in Urology* 2013; **23**(4): 331-6.
3. Mohler JL. The 2010 NCCN Clinical Practice Guidelines in Oncology on Prostate Cancer. *Journal of the National Comprehensive Cancer Network* 2010; **8**(2): 145.
4. Horwitz EM, et al. Ten-year follow-up of radiation therapy oncology group protocol 92-02: a phase III trial of the duration of elective androgen deprivation in locally advanced prostate cancer. *J Clin Oncol* 2008; **26**(15): 2497-504.
5. Bolla M, et al. Duration of androgen suppression in the treatment of prostate cancer. *N Engl J Med* 2009; **360**(24): 2516-27.
6. Bolla M, et al. External irradiation with or without long-term androgen suppression for prostate cancer with high metastatic risk: 10-year results of an EORTC randomised study. *Lancet Oncol* 2010; **11**(11): 1066-73.

7. Hanks GE, et al. Phase III trial of long-term adjuvant androgen deprivation after neoadjuvant hormonal cytoreduction and radiotherapy in locally advanced carcinoma of the prostate: the Radiation Therapy Oncology Group Protocol 92-02. *J Clin Oncol* 2003; **21**(21): 3972-8.
8. Xie D, et al. DAB2IP coordinates both PI3K-Akt and ASK1 pathways for cell survival and apoptosis. *Proceedings of the National Academy of Sciences* 2009; **106**(47): 19878-83.
9. Kong Z, et al. Downregulation of human DAB2IP gene expression in prostate cancer cells results in resistance to ionizing radiation. *Cancer research* 2010; **70**(7): 2829-39.
10. Xie D, et al. DAB2IP coordinates both PI3K-Akt and ASK1 pathways for cell survival and apoptosis. *Proceedings of the National Academy of Sciences of the United States of America* 2009; **106**(47): 19878-83.
11. Yu L, et al. DAB2IP regulates autophagy in prostate cancer in response to combined treatment of radiation and a DNA-PKcs inhibitor. *Neoplasia* 2012; **14**(12): 1203-12.
12. Tumati V, et al. Development of a locally advanced orthotopic prostate tumor model in rats for assessment of combined modality therapy. *International Journal of Oncology* 2013; **42**(5): 1613-9.
13. Duggan D, et al. Two genome-wide association studies of aggressive prostate cancer implicate putative prostate tumor suppressor gene DAB2IP. *Journal of the National Cancer Institute* 2007; **99**(24): 1836-44.
14. Jacobs C, et al. DOC-2/DAB2 Interacting Protein Status in High-Risk Prostate Cancer Correlates With Outcome for Patients Treated With Radiation Therapy. *International Journal of Radiation Oncology*Biology*Physics* 2014; **89**(4): 729-35.
15. Zhang T, et al. The ATM inhibitor KU55933 sensitizes radioresistant bladder cancer cells with DAB2IP gene defect. *International Journal of Radiation Biology* 2015; **91**(4): 368-78.
16. Xie D, et al. Role of DAB2IP in modulating epithelial-to-mesenchymal transition and prostate cancer metastasis. *Proceedings of the National Academy of Sciences* 2010; **107**(6): 2485-90.
17. Wu K, et al. The role of DAB2IP in androgen receptor activation during prostate cancer progression. *Oncogene* 2014; **33**(15): 1954-63.
18. Chen H, et al. Epigenetic regulation of a novel tumor suppressor gene (hDAB2IP) in prostate cancer cell lines. *The Journal of biological chemistry* 2003; **278**(5): 3121-30.
19. Chen H, et al. Differential Regulation of the Human Gene DAB2IP in Normal and Malignant Prostatic Epithelia: Cloning and Characterization. *Genomics* 2002; **79**(4): 573-81.
20. Chen H, et al. Epigenetic Regulation of a Novel Tumor Suppressor Gene (hDAB2IP) in Prostate Cancer Cell Lines. *Journal of Biological Chemistry* 2003; **278**(5): 3121-30.
21. Dote H, et al. Aberrant Promoter Methylation in Human DAB2 Interactive Protein (hDAB2IP) Gene in Breast Cancer. *Clinical Cancer Research* 2004; **10**(6): 2082-9.
22. Qiu G-H, et al. Differential expression of hDAB2IPA and hDAB2IPB in normal tissues and promoter methylation of hDAB2IPA in hepatocellular carcinoma. *Journal of Hepatology* 2007; **46**(4): 655-63.
23. Yano M, et al. Aberrant promoter methylation of human DAB2 interactive protein (hDAB2IP) gene in lung cancers. *International Journal of Cancer* 2005; **113**(1): 59-66.
24. Dote H, et al. Aberrant promoter methylation in human DAB2 interactive protein (hDAB2IP) gene in gastrointestinal tumour. *Br J Cancer* 2005; **92**(6): 1117-25.
25. Tsai Y-S, et al. The role of homeostatic regulation between tumor suppressor DAB2IP and oncogenic Skp2 in prostate cancer growth; 2014.
26. Shen Y-J, et al. Downregulation of DAB2IP results in cell proliferation and invasion and contributes to unfavorable outcomes in bladder cancer. *Cancer Science* 2014; **105**(6): 704-12.
27. Zhu JN, et al. DAB2IP expression in bladder transitional cell carcinoma and its correlation with clinical outcome. *Journal of Sichuan University Medical science edition* 2014; **45**(4): 591-4.

28. Calvisi DF, et al. Inactivation of Ras GTPase-activating proteins promotes unrestrained activity of wild-type Ras in human liver cancer. *Journal of Hepatology* 2011; **54**(2): 311-9.
29. Chen H, et al. Down-regulation of human DAB2IP gene expression mediated by polycomb Ezh2 complex and histone deacetylase in prostate cancer. *The Journal of biological chemistry* 2005; **280**(23): 22437-44.
30. Rhodes DR, et al. Multiplex biomarker approach for determining risk of prostate-specific antigen-defined recurrence of prostate cancer. *Journal of the National Cancer Institute* 2003; **95**(9): 661-8.
31. Varambally S, et al. The polycomb group protein EZH2 is involved in progression of prostate cancer. *Nature* 2002; **419**(6907): 624-9.
32. Wang Z, et al. The Mechanism of Growth-inhibitory Effect of DOC-2/DAB2 in Prostate Cancer: CHARACTERIZATION OF A NOVEL GTPase-ACTIVATING PROTEIN ASSOCIATED WITH N-TERMINAL DOMAIN OF DOC-2/DAB2. *Journal of Biological Chemistry* 2002; **277**(15): 12622-31.
33. Roach M, et al. Defining biochemical failure following radiotherapy with or without hormonal therapy in men with clinically localized prostate cancer: Recommendations of the RTOG-ASTRO Phoenix Consensus Conference. *International journal of radiation oncology, biology, physics* 2006; **65**(4): 965-74.
34. Kong Z, et al. Epothilone B confers radiation dose enhancement in DAB2IP gene knock-down radioresistant prostate cancer cells. *International journal of radiation oncology, biology, physics* 2010; **78**(4): 1210-8.
35. Wu K, et al. The Mechanism of DAB2IP in Chemoresistance of Prostate Cancer Cells. *Clinical Cancer Research* 2013; **19**(17): 4740-9.
36. Yang L, et al. A Common Genetic Variant (97906C>A) of DAB2IP/AIP1 Is Associated with an Increased Risk and Early Onset of Lung Cancer in Chinese Males. *PLoS ONE* 2011; **6**(10): e26944.
37. Xu S, et al. Association of the variant rs2243421 of human DOC-2/DAB2 interactive protein gene (hDAB2IP) with gastric cancer in the Chinese Han population. *Gene* 2013; **515**(1): 200-4.
38. Conway K, et al. DNA methylation profiling in the Carolina Breast Cancer Study defines cancer subclasses differing in clinicopathologic characteristics and survival. *Breast Cancer Research : BCR* 2014; **16**(5): 450.
39. Lai C-H, et al. Sensitization of radio-resistant prostate cancer cells with a unique cytolethal distending toxin. *Oncotarget* 2014; **5**(14): 5523-34.
40. W Z, et al. siRNA silencing EZH2 reverses cisplatin-resistance of human non-small cell lung and gastric cancer cells. *Asian Pacific Journal of Cancer Prevention* 2015; **16**(6): 2425-30.

Table and Figure Legends:

Table 1. Comparing clinicopathological factors based on tumor DAB2IP expression. PSA, prostate-specific antigen.

Table 2. Pretreatment tumor reduction of DAB2IP portends significantly worse outcome as calculated by log-rank. CRFS, castration resistance-free survival; DMFS, distant metastasis-free survival; FFBF, freedom from biochemical failure; PCSS, prostate cancer-specific survival.

Table 3. Stratified EZH2 expression was not statistically significant for any outcome as calculated by log-rank. CRFS, castration resistance-free survival; DMFS, distant metastasis-free survival; FFBF, freedom from biochemical failure; PCSS, prostate cancer-specific survival.

Table 4. Statistically significant variables on multivariate analysis by endpoint as calculated by Cox regression.

Figure 1. Kaplan Meier and log-rank analysis comparing (A) freedom from biochemical failure, (B) castration resistance-free survival, (C) distant metastasis-free survival, (D) prostate cancer-specific survival, and (E) overall survival based on pretreatment tumor DAB2IP status.

Table 1

Category		Reduced DAB2IP % (n)	Retained DAB2IP % (n)	P-value
Sample size, n=		22	57	N/A
Median follow up in months (range)		63.8 (50.3 - 85.4)	57.6 (42.1 - 74.3)	0.3196
Median age in years (range)		66 (63 - 71)	65 (59 - 71)	0.3492
T stage	T1c	4.5 (1)	20.0 (11)	0.0149
	T2a-c	54.5 (12)	67.3 (37)	
	T3a-b	40.9 (9)	12.7 (7)	
N stage	N0	90.9 (20)	96.4 (54)	0.3150
	N1	9.1 (2)	3.6 (2)	
Pretreatment PSA	<10	9.1 (2)	35.1 (20)	0.0379
	10-20	9.1 (2)	12.3 (7)	
	>20	81.8 (18)	52.6 (30)	
Gleason score	6-7	13.6 (3)	29.8 (17)	0.0048
	8	13.6 (3)	38.6 (22)	
	9-10	72.7 (16)	31.6 (18)	
Total radiation dose	73.8-79.0 Gy	40.9 (9)	24.6 (14)	0.1745
	79.2 Gy	59.1 (13)	75.4 (43)	
Hormone therapy	Yes	100.0 (22)	89.5 (51)	0.1782
	No	0 (0)	10.5 (6)	
Duration of hormone therapy	4-21 months	30.0 (6)	42.2 (19)	0.4160
	24-36 months	70.0 (14)	57.8 (26)	

Table 2

Biomarker status	FFBF		CRFS		DMFS		PCSS		OS	
	4 year	P-value	4 year	P-value	4 year	P-value	5 year	P-value	5 year	P-value
DAB2IP-retained	92%	<0.0001	96%	0.0039	100%	0.0006	100%	0.0102	92%	0.3327
DAB2IP-reduced	34%		58%		58%		83%		79%	

Table 3

Biomarker status	FFBF		CRFS		DMFS		PCSS		OS	
	4 year	P-value	4 year	P-value	4 year	P-value	5 year	P-value	5 year	P-value
EZH2 grade 0	100%	0.6324	100%	0.1125	100%	0.2536	100%	0.1715	100%	0.2432
EZH2 grade 1	90%		89%		90%		100%		80%	
EZH2 grade 2	75%		87%		85%		95%		89%	
EZH2 grade 3	69%		69%		75%		81.8%		77%	

Table 4

Freedom from Biochemical Failure		
DAB2IP	P = 0.0026	HR = 3.994
Gleason score	P = 0.0428	HR = 2.674
Castration Resistance-Free Survival		
DAB2IP	P = 0.0043	HR = 6.614
EZH2	P = 0.0566	HR = 9.615
Gleason score	P = 0.0409	HR = 4.274
Distant Metastasis-Free Survival		
DAB2IP	P = 0.0009	HR = 12.076
EZH2	P = 0.0160	HR = 25.641
Gleason score	P = 0.0174	HR = 6.049
T-stage	P = 0.0252	HR = 4.717

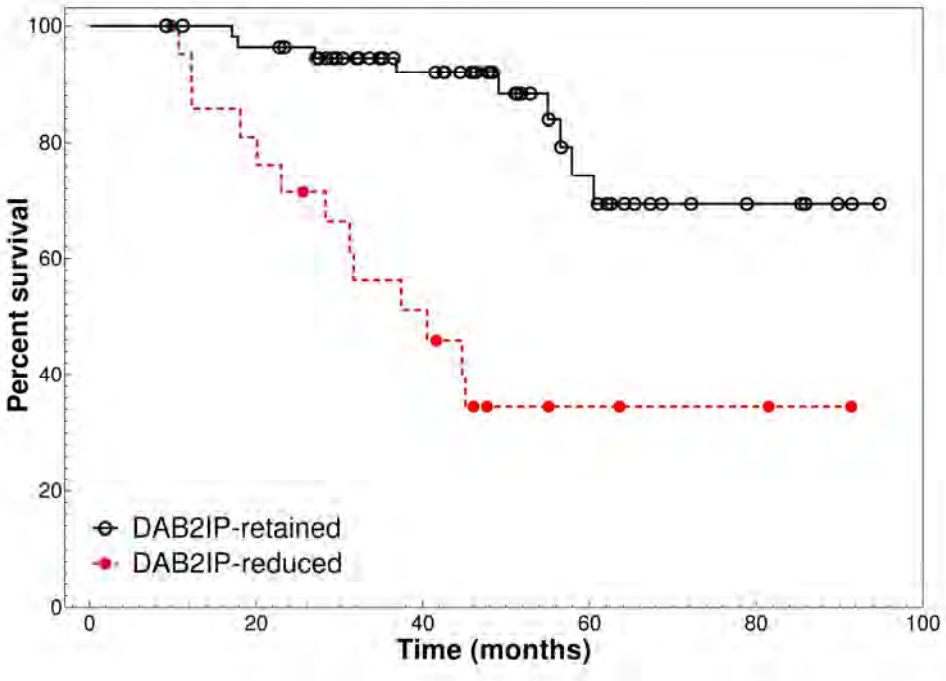

Figure 1A
153x109mm (300 x 300 DPI)

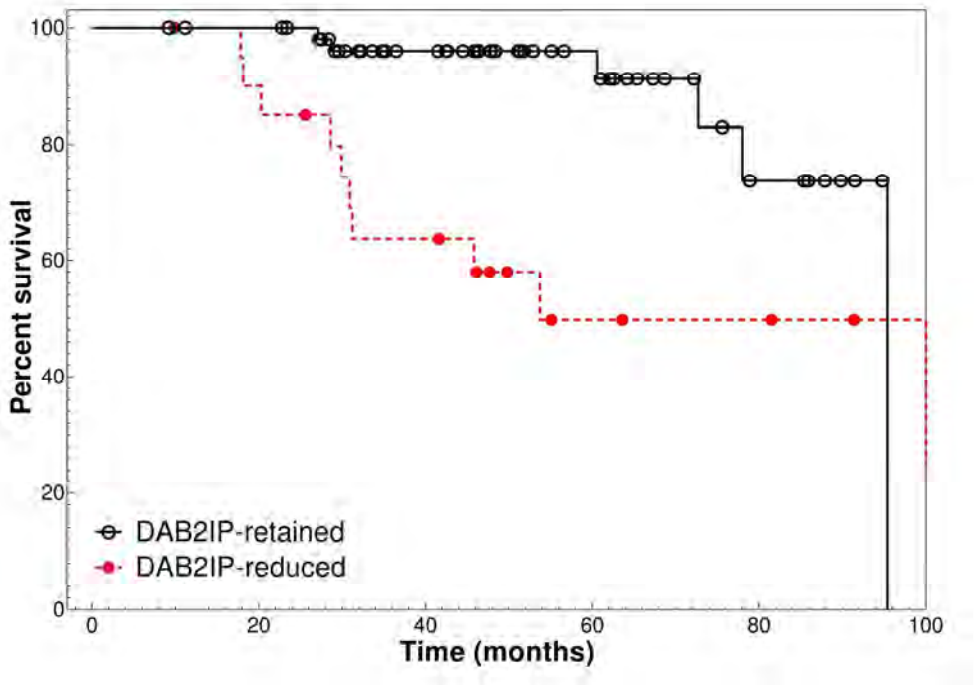

Figure 1B
153x109mm (300 x 300 DPI)

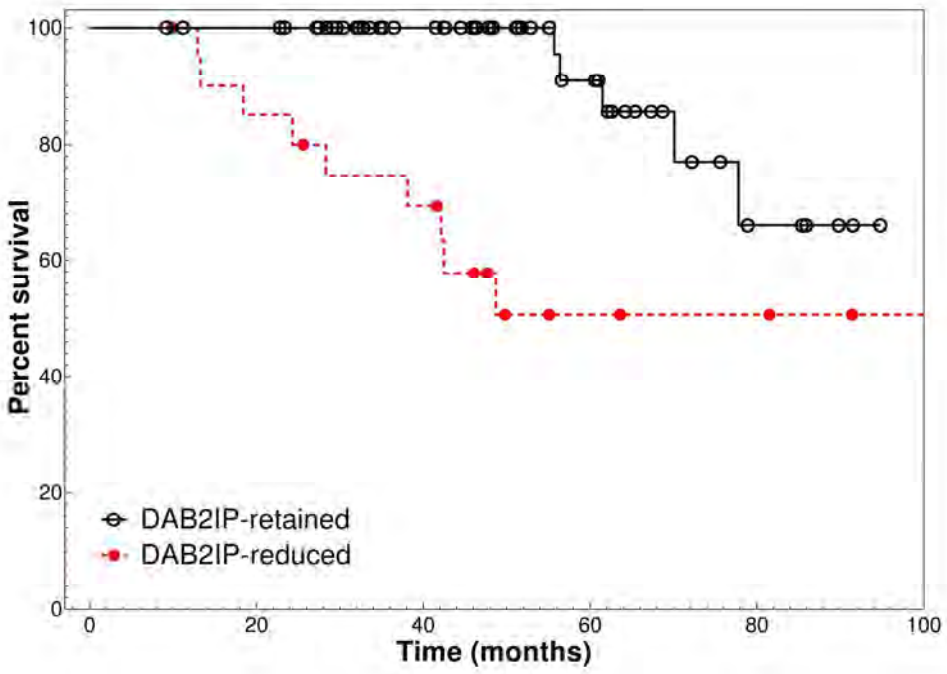

Figure 1C
153x109mm (300 x 300 DPI)

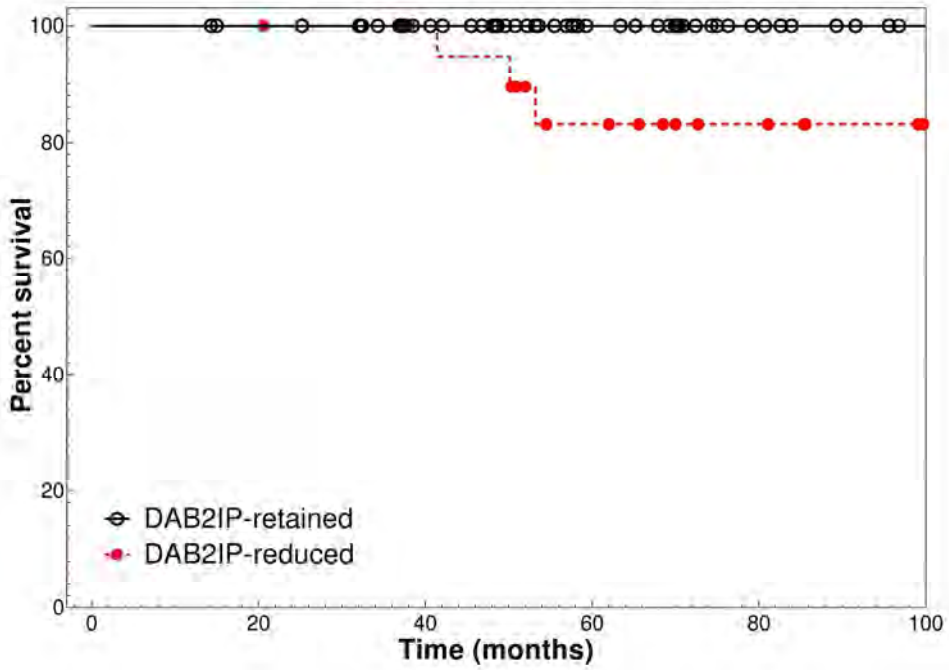

Figure 1D
153x109mm (300 x 300 DPI)

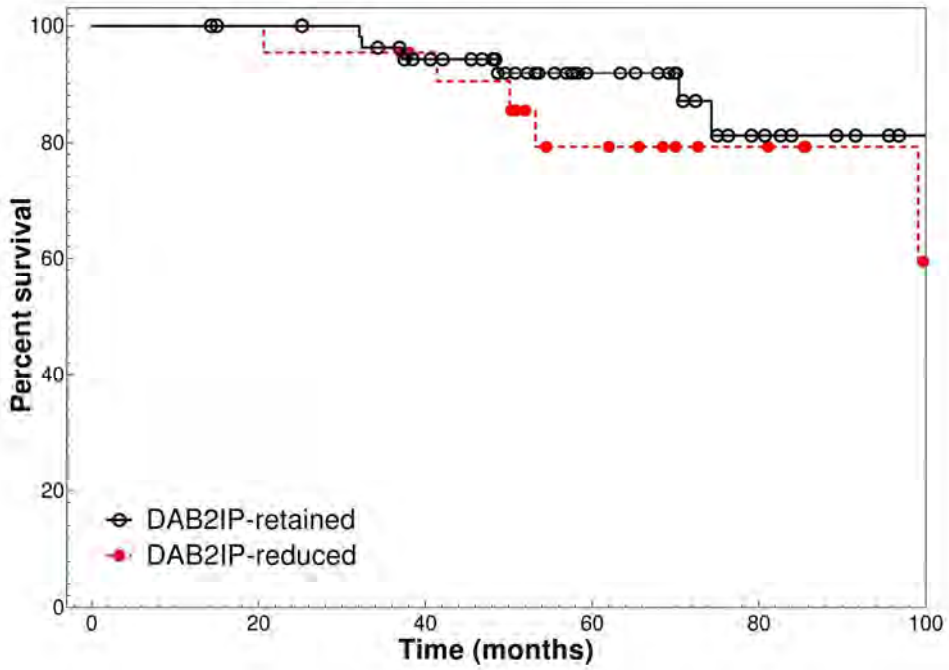

Figure 1E
153x109mm (300 x 300 DPI)

OXFORD UNIVERSITY PRESS | Carcinogenesis

Tumor Suppressor Protein DAB2IP Participates in Spindle Assembly Checkpoint and Maintains Chromosomal Stability

Journal:	*Carcinogenesis*
Manuscript ID:	Draft
Manuscript Type:	Original Manuscript
Date Submitted by the Author:	n/a
Complete List of Authors:	Saha, Debabrata; UTSouthwestern Medical Center, Radiattion Oncology Yu, Lan; UTSouthwestern Medical Center, Radiation Oncology Shang, Zeng-Fu; Medical College of Soochow University, Radiation Medicine and Protection Tumati, Vasu; UTSouthwestern Medical Center, Radiation Oncology Hsieh, Jer-Tsong; UTSouthwestern Medical Center, Urology Habib, Amyn; UTSouthwestern Medical Center, Neurology & Neurotherapeutics Chen, Benjamin; UTSouthwestern Medical Center, Radiation Oncology
Keywords:	DAB2IP, APC/C-MCC, spindle assembly checkpoint, chromosomal stability, Prostate Cancer

Tumor Suppressor Protein DAB2IP Participates in Spindle Assembly Checkpoint and Maintains Chromosomal Stability

Lan Yu[1*], Zeng-Fu Shang[1,2*], Vasu Tumati[1], Jer-Tsong Hsieh[3,5,7], Amyn A. Habib [4,5,6], Benjamin Chen[1,4] and Debabrata Saha[1,4]

[1]Department of Radiation Oncology, [3]Department of Urology, [4]Department of Neurology and Neurotherapeutics, [5]Simmons Comprehensive Cancer Center University of Texas Southwestern Medical Center, Dallas, TX 75390, USA; [6]VA North Texas Health Care System, Dallas, TX, USA; [2]School of Radiation Medicine and Protection, Medical College of Soochow University; Collaborative Innovation Center of Radiation Medicine of Jiangsu Higher Education Institutions, Suzhou, Jiangsu 215123, China; [7]Department of Oncology, National Taiwan University Hospital, National Taiwan University College of Medicine, Taipei 10048, Taiwan.

* These authors contributed equally as first authors

Running title: DAB2IP in spindle assembly checkpoint regulation

Corresponding Author

Debabrata Saha, Ph.D.

Assistant Professor

Department of Radiation Oncology

University of Texas Southwestern Medical Center

2201 Inwood Road, Dallas, TX 75390-9187; USA

Email: debabrata.saha@utsouthwestern.edu

Tel: (214) 648-7750

FAX: (214) 648-5995

Abstract

DAB2IP, a tumor suppressor, is known to suppress the PI3K-Akt pro-survival pathway and enhance ASK1-mediated apoptosis. Decreased expression of DAB2IP is often detected in advanced prostate cancer (PCa) and is associated with poor prognosis. Loss of DAB2IP, which is primarily due to epigenetic regulation and promoter methylation, is correlated with aggressive cancers and poor prognosis. Our current findings reveal a novel activity of DAB2IP in modulating the spindle assembly checkpoint (SAC). SAC is a molecular fail-safe mechanism that prevents premature separation of sister chromatids until sister chromatids are attached to microtubule fibers oriented from opposite poles of the spindle. SAC is maintained by the mitotic checkpoint complex (MCC) through its inhibition of Cdc20, an activator of the anaphase-promoting APC/C E3 ubiquitin ligase. Several studies have proposed that the autoubiquitylation of Cdc20 by APC/C-MCC is correlated with MCC disassembly. Here, we report that DAB2IP directly interacts with the APC/C co-activator Cdc20 and prevents its ubiquitylation during prometaphase. Furthermore, RNAi-mediated inhibition of DAB2IP leads to less Mad2 bound to Cdc20 and APC/C complex, which promotes premature mitotic exit in the presence of microtubule inhibitor nocodazole or stabilizer paclitaxel. Consistent with this observation, we observe that DAB2IP-deficient cells display an increased outcome of chromosome lagging in anaphase and chromosomal instability, which is recognized as a major driving force of carcinogenesis and chemoresistence. In conclusion, a novel function of DAB2IP on mitotic SAC regulation is identified which is essential for maintaining chromosomal stability that is often lost in cancer cells.

Key words: DAB2IP, APC/C-MCC, spindle assembly checkpoint, chromosomal stability, Prostate Cancer

Summary

The tumor suppressor protein, DAB2IP, plays an essential role in modulating the spindle assembly checkpoint (SAC) and maintaining chromosome stability. Our finding demonstrates a new mechanism by which down regulation of DAB2IP contributes to carcinogenesis and chemoresistance.

Introduction

DAB2IP, also known as apoptosis signal-regulating kinase 1-interacting protein-1 (AIP1), is a novel Ras-GTPase activating factor and often downregulated by epigenetic silencing in many cancers (1-5). DAB2IP acts as a scaffold protein and is capable of bridging both survival and death signaling cascades to maintain a state of cellular homeostasis through suppression of the PI3K-Akt pathway and enhancement of ASK1-JNK-mediated apoptosis (6). Moreover, the tumor suppressor function of DAB2IP also relies on its ability to prevent epithelial-mesenchymal transition (EMT) through inhibition of the Ras-PI3-Akt and Ras-NFκB signaling pathways (3-5,7,8). The expression status of DAB2IP in high-risk prostate cancer is highly correlated with outcome for patients treated with definitive external beam radiation (9-11). All the studies support the idea that loss of DAB2IP is correlated with aggressive cancers and predicts poor prognosis. However, how DAB2IP deficiency contributes to cancer development has not been fully elucidated.

Both chromosomal instability (CIN) and the consequent aneuploidy (the 'state' of the karyotype) have long been associated with carcinogenesis, poor prognosis, metastasis, and drug resistance (12-14). Previous studies have demonstrated that there is a strong correlation between CIN and defectsin SAC (14,15). The SAC is a pivotal cell-cycle surveillance system that prevents premature separation of sister chromatids until all sister chromatids are correctly attached to spindle microtubule fibers through their kinetochores (16). The unattached kinetochores activate SAC and inhibit the activation of a multisubunit ubiquitin ligase called anaphase promoting complex or cyclosome (APC/C). The SAC promotes the association of Cdc20, a co-activator of APC/C, with three other mitotic proteins, Mad2, BubR1, and Bub1, forming the mitotic checkpoint complex (MCC) (17).

The MCC is also able to bind with APC/C, but unlike APC/C-Cdc20, APC/C-MCC can't recognize and ubiquitylate their target securin and cyclin B1 and thereby blocks mitosis exit

(18-20). Recent studies demonstrated that assembly and disassembly of APC/C-MCC continuously occurs in the presence the SAC. The highly dynamic character of MCC assembly and disassembly is a key feature that allows rapid checkpoint silencing when SAC turns off (20-22). The APC/C-mediated Cdc20 autoubiquitylation and degradation in prometaphase, contributes to APC/C-MCC disassembly (23). However, the underlying molecular mechanisms that control the level of Cdc20 ubiquitylation and APC/C disassembly from checkpoint inhibition after proper kinetochore attachment are still largely unknown. In this study, DAB2IP is identified as a negative regulator of Cdc20 ubiquitylation and MCC disassembly during SAC silencing progression. Loss of DAB2IP leads to comprise of SAC and increases the number of aneuploid cells through aberrant chromosome segregation. Our findings reveal a unique functional role for DAB2IP in maintaining chromosome stability and highlight a new mechanism by which downregulation of DAB2IP contributes to carcinogenesis and chemoresistance.

Materials and Methods

Cell lines and treatment

C4-2 D2 and its control (Neo) cells were generated from C4-2 cells as described previously (7) and maintained in T medium (Invitrogen, Carlsbad, CA) containing 5% fetal bovine serum (HyClone, Hudson, NH), 10 mM HEPES and 1 mM sodium bicarbonate in a humidified incubator at 37 °C with 5% CO2. The cell lines HeLa, HCT116and 293T were purchased from the American Type Culture Collection (ATCC, Manassas, VA) and maintained in DMEM (Invitrogen, Carlsbad, CA) supplemented with 10% FBS (HyClone, Hudson, NH). All the cell lines were authenticated through cell morphology monitoring, species verification, growth curve and mycoplasma contamination using MycoAlert PLUS mycoplasma detection kit (Lonza, Allendale, NJ) once a month. For mitotic arrest, cells were treated with 50ng/mL nocodazole (Sigma, St Louis, MO) or 10nM paclitaxel (Sigma, St Louis, MO) for indicated times.

siRNAs and plasmids

Duplex siRNAs were synthesized (Invitrogen, Carlsbad, CA) based on experimentally validated target sequences for DAB2IP (5'-GGAGCGCAACAGUUACCUGTT-3') (6), MAD2 (5'-GGGAAGAGUCGGGACCACAGUUUAU-3') (24) or control siRNA (5'-CTGGACTTCCAGAAGAACA-3') (6). siRNAs were transfected into cells using Lipofectamine 2000 (Invitrogen, Carlsbad, CA) according to the manufacturer's protocol. HCT116 cells were transfected with pGIPZDAB2IP-lentiviral-shRNAmir and pGIPZ-non-silencing-lentiviral shRNAmir (7) according to the manufacturer's protocol, then the cells were selected by puromycin at concentration of 0.5 μg/ml for 3-4 weeks.

Various expression plasmids for DAB2IP were described previously (6), HA-Cdc20 and Myc-Cdc20 were purchased from Addgene (Cambridge, MA), HA-Ubi plasmid was given by Dr. Hongtao Yu at UT Southwestern (25).

Antibodies and immunoprecipitation

The following primary antibodies were used: rabbit anti-DAB2IP, anti-Cdc20, anti-BubR1 (Bethyl Laboratories, Montgomery, TX); mouse anti-Ku80, rabbit anti-HA, control mouse IgG, and rabbit IgG (Santa Cruz Biotechnology, Inc, Dallas, TX); mouse anti-Cyclin B1, rabbit anti-Hsp70, anti-PARP (Cell Signaling Technology Danvers, MA); rabbit anti-phospho–histone H3 (Ser-10) (Millipore, Bellerica, MA); mouse anti-α-tubulin, anti-Flag, rabbit anti-β-actin (Sigma-Aldrich, St. Louis, MO); mouse anti-securin (MBL international, Woburn, MA); mouse anti-Cdc27, anti-MAD2 (BD Biosciences San Jose, CA). EasyBlot anti Rabbit and Mouse IgG (HRP) (GeneTex Irvine, CA). Secondary antibodies used for immunofluorescence labeling were Alexa Fluor 488 goat anti–mouse IgG, Alexa Fluor 488 goat anti–rabbit IgG, Alexa Fluor 488 goat anti–human IgG, Alexa Fluor 568 goat anti–mouse IgG, and Alexa Fluor 568 goat anti–rabbit IgG (Invitrogen Carlsbad, CA).

C4-2 D2 and HeLa cells were synchronized with nocodazole at prometaphase and cell lysates were incubated with anti-DAB2IP, Cdc20, Cdc27 antibodies and protein A/G sepharose overnight. The sepharose beads were washed with lysis buffer three times and resuspended in SDS-PAGE loading buffer for Western blotting analysis using anti-DAB2IP, Cdc20, Cdc27, Mad2 and BubR1 antibodies.

Immunofluorescence

The cells were fixed in 4% paraformaldehyde/PBS for 30 min, permeabilized in 0.5% Triton X-100/PBS for 15 min, and blocked in 5% bovine serum albumin for 30 min. The samples were incubated with anti-α-tubulin (1:1,000) for 3 hours, washed in PBS for 10 min three times, and incubated with rhodamine red-conjugated goat anti-mouse secondary antibodies (1:1,000) for 1 hour. The cells were washed for 10 min three times and mounted using VECTASHIELD mounting medium with 4', 6-diamidino-2-phenylindole (DAPI) (Vector Laboratories, Burlingame, CA). The images were taken in a fluorescence microscope

(Axio Imager M2, Carl Zeiss, Thornwood, NY) with AxioVision SE64 Rel.4.8software (Carl Zeiss, Thornwood, NY).

Chromosome spread assays

HCT116 cells were treated with 100ng/ml colcemid (Irvine Scientific, Santa Ana, CA) for 6 hours. Then cells were collected and hypotonically swollen in pre-warmed 75 mM KCl for 13 min at 37 ℃. Cells were fixed in freshly made Carnoys fixative solution (methanol: acetic acid 3:1) with 2-3 times changes of the fixative. Cells were dropped onto warmed glass slides and dried overnight. Slides were stained in 5% Giemsa for 10 min at room temperature, rinsed with running water, air dried and mounted. The slides were visualized using a microscope (BX51, Olympus, Tokyo, Japan) and the images were recorded with SPOT Advanced software (SPOT Imaging Solutions, Sterling Heights, MI).

The MTT cell proliferation assays

Exponentially growing DAB2IP-proficient and -deficient C4-2 cells, and HeLa cells were transfected with DAB2IP-siRNA and control-siRNA, trypsinized and counted. One thousand cells were seeded per well in 96-well plates. Cells were treated with indicated dose of paclitaxel and docetaxel for 48 hours and then assayed for viability using the previously described MTT assay (26).

Cdc20 Ubiquitylation assay

HeLa and 293T cells were transfected with 1.0 μg Flag-DAB2IPor Flag empty plasmid along with 2.0 μg HA-ubiquitin, and Myc-Cdc20. 24 hours after transfection, cells were incubated with 10 μM MG132 for 12 hours. The cells then were lysed and Cdc20 was immunoprecipitated by anti-Myc antibody. The ubiquitylation levels of Cdc20 were determined by Western blotting.

Statistical Analysis

Data is presented as the mean ± SD of at least three independent experiments. The results were tested for significance using the unpaired Student's t test, and **P< 0.01, *P < 0.05 was considered significant.

Results

DAB2IP maintains a robust spindle checkpoint and inhibits aneuploidy from aberrant chromosome segregation

We first analyzed the chromosome number in chromosome-stable human colon carcinoma HCT116 cells. Knockdown of DAB2IP in HCT116 cells led to significantly increased aneuploid event and the proportion of aneuploid cells was correlated with the efficiency of DAB2IP-depletion (Figure 1A-C). The generation of aneuploid cells is highly correlated with aberrant mitotic progression, and the most common event leading to chromosomal instability is chromosome lagging in anaphase (27). Therefore, chromosome lagging was analyzed in DAB2IP-proficientand deficient cells. The expression DAB2IP caused a significant decrease in lagging chromosomes in C4-2 cells (Figure1D-E), whereas, knockdown of DAB2IP induced an increased level of lagging chromosomes in HeLa cells (Figure 1F). Chromosome lagging may result from premature segregation of chromosomes in cells with a weakened SAC (28). Consistent with this observation, our results further revealed that C4-2 D2 cells showed a significant increase in metaphase cells compared to control cells (C4-2 Neo) which suggests a robust SAC in mitotic cells (Figure 2A and B). To further demonstrate the effect of DAB2IP on the SAC, we treated cells with nocodazole which promotes depolymerization of microtubules and induces SAC. The mitotic index (MI) was determined by staining with a pH3-specific antibody and propidium iodide (PI). As shown in Figure 2C, C4-D2 cells exhibited a dramatically higher mitotic index (MI) when compared to C4-2 neo cells. Similarly, the MI was also elevated in DAB2IP-expressing C4-2 cells when treated with paclitaxel (Figure 6A). Consistent with this, the expression of cyclin B1 in DAB2IP-expressing cells was much higher than that of control C4-2 cells (Figure 2D). In addition, DAB2IP-depleted HeLa cells (Figure 2E and F) and DAB2IP-knockout mouse embryonic fibroblasts (MEFs) exhibited reduction of mitotic index when exposed to

nocodazole at different time points (Supplementary Figure1A and B). These experiments indicated that expression of DAB2IP induced a strong SAC, through which DAB2IP blocked premature chromosome segregation and aneuploidy generation.

DAB2IP interacts with Cdc20

To further determine the effect of DAB2IP on SAC, the kinetochore localizations of Bub1, BubR1 and Mad2 were investigated. The kinetochore signals of Bub1, BubR1 and Mad2 in prometaphase seemed to be unaffected by DAB2IP status (Supplementary Figure 2A-C). Our findings suggested that DAB2IP can affect checkpoint inactivation, but not SAC activation at kinetochores. Therefore, we further tested whether DAB2IP could form a complex with MCC during mitosis. To test this, mitotic cells were harvested by shaking off the prometaphase C4-2D2 cells which were synchronized using nocodazole. The synchronized M-phase C4-2 D2 cell lysates were then subjected to co-immunoprecipitation analysis. As shown in Figure 3A, Cdc20 and Cdc27, the activator and a component of APC/C, were immuno-precipitated by anti-DAB2IP antibodies. Mad2 doesn't interact with DAB2IP directly. Conversely, DA2BIP was immune-precipitated by the anti-Cdc20 antibody. DAB2IP also formed a complex with Cdc20 and Cdc27 in HeLa cells (Supplementary Figure 3). We then co-transfected Flag-DAB2IP or Flag empty vectors with HA-Cdc20 and performed the immunoprecipitation using anti-Flag antibodies (Figure 3C). Data indicated that HA-Cdc20 could interact with Flag-DAB2IP in cells (Figure 3C). We further defined that the CPR domain of DAB2IP mediated its interaction with Cdc20 (Figure 3E).

DAB2IP contributes to APC/C-MCC stability through blocking the ubiquitylation of Cdc20 in prometaphase

Our data demonstrated that DAB2IP maintained a robust spindle assembly checkpoint and

interacted with Cdc20.The activity of APC/C-Cdc20 is inhibited by Mad2 and BubR1. Therefore, we further examined whether DAB2IP might alter SAC via affecting the interaction pattern of the APC/C-MCC complex. We shook off prometaphase C4-2 D2 and C4-2 Neo cells which were blocked by nocodazole, and then immunoprecipitated MCC using anti-Cdc20 and -Cdc27 antibodies. As shown in Figure 4A, the levels of Mad2 and BubR1 bound to Cdc20 and Cdc27 were higher in C4-2D2 cells. Consistent with this result, depletion of DAB2IP in HeLa cells also led to markedly decreased expression of Mad2 and BubR1 on Cdc20 and Cdc27 (Figure 4B). The disassembly of MCC is important for SAC silencing and mitosis exit. As shown in Figure 4C, in C4-2D2 cells, interaction of Mad2 with Cdc20 was greatly stabilized following release from nocodazole arrest. Cyclin B1 and securin are targets of APC/C-Cdc20 when SAC turns off. To further support that DAB2IP is required for checkpoint maintenance, we tested the degradation kinetics of cyclin B1 and securin in C4-2 cells after release from nocodazole-mediated prometaphase arrest. When compared with control cells, cyclin B1 and securin were dramatically stabilized in C4-2 D2 cells (Figure 4D). Since Cdc20 autoubiquitylation by APC/C-MCC is necessary for MCC disassembly and SAC silencing, we then tested DAB2IP's effect on the ubiquitylation level of Cdc20 during prometaphase. We co-transfected Myc-Cdc20, Flag-DAB2IP (or Flag empty vector) and HA-Ubi expression vector in HeLa cells, synchronized in prometaphase by nocodazole followed by MG132 treatment, a specific inhibitor of proteosome-mediated protein degradation. The signal of polyubiquitylated Cdc20 in DAB2IP-expressing HeLa cells was much weaker than in cells without DAB2IP (Figure 5A). A similar effect was also observed in 293T cells (Figure 5B).

DAB2IP sensitizes cells to microtubule-stabilizing drugs relying on its role in SAC maintenance

Microtubule-stabilizing agents have been extensively used in the treatment of solid tumors (29,30). However, resistance to chemotherapy can develop that leads to poor clinical outcomes for patients (31,32). These anti-mitotic drugs, such as paclitaxel, kill cancer cells by relying on spindle checkpoint-mediated mitotic arrest (33). DAB2IP increased paclitaxel-induced mitotic arrest in PCa cells (Figure 6A). In addition, the expression of DAB2IP sensitized C4-2 cells to paclitaxel or docetaxel treatment (Figure 6 B-C). Consistently, IB was performed to detect cleaved PARP-1, which was greater in C4-2 D2 cells compared to C4-2 Neo in response to paclitaxel (Figure 6D). A similar effect was observed in HeLa cells (Supplementary Figure 4). Further, Mad2, which is essential for SAC maintenance, was depleted resulting in an abrogation of paclitaxel sensitivity even in C42-D2 cells (Figure 6E). Additionally, DAB2IP expression was significantly increased upon MAD2 suppression indicating that DAB2IP's function in SAC relies on the Mad2 pathway and that their simultaneous presence is required to induce paclitaxel sensitivity.

Discussion

It has been shown that the checkpoint silencing process is initiated though stripping of SAC proteins and turning off the production of MCC at the kinetochore (20,34,35). However, the process by which disassembly of the existing cytosolic MCC occurs is still unknown. In this study, we reveal a novel role of DAB2IP in SAC maintenance by stabilizing APC/C-MCC. The presence of DAB2IP promotes binding of Mad2 and BubR1 with Cdc20 and the APC/C complex. On the other hand, loss of DAB2IP contributes to the disassociation of MCC from the APC/C, leading to premature SAC inactivation and APC/C activation. Consistent with its role in SAC, expression of DAB2IP in C4-2 cells leads to a significantly higher incidence of mitotic arrest when exposed to nocodazole and paclitaxel (Figure 2C and 6A).

To date, several proteins have been identified as components of the MCC complex and have been suggested to be participants in checkpoint silencing, including PP1 (36), $p31^{comet}$ (36,37), UbcH10 (38), CUEDC2 (24) and APC15 (21,39,40). Our study demonstrates that DAB2IP plays an opposing role to these aforementioned regulators and contributes to SAC maintenance and prevention of premature mitotic exit. Previous studies revealed that Cdc20 autoubiquitylation is necessary for MCC release. Moreover, proteasome inhibition leads to accumulation of large amounts of MCC-APC/C during SAC activation (40,41). Uzuova et al. proposed that continuous cycles of synthesis and degradation of Cdc20 during prometaphase is helpful for rapid MCC turnover and SAC silencing when MCC production is stopped at the kinetochore. Several groups have reported that APC15, a subunit of the APC/C complex is responsible for Cdc20 autoubiquitylation and proteasomal degradation during prometaphase, which triggers MCC disassembly. Here, we found that DAB2IP can interact with Cdc20 and inhibit Cdc20 ubiquitylation during prometaphase. Therefore, DAB2IP negatively regulates APC/C-MCC turnover and slows down the degradation of cyclin B1 and securin after nocodazole release (Figure 4). How DAB2IP-mediated SAC arrest releasing occurs is still an

unanswered question. Based on our study, we propose two possible scenarios: (1) DAB2IP is post-translationally modified during prometaphase and the modification can be removed when the SAC is silenced (Figure 6F); (2) DAB2IP might be also ubiquitylated and degraded by APC/C during the metaphase-anaphase transition (Figure 6G). We will investigate these two models in our future studies.

SAC plays an essential role in faithful chromosome segregation during anaphase and maintenance of chromosome stability. Complete loss of SAC is lethal even for tumor cells. However, partial loss of the SAC is responsible for causing chromosome missegregation and aneuploidy, which is a common feature of many cancers. Evidence to support this idea came from studies using mice with weakened SAC function that were found to have a high incidence of aneuploidy and tumor formation (42-44). Consistent with its role as a tumor suppressor, our work shows that DAB2IP can significantly inhibit missegregation and aneuploidy. Our previous studies demonstrated that DAB2IP participates in DNA damage response and that loss of DAB2IP leads to increased radiation resistance and poor prognosis (9-11). We and others also revealed that many DNA damage repair -related factors play important roles in mitotic regulation, including microtubule organization, spindle checkpoint and centromeric cohesion (45-48). We speculate that DAB2IP may couple the DNA damage response and mitotic regulation to ensure genomic and chromosomal stability, which in turn prevents tumor growth.

Microtubule damaging agents suppress microtubule dynamics and activate the SAC by destroying the kinetochore-microtubule (k-MT) attachment. Persistent trapping of cells in mitosis by SAC will lead to apoptosis in a Cdk1-dependent manner (49). However, mitotic slippage limits the efficacy of these classes of drugs. Ma et al. found that depletion of $p31^{comet}$ sensitized tumor cells to spindle damaging agents occurs by delaying checkpoint silencing and increasing the duration of mitotic arrest (50). Our results demonstrated that presence of

DAB2IP, which is similar to loss-of-function of $p31^{comet}$, could also increase the sensitivity of C4-2 cells to microtubule damaging agents, including paclitaxel and docetaxel. Wu et al. revealed that DAB2IP negatively regulated the expression of clusterin (sCLU), which is an important anti-apoptosis factor, and correlated with chemoresistance of PCa cells, through which DAB2IP increased chemosensitivity (29). More importantly, we also found that knockdown of Mad2 completely abrogates chemosensitivity of C4-2 D2 cells, suggesting that the increased cytotoxicity induced by microtubule damaging drugs partially stems from the prolonged mitotic block mediated by robust SAC in C4-2 D2 cells.

In summary, we propose a model for DAB2IP's role in SAC (Figure 6F and G). DAB2IP, as a component of APC/C-MCC, could inhibit ubiquitylation and degradation of Cdc20 during prometaphase, which then blocks the disassembly of APC/C-MCC and inhibits premature SAC silencing. Loss of DAB2IP increases chromosome missegragation and aneuploidy, which contributes to tumorigenesis and chemoresistance. In conclusion, our work shed lights on a novel function of DAB2IP contributing to chromosome stability maintenance.

Supplementary Material

Supplementary Figures 1–10 are available at Carcinogenesis Online at http://carcin.oxfordjournals.org/

Funding

This work was supported by the National Institute of Health grants CA175879 (DS), CA166677 (BPC), Department of Defense W81XWH-11-1-0270 (DS), Department of Veterans Affairs (AH) and National Natural Science Foundation of China. Grant # 81472919 (ZS).

Acknowledgment

We thank Dr. Hongtao Yu (University of Texas Southwestern Medical Center, Dallas, Texas) for kindly providing the HA-Ubi plasmid.

Conflict of Interest Statement: None declared.

Reference

1. Dote, H., *et al.* (2004) Aberrant promoter methylation in human DAB2 interactive protein (hDAB2IP) gene in breast cancer. *Clin Cancer Res*, **10**, 2082-9.
2. Chen, H., *et al.* (2002) Differential regulation of the human gene DAB2IP in normal and malignant prostatic epithelia: cloning and characterization. *Genomics*, **79**, 573-81.
3. Shen, Y.J., *et al.* (2014) Downregulation of DAB2IP results in cell proliferation and invasion and contributes to unfavorable outcomes in bladder cancer. *Cancer Sci*, **105**, 704-12.
4. Zhang, X., *et al.* (2012) Low expression of DAB2IP contributes to malignant development and poor prognosis in hepatocellular carcinoma. *J Gastroenterol Hepatol*, **27**, 1117-25.
5. Smits, M., *et al.* (2012) EZH2-regulated DAB2IP is a medulloblastoma tumor suppressor and a positive marker for survival. *Clin Cancer Res*, **18**, 4048-58.
6. Xie, D., *et al.* (2009) DAB2IP coordinates both PI3K-Akt and ASK1 pathways for cell survival and apoptosis. *Proc Natl Acad Sci U S A*, **106**, 19878-83.
7. Xie, D., *et al.* (2010) Role of DAB2IP in modulating epithelial-to-mesenchymal transition and prostate cancer metastasis. *Proc Natl Acad Sci U S A*, **107**, 2485-90.
8. Min, J., *et al.* (2010) An oncogene-tumor suppressor cascade drives metastatic prostate cancer by coordinately activating Ras and nuclear factor-kappaB. *Nat Med*, **16**, 286-94.
9. Kong, Z., *et al.* (2010) Downregulation of human DAB2IP gene expression in prostate cancer cells results in resistance to ionizing radiation. *Cancer Res*, **70**, 2829-39.
10. Yu, L., *et al.* (2012) DAB2IP regulates autophagy in prostate cancer in response to combined treatment of radiation and a DNA-PKcs inhibitor. *Neoplasia*, **14**, 1203-12.
11. Jacobs, C., *et al.* (2014) DOC-2/DAB2 interacting protein status in high-risk prostate cancer correlates with outcome for patients treated with radiation therapy. *Int J Radiat Oncol Biol Phys*, **89**, 729-35.
12. Rajagopalan, H., *et al.* (2003) The significance of unstable chromosomes in colorectal cancer. *Nat Rev Cancer*, **3**, 695-701.
13. McGranahan, N., *et al.* (2012) Cancer chromosomal instability: therapeutic and diagnostic challenges. *EMBO Rep*, **13**, 528-38.
14. Gordon, D.J., *et al.* (2012) Causes and consequences of aneuploidy in cancer. *Nat Rev Genet*, **13**, 189-203.
15. Fang, X., *et al.* (2011) Aneuploidy and tumorigenesis. *Semin Cell Dev Biol*, **22**, 595-601.
16. Lara-Gonzalez, P., *et al.* (2012) The spindle assembly checkpoint. *Curr Biol*, **22**, R966-80.
17. Kim, S., *et al.* (2011) Mutual regulation between the spindle checkpoint and APC/C. *Semin Cell Dev Biol*, **22**, 551-8.
18. Lara-Gonzalez, P., *et al.* (2011) BubR1 blocks substrate recruitment to the APC/C in a KEN-box-dependent manner. *J Cell Sci*, **124**, 4332-45.
19. Sczaniecka, M., *et al.* (2008) The spindle checkpoint functions of Mad3 and Mad2 depend on a Mad3 KEN box-mediated interaction with Cdc20-anaphase-promoting

complex (APC/C). *J Biol Chem*, **283**, 23039-47.

20. Jia, L.*, et al.* (2013) Tracking spindle checkpoint signals from kinetochores to APC/C. *Trends Biochem Sci*, **38**, 302-11.
21. Uzunova, K.*, et al.* (2012) APC15 mediates CDC20 autoubiquitylation by APC/C(MCC) and disassembly of the mitotic checkpoint complex. *Nat Struct Mol Biol*, **19**, 1116-23.
22. Musacchio, A.*, et al.* (2012) The spindle-assembly checkpoint and the beauty of self-destruction. *Nat Struct Mol Biol*, **19**, 1059-61.
23. Reddy, S.K.*, et al.* (2007) Ubiquitination by the anaphase-promoting complex drives spindle checkpoint inactivation. *Nature*, **446**, 921-5.
24. Gao, Y.F.*, et al.* (2011) Cdk1-phosphorylated CUEDC2 promotes spindle checkpoint inactivation and chromosomal instability. *Nat Cell Biol*, **13**, 924-33.
25. Potts, P.R.*, et al.* (2005) Human MMS21/NSE2 is a SUMO ligase required for DNA repair. *Mol Cell Biol*, **25**, 7021-32.
26. van Meerloo, J.*, et al.* (2011) Cell sensitivity assays: the MTT assay. *Methods Mol Biol*, **731**, 237-45.
27. Thompson, S.L.*, et al.* (2010) Mechanisms of chromosomal instability. *Curr Biol*, **20**, R285-95.
28. Kops, G.J.*, et al.* (2005) On the road to cancer: aneuploidy and the mitotic checkpoint. *Nat Rev Cancer*, **5**, 773-85.
29. Wu, K.*, et al.* (2013) The mechanism of DAB2IP in chemoresistance of prostate cancer cells. *Clin Cancer Res*, **19**, 4740-9.
30. Ahmed, A.A.*, et al.* (2007) The extracellular matrix protein TGFBI induces microtubule stabilization and sensitizes ovarian cancers to paclitaxel. *Cancer Cell*, **12**, 514-27.
31. Seruga, B.*, et al.* (2011) Drug resistance in metastatic castration-resistant prostate cancer. *Nat Rev Clin Oncol*, **8**, 12-23.
32. Galsky, M.D.*, et al.* (2010) Docetaxel-based combination therapy for castration-resistant prostate cancer. *Ann Oncol*, **21**, 2135-44.
33. Yamada, H.Y.*, et al.* (2006) Spindle checkpoint function and cellular sensitivity to antimitotic drugs. *Mol Cancer Ther*, **5**, 2963-9.
34. Wang, Y.*, et al.* (2014) The current view for the silencing of the spindle assembly checkpoint. *Cell Cycle*, **13**, 1694-701.
35. Sacristan, C.*, et al.* (2014) Joined at the hip: kinetochores, microtubules, and spindle assembly checkpoint signaling. *Trends Cell Biol*.
36. Vanoosthuyse, V.*, et al.* (2009) A novel protein phosphatase 1-dependent spindle checkpoint silencing mechanism. *Curr Biol*, **19**, 1176-81.
37. Westhorpe, F.G.*, et al.* (2011) p31comet-mediated extraction of Mad2 from the MCC promotes efficient mitotic exit. *J Cell Sci*, **124**, 3905-16.
38. Stegmeier, F.*, et al.* (2007) Anaphase initiation is regulated by antagonistic ubiquitination and deubiquitination activities. *Nature*, **446**, 876-81.
39. Foster, S.A.*, et al.* (2012) The APC/C subunit Mnd2/Apc15 promotes Cdc20 autoubiquitination and spindle assembly checkpoint inactivation. *Mol Cell*, **47**, 921-32.

40. Mansfeld, J., *et al.* (2011) APC15 drives the turnover of MCC-CDC20 to make the spindle assembly checkpoint responsive to kinetochore attachment. *Nat Cell Biol*, **13**, 1234-43.
41. Varetti, G., *et al.* (2011) Homeostatic control of mitotic arrest. *Mol Cell*, **44**, 710-20.
42. Michel, L.S., *et al.* (2001) MAD2 haplo-insufficiency causes premature anaphase and chromosome instability in mammalian cells. *Nature*, **409**, 355-9.
43. Dai, W., *et al.* (2004) Slippage of mitotic arrest and enhanced tumor development in mice with BubR1 haploinsufficiency. *Cancer Res*, **64**, 440-5.
44. Orr, B., *et al.* (2013) A double-edged sword: how oncogenes and tumor suppressor genes can contribute to chromosomal instability. *Front Oncol*, **3**, 164.
45. Shang, Z., *et al.* (2014) DNA-PKcs activates the Chk2-Brca1 pathway during mitosis to ensure chromosomal stability. *Oncogenesis*, **3**, e85.
46. Shang, Z.F., *et al.* (2010) Inactivation of DNA-dependent protein kinase leads to spindle disruption and mitotic catastrophe with attenuated checkpoint protein 2 Phosphorylation in response to DNA damage. *Cancer Res*, **70**, 3657-66.
47. Yang, C., *et al.* (2011) Aurora-B mediated ATM serine 1403 phosphorylation is required for mitotic ATM activation and the spindle checkpoint. *Mol Cell*, **44**, 597-608.
48. Wang, R.H., *et al.* (2004) A requirement for breast-cancer-associated gene 1 (BRCA1) in the spindle checkpoint. *Proc Natl Acad Sci U S A*, **101**, 17108-13.
49. Castedo, M., *et al.* (2002) Cyclin-dependent kinase-1: linking apoptosis to cell cycle and mitotic catastrophe. *Cell Death Differ*, **9**, 1287-93.
50. Ma, H.T., *et al.* (2012) Depletion of p31comet protein promotes sensitivity to antimitotic drugs. *J Biol Chem*, **287**, 21561-9.

Figure Legends

Figure1. Expression of DAB2IP inhibits missegragation and aneuploidy and loss of DAB2IP leads to CIN. **A.** Western blots showing the shRNA-mediated suppressed expression of DAB2IP in HCT116 cells. **B.** Representative images of diploidy and aneuploidy chromosome spread. **C.** Chromosome numbers from individual metaphase spreads of control- and DAB2IP- shRNA transfected HCT116 cells. **D.** The representative images of normal and missegragation (lagging) chromosomes in C4-2 Neo and D2 cells. The cells were stained with anti-α-tubulinantibodies. **E.** The proportion of cells with chromosome-missegregation in C4-2 Neo and D2 cells are presented as the mean and SD from three independent experiments (**$p < 0.01$ as compared with control cells). **F.** The proportion of cells with chromosome-missegregation in HeLa siCon and siD2 cells are presented as the mean and SD from three independent experiments (*$p < 0.05$ as compared with control cells). Westernblot shown in Fig. 1 (A) is cropped and the full-length image is shown in Supplementary Figure 5 available at Carcinogenesis Online.

Figure 2. DAB2IP maintains a robust spindle assembly checkpoint. **A and B.** Exponentially growing C4-2 Neo and D2 cells were subjected to the same immunofluorescent staining protocol. The percentage of each mitotic substage among mitotic cells was determined with the presented morphology. **C and D**. C4-2 Neo and D2 cells or HeLa siCon and siD2 cells were treated with 50ng/ml nocodazole for different times. Cells were collected and fixed at the indicated time and the percentage of pH3-positive cells were determined by flow cytometry. Mitotic index represented is from three independent experiments. **E and F.** The expression levels of DAB2IP, cyclin B1, and actin were analyzed by immunoblotting. Westernblots shown in Fig.2 (E-F) are cropped and the full-length images are shown in Supplementary Figure 6 available at Carcinogenesis Online.

Figure 3. DAB2IP interacts with Cdc20 through its CPR region. **A and B.** C4-2 D2 cells were synchronized at prometaphase using nocodazole arrest and the mitotic cells were collected by shaking off. Cells lysates were immunoprecipitated with an anti-DAB2IP (A) or anti-Cdc20 (B) or Ig G and then Cdc20, DAB2IP, Cdc27 and Mad2 were analyzed by western blotting. **C.** Flag conjugated DAB2IP, Flag- empty vector and HA-Cdc20 were transfected into 293T cells. The cells were then treated with 50ng/ml nocodazole for 16hours and cells lysates were IP with anti-Flag antibody, the HA signal was examined by western blotting. **D.** Schema of different truncated domains of DAB2IP. **E.** Various cDNA constructs of DAB2IP truncations were co-transfected with HA-Cdc20 into 293T cells and then were immunoprecipitated using anti-Flag antibody. IP-Westernblots shown in Fig. 3 (A-C, E) are cropped and the full-length images are shown in Supplementary Figure 7 available at Carcinogenesis Online.

Figure 4. DAB2IP maintains MCC stability. **A and B**. Western blots showing Cdc20 and APC/C immunoprecipitation from nocodazole blocked C4-2 D2 and Neo or HeLa siCon and siD2 prometaphase cells lysates. The amounts of Mad2 and BubR1 binding with Cdc20 and Cdc27 were determined. **C.** DAB2IP-proficient and -deficient C4-2 cells were synchronized with nocodazole and Cdc20 was IP at the indicated times after nocodazole release. The amount of Mad2 binding with Cdc20 was visualized by immunoblotting. Whole cell lysates were analyzed with the indicated antibodies. **D.** C4-2 Neo and D2 cells were synchronized in prometaphase using nocodazole and then released into fresh media. Cells were collected at the indicated times after release. The expression levels of DAB2IP, cyclin B1, securin, Cdc27 and HSP70 were analyzed by immunoblotting. IP-Westernblots shown in Fig. 4 (A-D) are cropped and the full-length images are shown in Supplementary Figures 8 available at Carcinogenesis Online.

Figure 5. DAB2IP inhibites the ubiquitylation of Cdc20 in prometaphase. Myc-Cdc20 and HA-Ubi were co-transfected with Flag-DAB2IP or empty vector in HeLa (A) and 293T (B) cells. Cells were harvested at 12hours after MG132 (1μM) treatment. Cdc20 was immunoprecipitated using anti-Myc antibody. CoIP products were analyzed by Western blotting using anti-HA antibody. Equal loading of whole cell lysates were subjected to immunoblotting with anti-Flag and anti-Myc antibodies. IP-Westernblots shown in Fig. 5 (A-B) are cropped and the full-length images are shown in Supplementary Figure 9 available at Carcinogenesis Online.

Figure 6. DAB2IP enhances chemosensitivity in a Mad2-dependent manner. **A.** C4-2 D2 and Neo cells were treated with paclitaxel and collected at 24 hours. The proportion of pH3-positive cells were analyzed by flow cytometry. Mitotic index is representative of three independent experiments. **B and C.** C4-2 D2 and Neo cells were exposed to different concentrations of the indicated chemotherapeutic drugs for 48 hours, and the cell number was tested with MTT assay. Results obtained from three independent experiments (means $\pm$ SEM). **D.** Cells were lysed 20 hours after exposure to indicated concentration of paclitaxel and subjected to Western blots. **E.** Right, C4-2 D2 and Neo cells were treated with control and Mad2 siRNA for 24 hours, and the cells seeded and exposed to different concentrations of the indicated paclitaxel for 48 hours, then the cell number was tested with MTT assay; left, Western blot showed levels of indicated proteins from extracts of C4-2 D2 and Neo cells treated with indicated siRNAs. **F and G.** DAB2IP blocks the turnover of the MCC during prometaphse. F. The spindle assembly checkpoint signal is generated from unoccupied kinetochore and transmits to cytosol by promoting formation APC/C-MCC. The Cdc20 in MCC can also be autoubiquitylated even in the prometaphase with the activated SAC. When generation of MCC is stopped, newly synthesized Cdc20 will bind with APC/C. In

DAB2IP-deficient cells, Cdc20 may prone to degradation, which leads to premature mitosis exit and increases chromosomal instability and tumorigenesis. G. DAB2IP can interact with Cdc20 and contribute to maintain Cdc20 stability in prometaphase and a robust SAC. This progression may rely on the post-translational modification of DAB2IP. Westernblots shown in Fig. 6 (D, E) are cropped and the full-length images are shown in Supplementary Figure 10 available at Carcinogenesis Online.

Figure 1

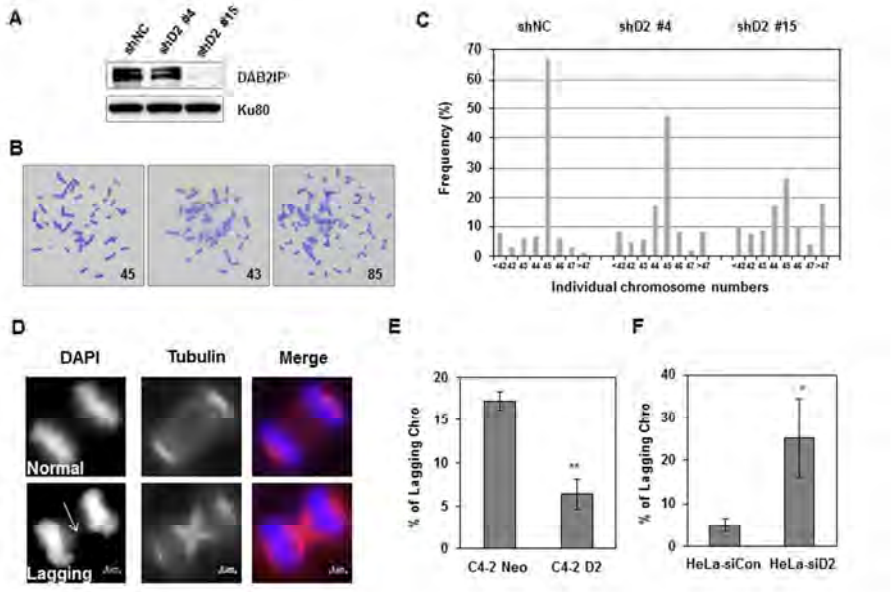

254x190mm (96 x 96 DPI)

Figure 2

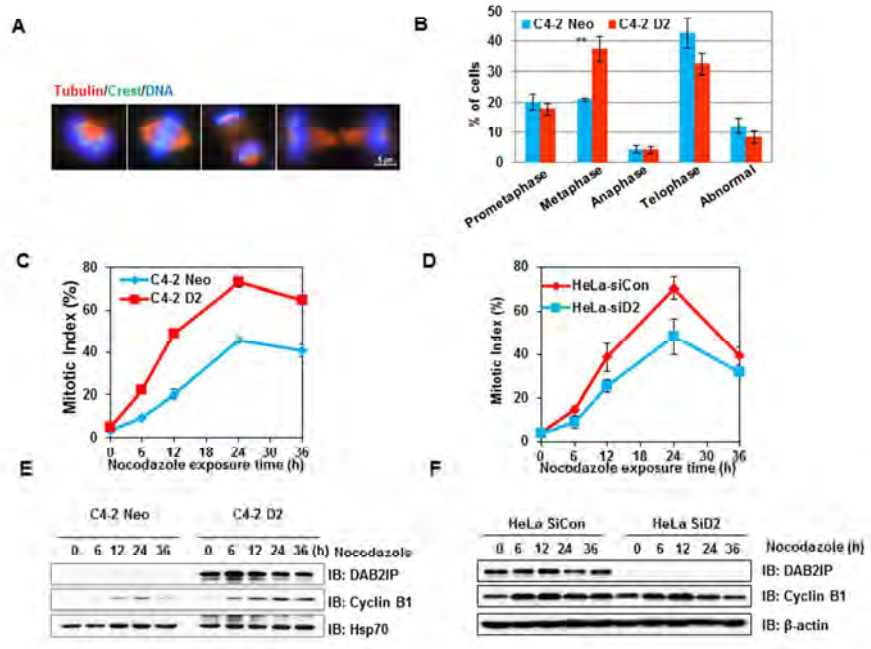

254x190mm (96 x 96 DPI)

Figure 3

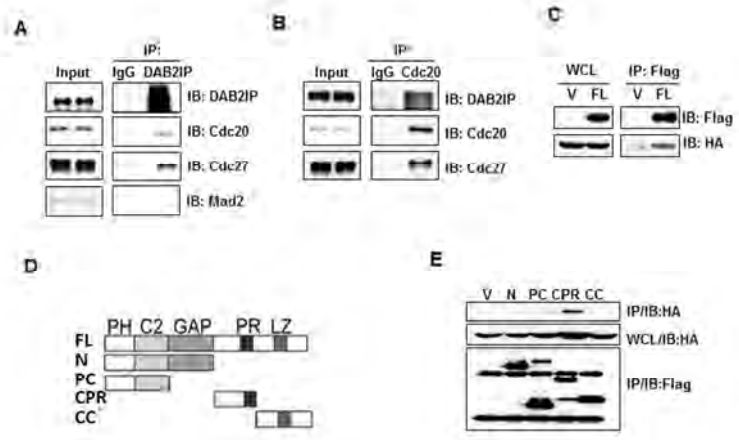

254x190mm (96 x 96 DPI)

Figure 4

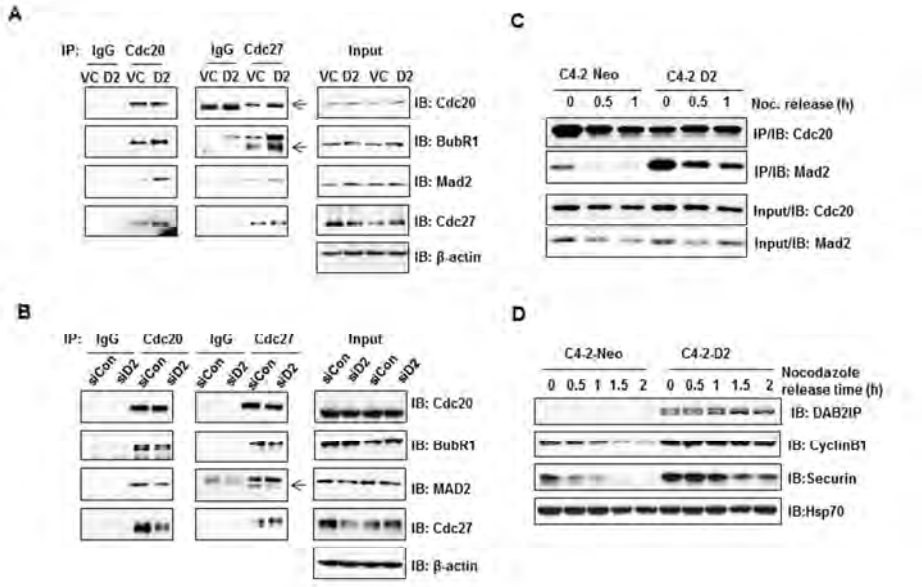

254x190mm (96 x 96 DPI)

Figure 5

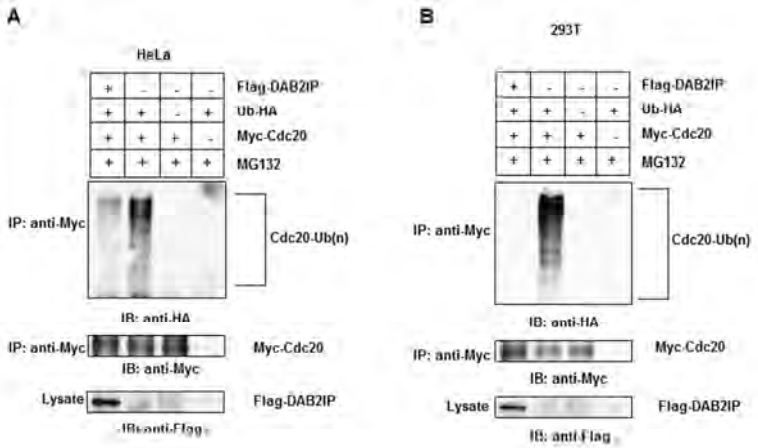

254x190mm (96 x 96 DPI)

Figure 6

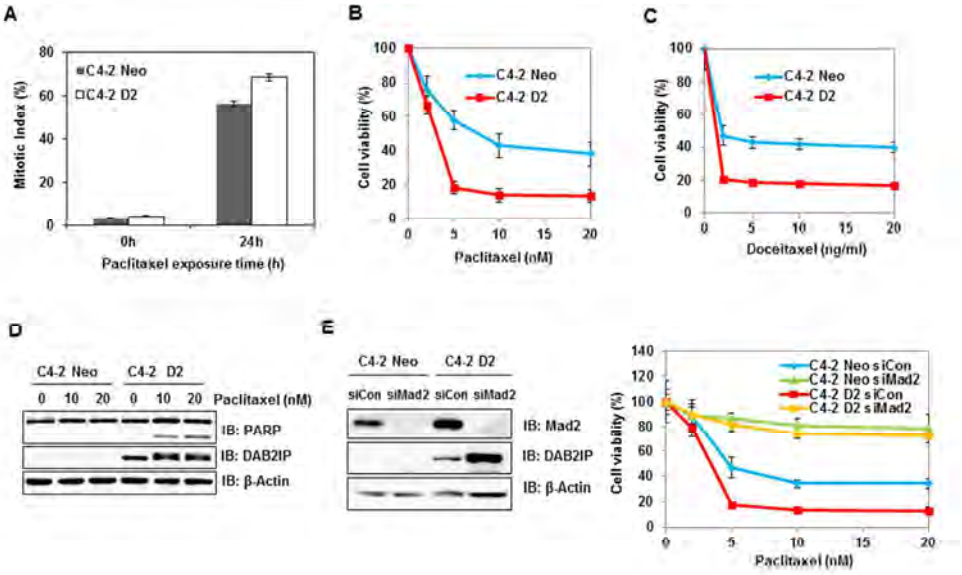

254x190mm (96 x 96 DPI)

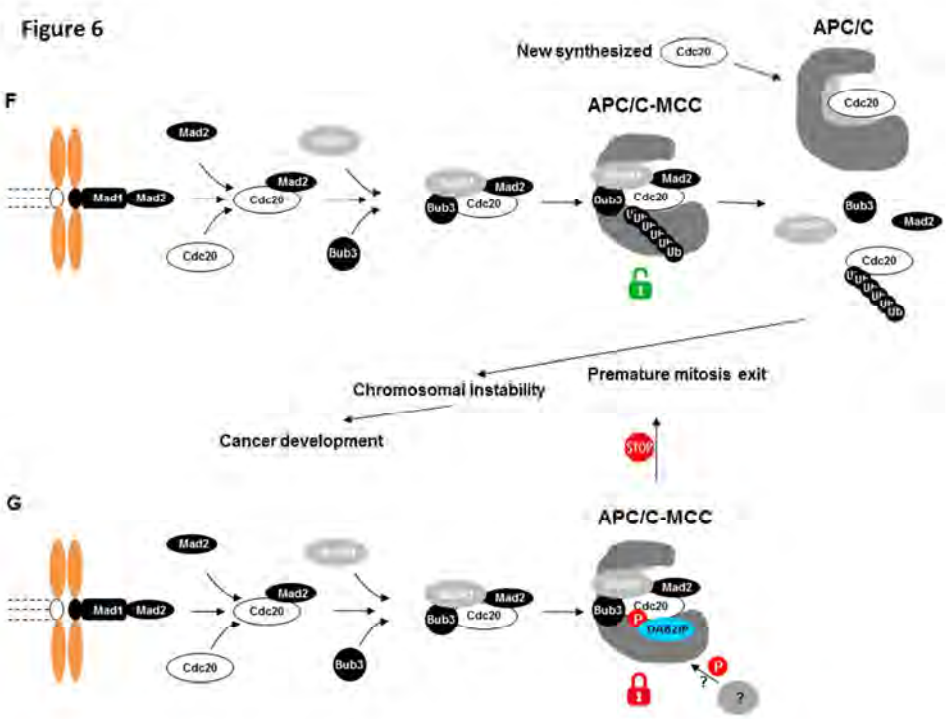

254x190mm (96 x 96 DPI)

Supplementary Figure 1. Depletion of DAB2IP weakens SAC in MEFs cells. **A.** DAB2IP-knockout or wild-type MEFs were treated with 50ng/ml nocodazole and collected at indicated time. The percentage of pH3-positive cells were performed by flow cytometry. Mitotic index were representative of three independent experiments. **B.** The expression levels of DAB2IP, and cyclin B1 were analyzed by immunoblotting.

Supplementary Figure 2. DAB2IP didn't affect the localization of spindle checkpoint proteins at kinetochore in prometaphase. **A , B and C**. Exponentially growing C4-2 D2, Neo cells were subjected to the same immunofluorescent staining protocol using anti-Mad2, BubR1 and Bub1 antibodies.

Supplementary Figure 3. DAB2IP interacts with Cdc20 in HeLa cells. Cells lysates from HeLa cells were immunoprecipitated with anti-DAB2IP antibody or IgG, the Cdc20, DAB2IP, Cdc27 and Mad2 were analyzed by immunoblotting.

Supplementary Figure 4. Loss of DAB2IP enhances chemoresistance in HeLa cells. **A.** HeLa cells were transfected with control- or DAB2IP-siRNA and were then treated with paclitaxel and collected at indicated time. The proportion of pH3-positive cells was analyzed by flow cytometry. Mitotic index is representative of three independent experiments. **B and C**. Control- and DAB2IP-siRNA-treated HeLa cells were exposed to different concentrations of indicated chemotherapeutic drugs for 48 hours, and the cell number was tested by MTT assay. Results obtained from three independent experiments (means $\pm$ SEM). **D.** Cells were lysed 20 hours after exposure to indicated concentration of paclitaxel and subjected to Western blotting analysis.

Supplementary Figure 1

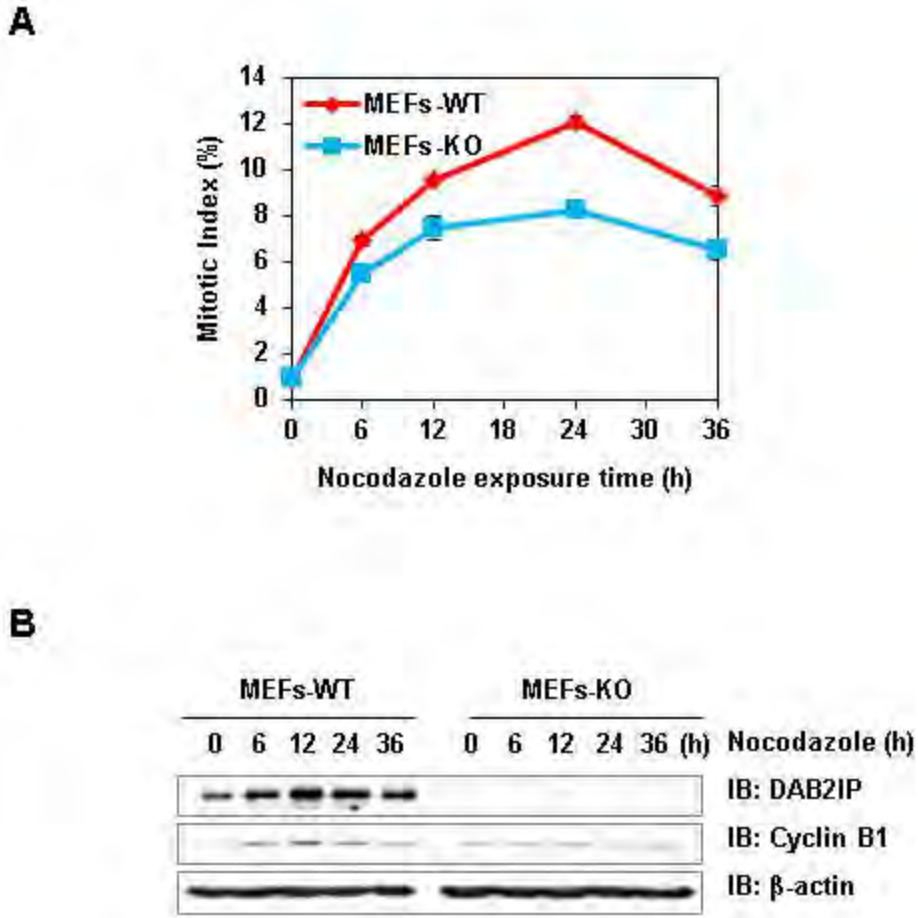

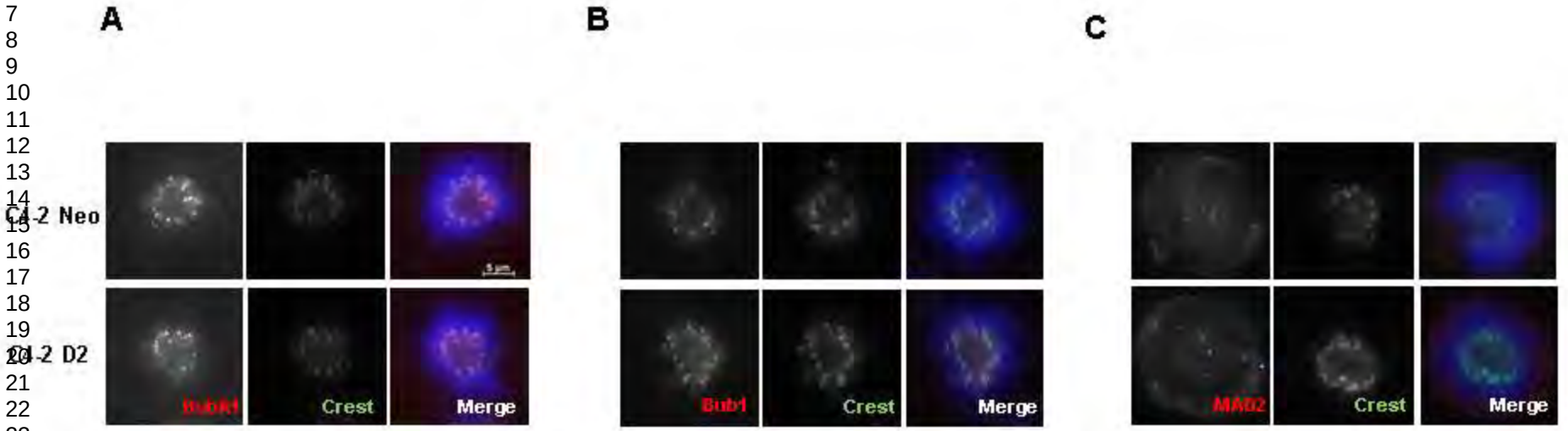
A
B
C
C4-2 Neo
C4-2 D2
BubR1
Bub1
MAD2
Crest
Merge
Crest
Merge
Crest
Merge

Supplementary Figure 3

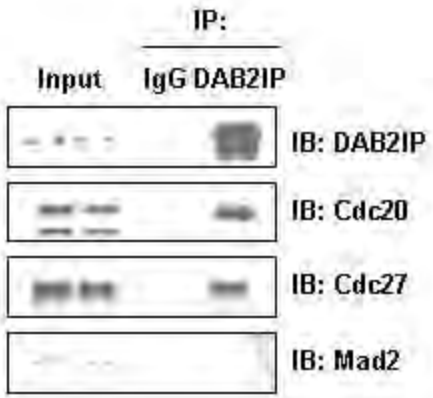

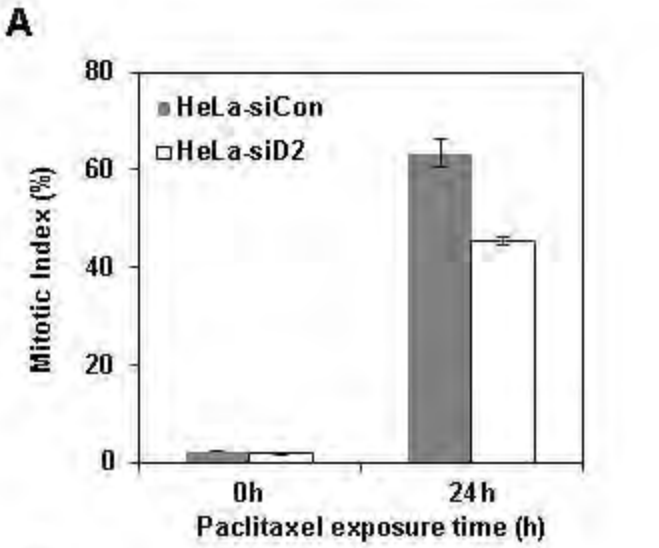
A
80
60
40
20
0
HeLa-siCon
HeLa-siD2
Mitotic Index (%)
0h
24h
Paclitaxel exposure time (h)

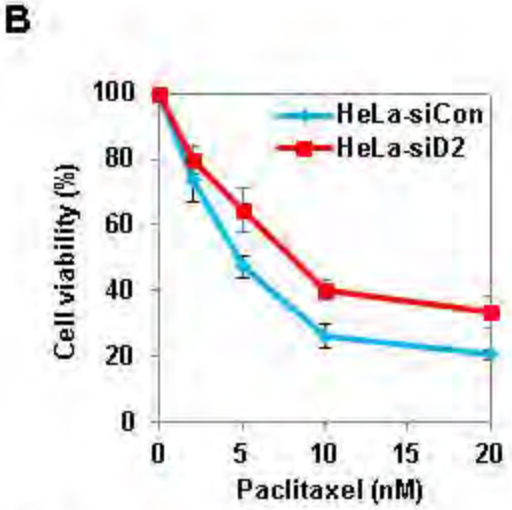
B
100
80
60
40
20
0
HeLa-siCon
HeLa-siD2
Cell viability (%)
0
5
10
15
20
Paclitaxel (nM)

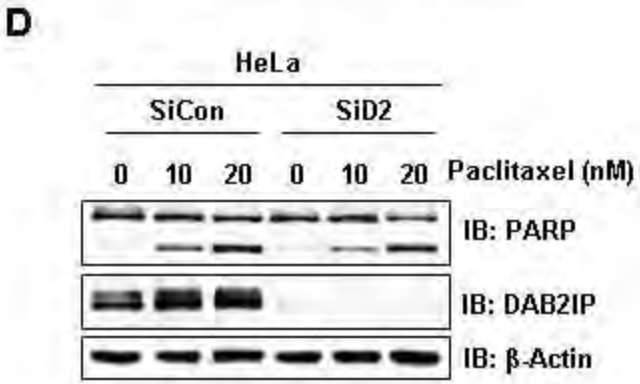
D
HeLa
SiCon
SiD2
0 10 20 0 10 20 Paclitaxel (nM)
IB: PARP
IB: DAB2IP
IB: β-Actin

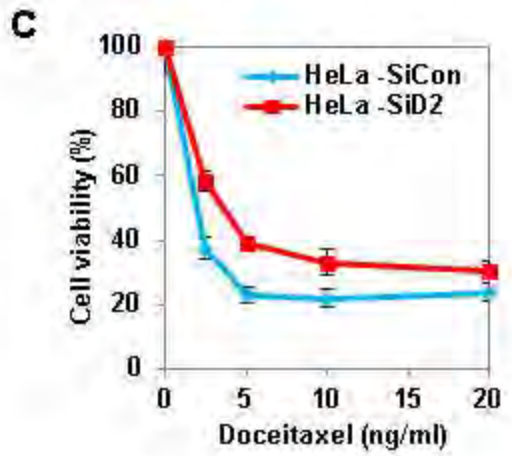
C
100
80
60
40
20
0
HeLa -SiCon
HeLa -SiD2
Cell viability (%)
0
5
10
15
20
Doceitaxel (ng/ml)

Supplementary Figure 5

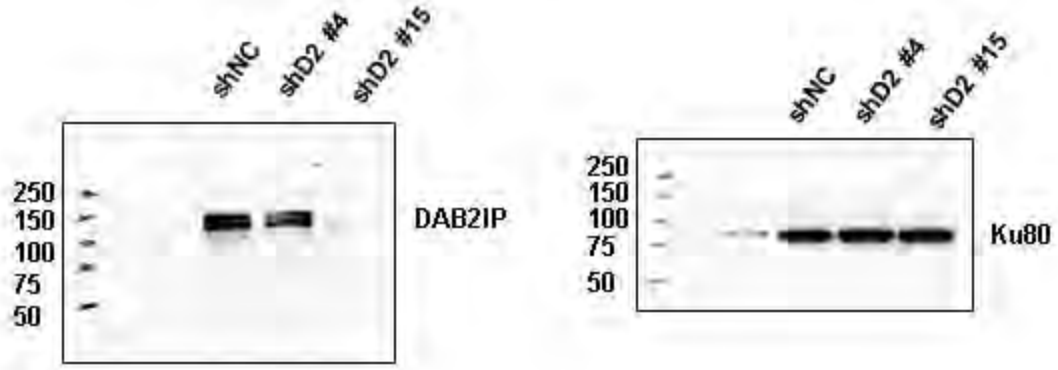

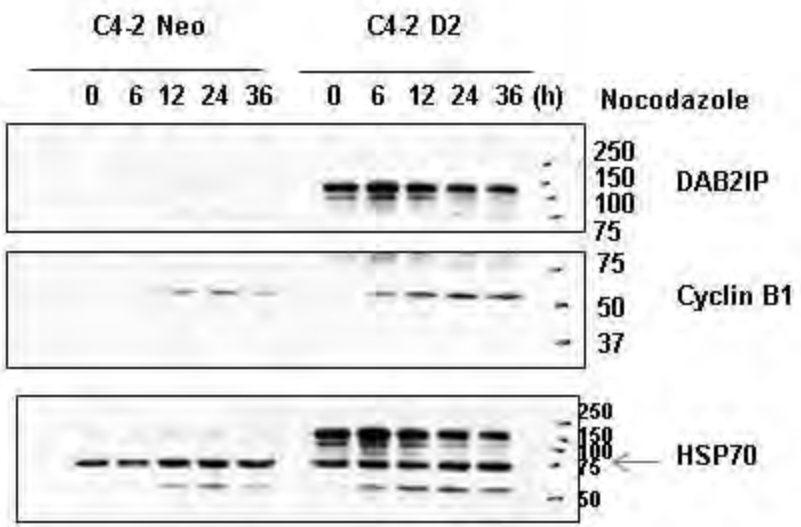
C4-2 Neo
C4-2 D2
0 6 12 24 36 0 6 12 24 36 (h)
Nocodazole
250
150
100
75
DAB2IP
75
50
37
Cyclin B1
250
150
100
75
50
HSP70


HeLa SiCon
HeLa SiD2
0 6 12 24 36 0 6 12 24 36
Nocodazole (h)
250
150
100
75
DAB2IP
75
50
37
Cyclin B1
50
37
actin

Supplementary Figure 7

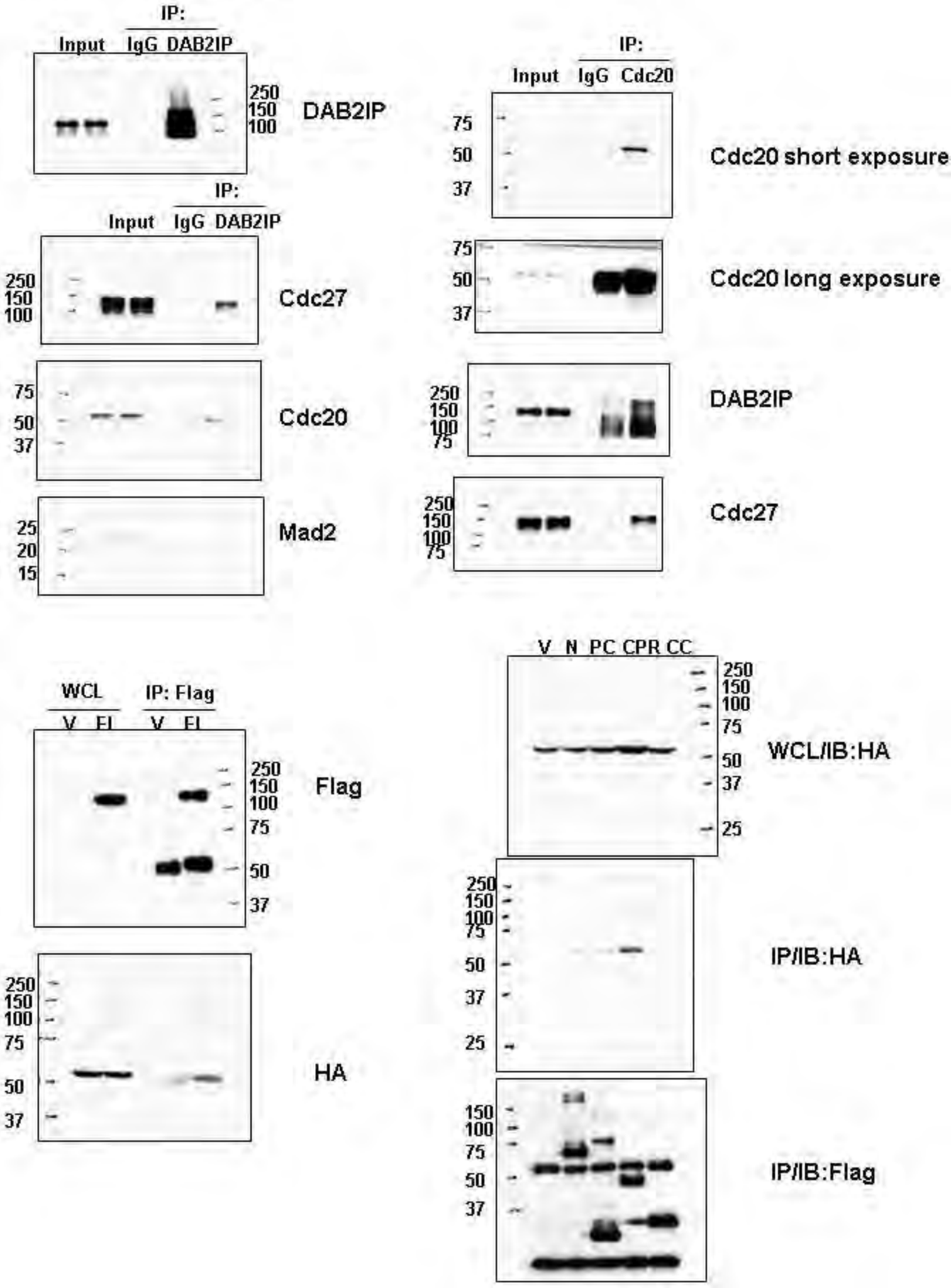

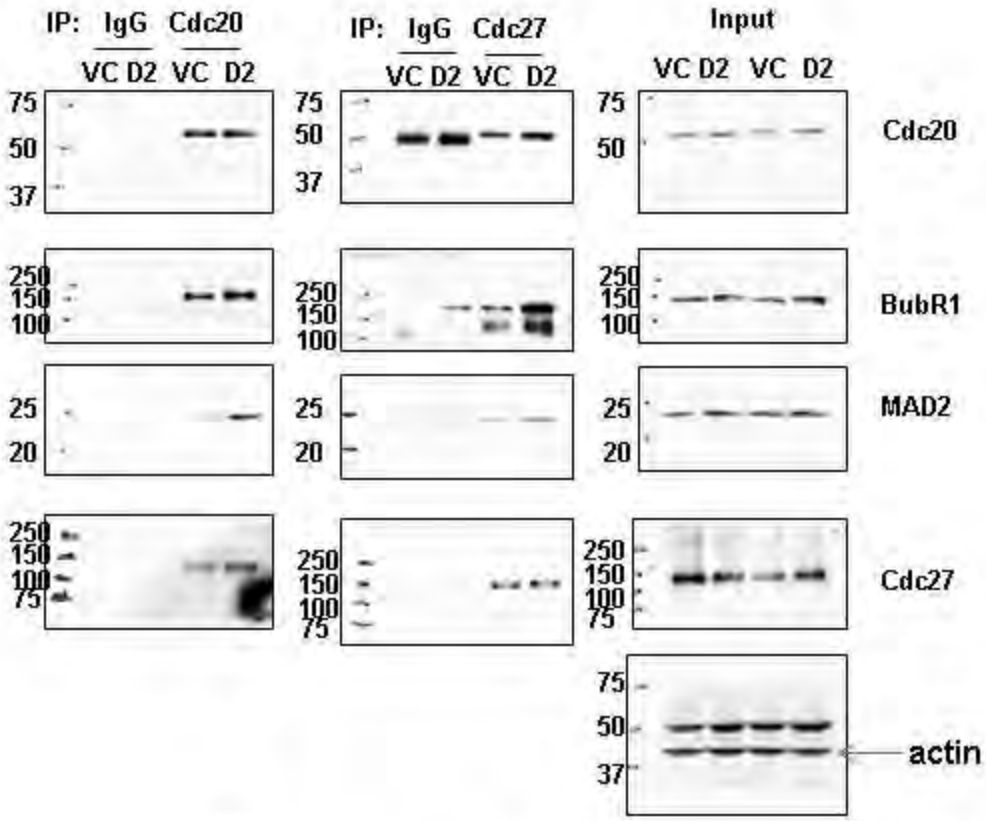
IP: IgG Cdc20
VC D2 VC D2
IP: IgG Cdc27
VC D2 VC D2
Input
VC D2 VC D2
75
50
37
Cdc20
250
150
100
BubR1
25
20
MAD2
250
150
100
75
Cdc27
75
50
37
actin

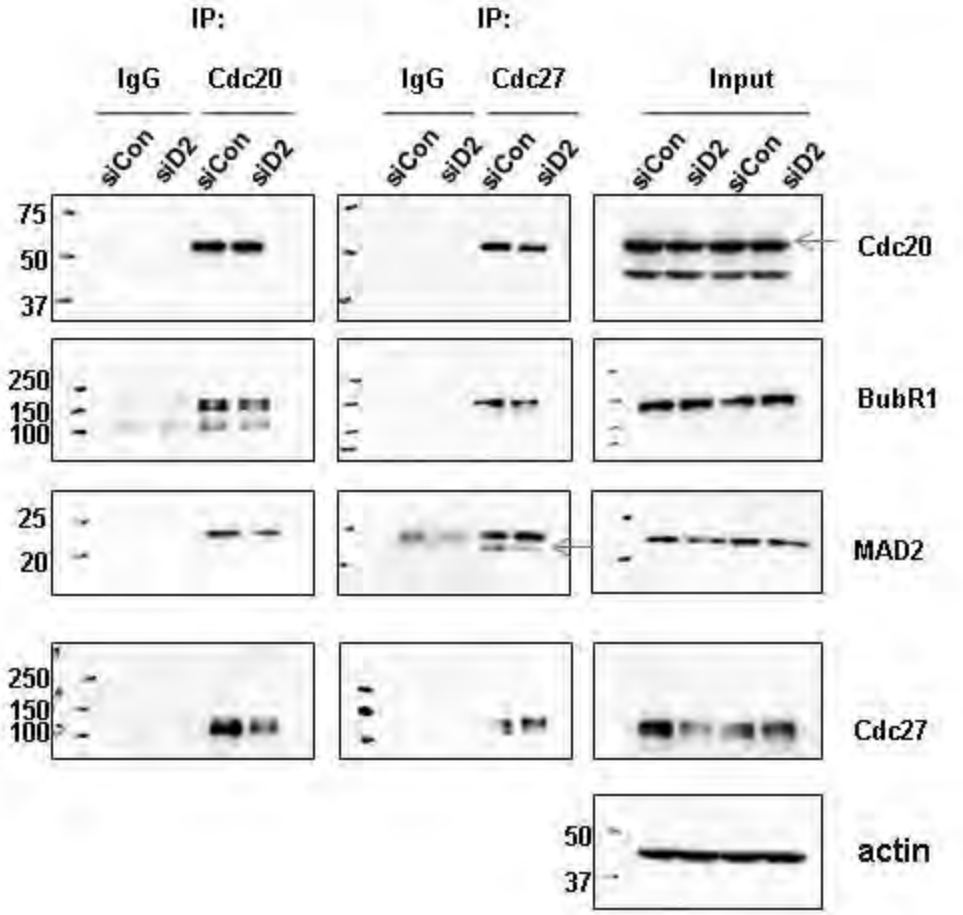
IP:
IgG Cdc20
IP:
IgG Cdc27
Input
siCon siD2 siCon siD2
siCon siD2 siCon siD2
siCon siD2 siCon siD2
75
50
37
Cdc20
250
150
100
BubR1
25
20
MAD2
250
150
100
Cdc27
50
37
actin

Supplementary Figure 8

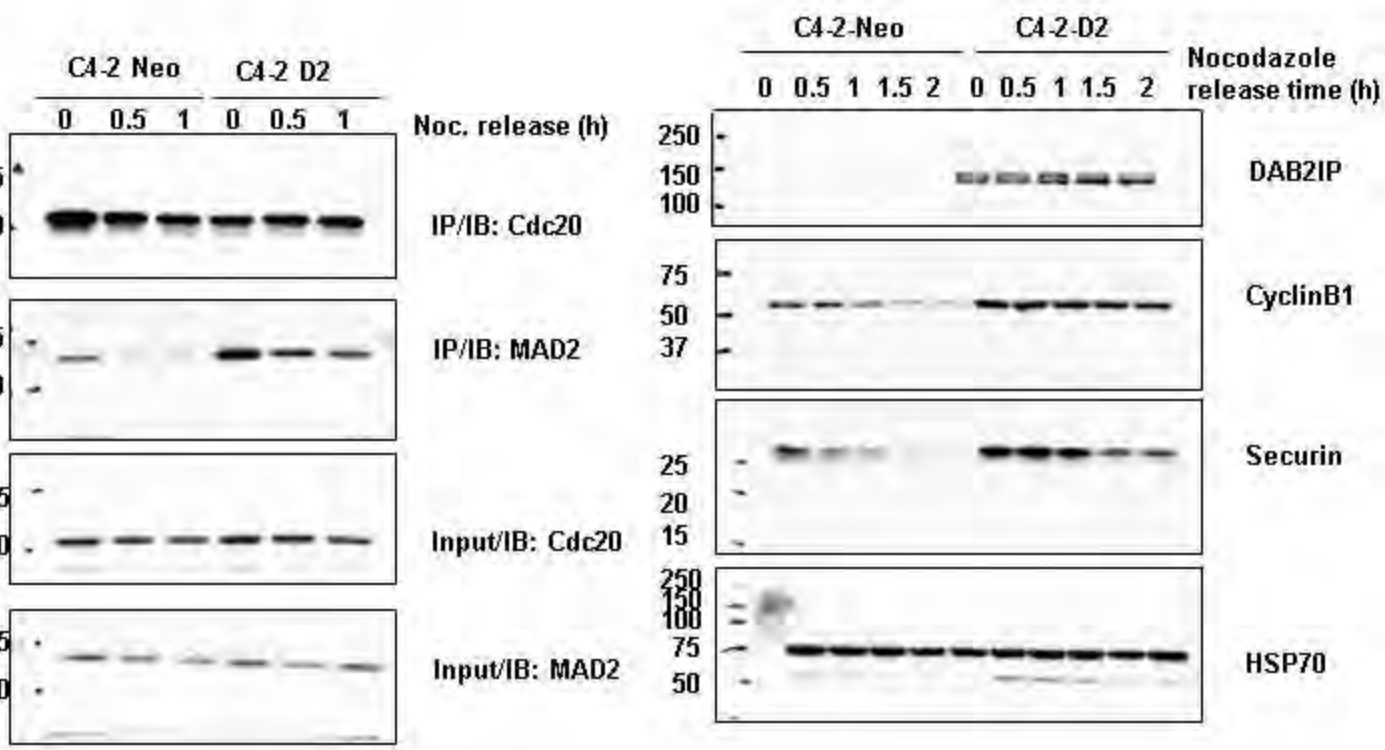

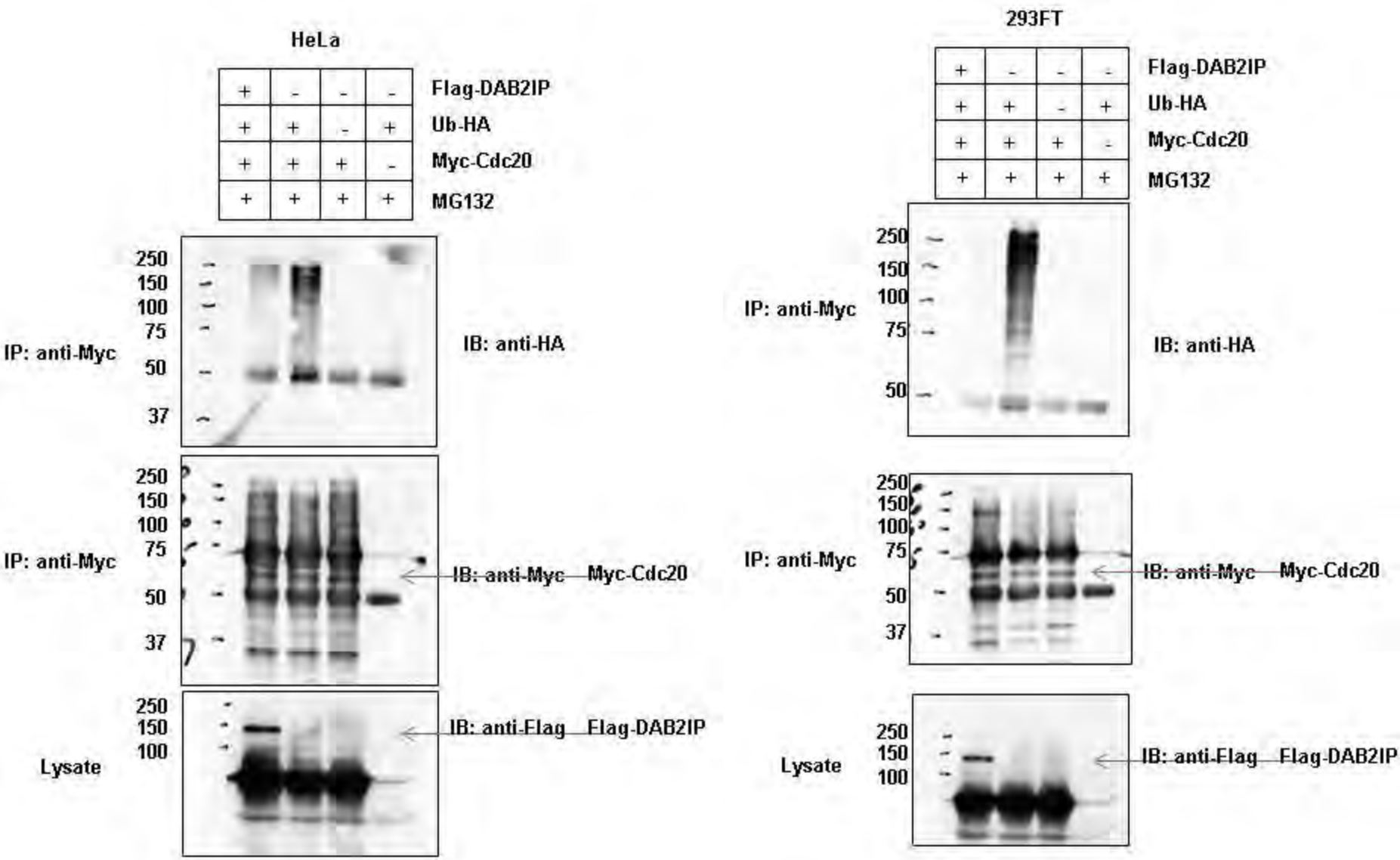
HeLa
293FT
Flag-DAB2IP
Ub-HA
Myc-Cdc20
MG132
IP: anti-Myc
IB: anti-HA
IB: anti-Myc
Myc-Cdc20
IB: anti-Flag
Flag-DAB2IP
Lysate
250
150
100
75
50
37

Supplementary Figure 10

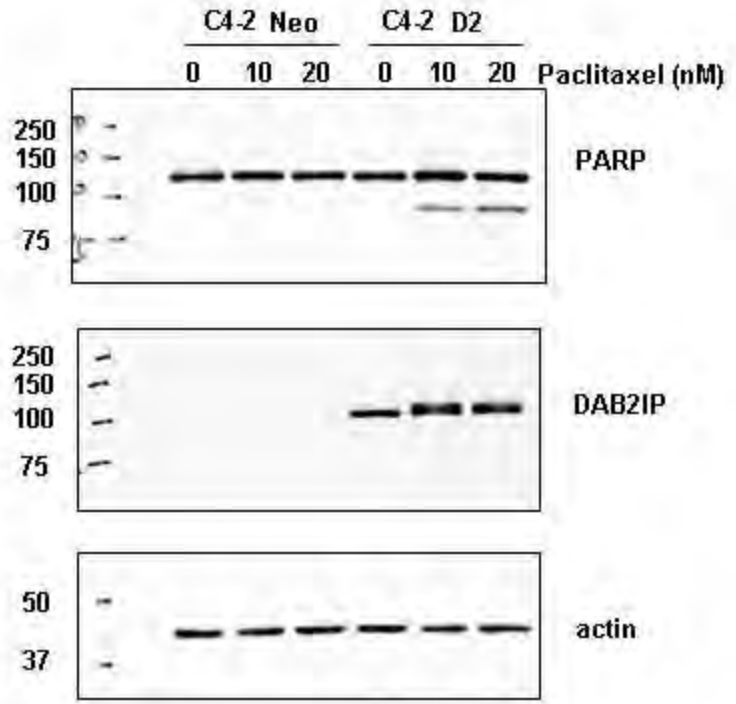

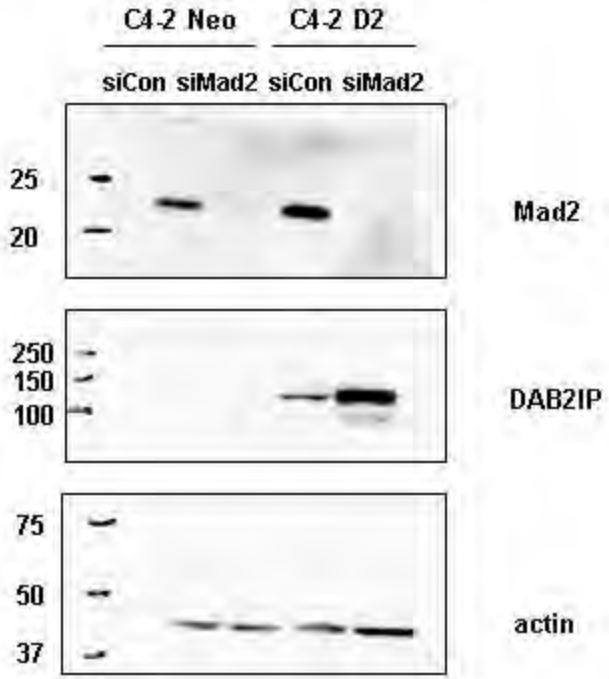

suppress the PI3K-Akt pro-survival pathway and enhance ASK1 mediated apoptosis. Decreased expression of DAB2IP is often detected in advanced prostate cancer (PCa) and is associated with poor prognosis. Loss of DAB2IP is primarily due to epigenetic regulation and promoter methylation resulting in radioresistance attributed to increased DNA repair capacity and decreased apoptosis. Our current findings reveal a novel role for DAB2IP in modulating the spindle assembly checkpoint (SAC). SAC is a molecular fail-safe mechanism that prevents premature separation of sister chromatids until they are attached to microtubule fibers oriented toward the opposite poles of the spindle. We found DAB2IP, is an integral component of APC/C-MCC, inhibit ubiquitylation and degradation of Cdc20 during prometaphase, which then blocks the disassembly of APC/C-MCC and inhibits premature SAC silencing. Presence of DAB2IP promotes binding of Mad2 and BubR1 with Cdc20 and the APC/C complex. On the other hand, loss of DAB2IP contributes to the dissociation of MCC from the APC/C causing degradation of Cdc20 and eventually leading to premature SAC inactivation and APC/C activation. Therefore, DAB2IP is identified as a negative regulator of Cdc20 degradation and MCC disassembly during SAC silencing progression. In conclusion loss of DAB2IP increases chromosome missegragation and aneuploidy, which contributes to tumorigenesis and chemo and radiation resistance to prostate cancer.

RESULTS

Figure 1: DAB2IP pathway

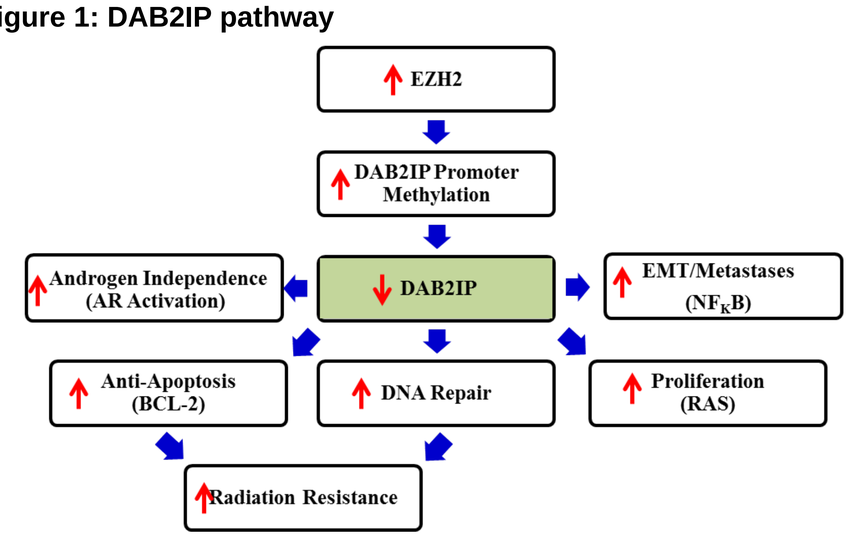

Figure 2: Decreased tumor expression of DAB2IP portends of worse outcome

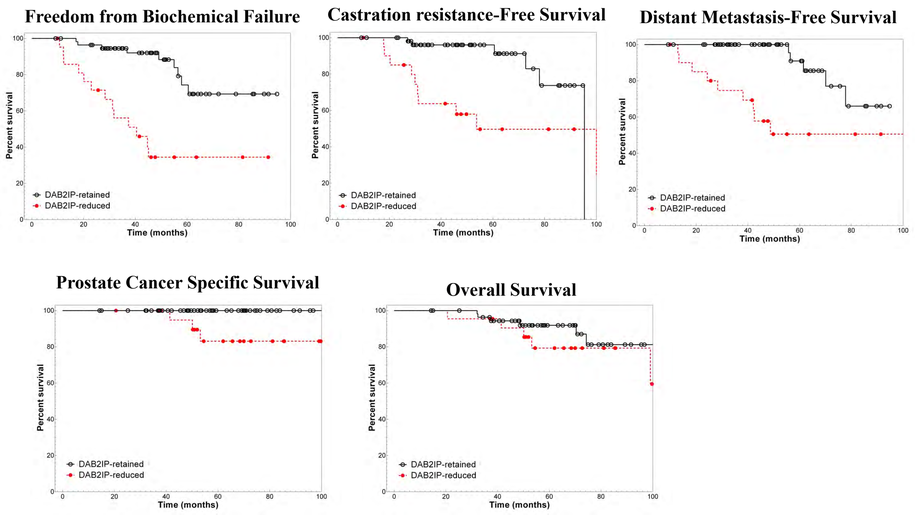

Table 1: Clinical Endpoints

Biomarker status	FFBF		CRFS		DMFS		PCSS		OS	
	4 year	P-value	4 year	P-value	4 year	P-value	5 year	P-value	5 year	P-value
DAB2IP-retained	92%	<0.0001	96%	0.0039	100%	0.0006	100%	0.0102	92%	0.3327
DAB2IP-reduced	34%		58%		58%		83%		79%	

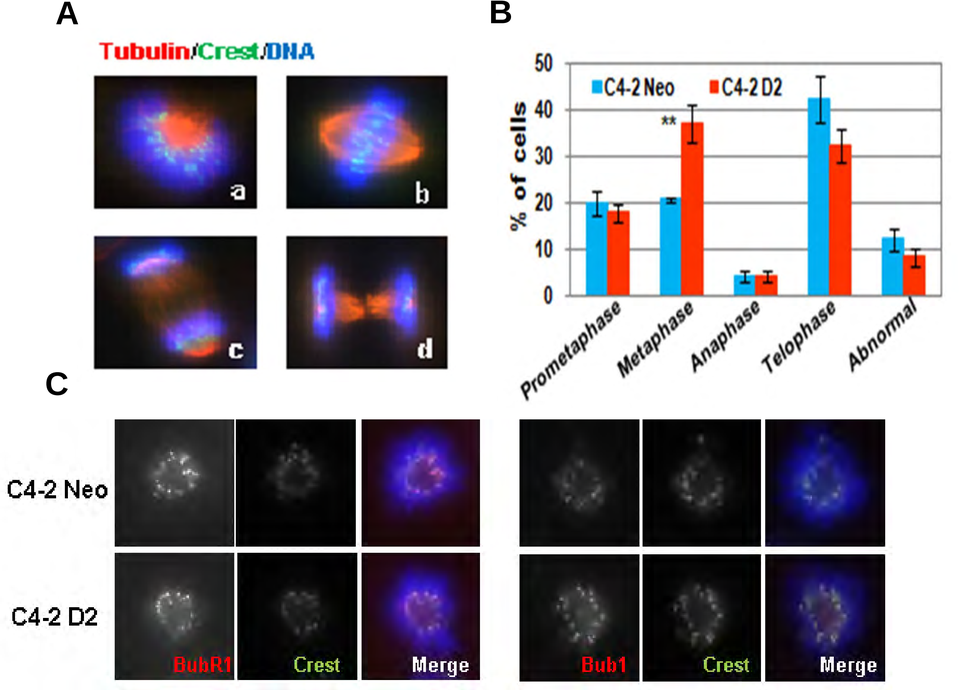

Figure 3. **DAB2IP regulates the SAC in prostate cancer cells** (A) Unperturbed DAB2IP overexpressed C4-2 cells and control cells undergoing mitosis were stained for tubulin (red), crest (green) and DAPI (blue). a, prometaphase; b, metaphase; c, anaphase; d, telophase. (B) Percentage distribution (mean + SE) of cells in different phases of mitosis and cytokinesis was analyzed. (C) DAB2IP does not affect the kinetochore localization of Bub1 and BubR1. DAB2IP-deficient and -proficient C4-2 cells are immunostained with anti-BubR1, Bub1 and CREST antibodies. Colocalization of BubR1 and Bub1 with CREST (kinetochores) was determined using a confocal microscope.

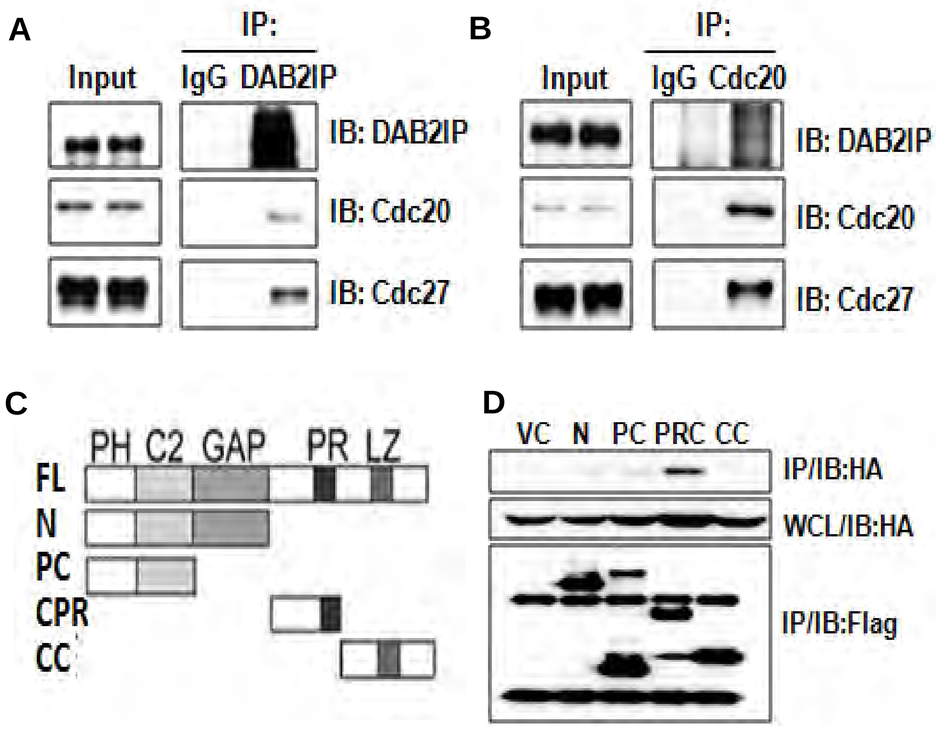

Figure 4. DAB2IP interacts with Cdc20 (A, B) IP experiment revealed that DAB2IP could interact with Cdc20 directly. (C) Schematic of the DAB2IP truncated constructs. (D) Immunoassay of 293T cells co-transfected with vectors expressing HA-tagged Cdc20 and Flag-tagged deletion mutants of DAB2IP; cells were treated with nocodazole, lysates were immunoprecipitated with anti-Flag M2 beads and immunoprecipitates were probed with an anti-HA or anti-Flag antibody.

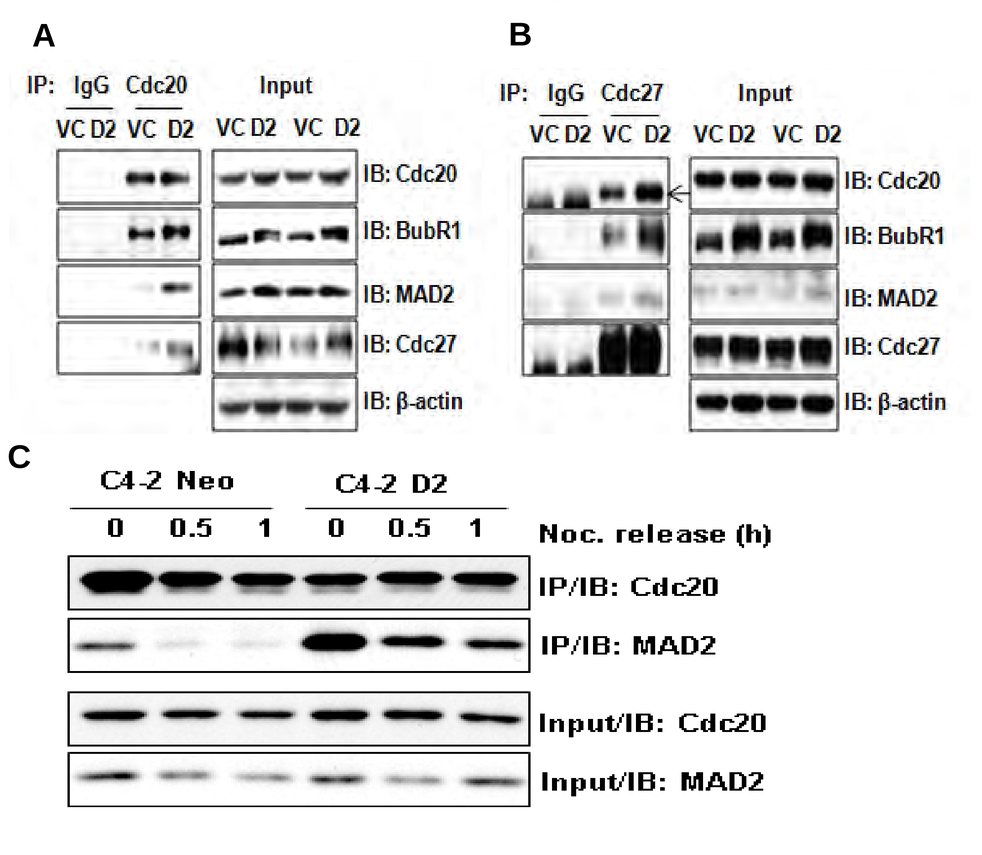

Figure 6. **Cdc20 turnover in prometaph**
Western blot showing Cdc20 degradation DAB2IP-deficient and -proficient C4-2 cel cycloheximide to block protein synthesis Cdc20 protein levels in cycloheximide-tre proficient C4-2 cells (n = 3; error bars, s.e

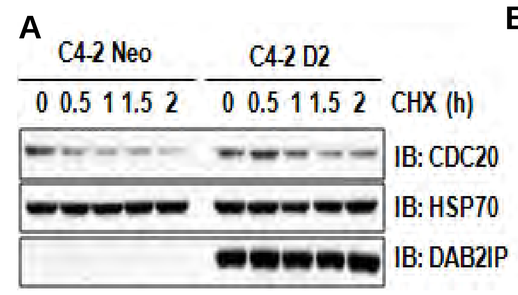

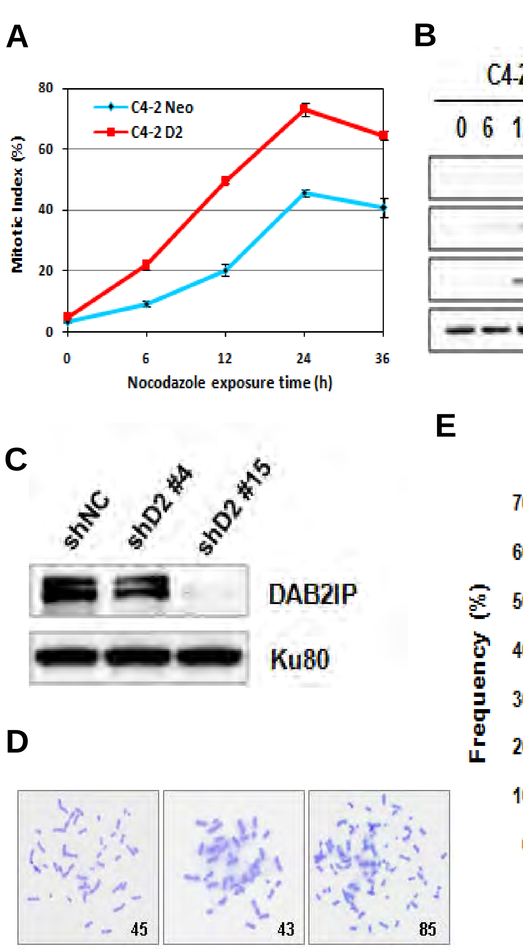

Figure 5. DAB2IP is required for chrome
(A) Nocodazole treated C4-2 Neo and D2 pH3 positive cells were detected. (B) West of cyclin B1 and pH3 after nocodazole trea DAB2IP in HCT116 cells using shRNA. (D aneuploidy and duploidy chromosomes. (E individual metaphase spreads of DAB2IP- cells (N >100).

WORKING

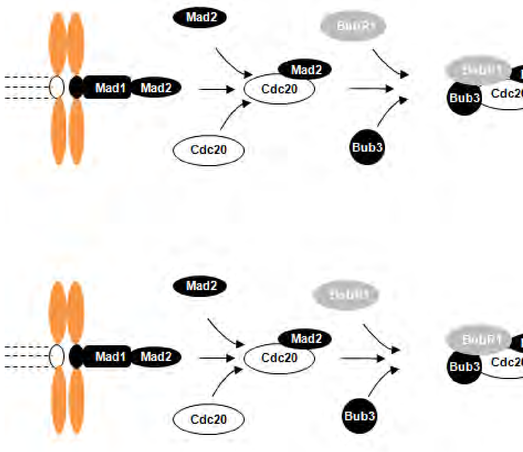

Acknowledgements:
CA175879 (DS), CA166677 (BPC), W